School of Earth and Planetary Sciences
Exploration Geophysics

Methods for high-precision subsurface imaging using spatially dense seismic data

Sasha Ziramov

0000-0001-5346-1124

This thesis is presented for the Degree of
Doctor of Philosophy
Of
Curtin University

May 2023

Dedication

In loving
memory of my late parents
Milena and Radisa,

and to my dear family,
Irina, Milena and Alex.

Abstract

Migration is a crucial step in seismic processing as it transforms seismograms into an image of underground rock formations. Current state-of-the-art depth migration techniques are regularly applied in marine seismic exploration, where they deliver accurate and reliable pictures of Earth's interior, under relatively few assumptions, supported often by only sparse a priori geological information. The question is how these algorithms will perform in different environments, not related to oil and gas exploration. For example, how to utilise those techniques in an elusive environment of hard rocks? The main challenge there is to image highly complex, subvertical piece-wise geology, represented by often low reflectivity, in a noisy environment.

Similarly, can we utilise the latest algorithms to image precisely shallow underground, intervened by complex fault and fracture systems, using high-resolution, high trace density, but limited signal-to-noise ratio (SNR) and survey size? To apply a high-precision pre-stack depth migration on such data that targets near surface, we need a specific approach to estimate the velocity at depths surrounding a complex overburden.

Three journal papers are presented and summaries in this thesis, with a solution to various problems faced by seismic exploration. The papers aim at maximizing information extraction from high-resolution, high-density 3D surveys by implementing innovative methods of acquisition, processing and high-precision imaging of rocks, structures and fluids at all depths, and in particular the near surface.

First publication shows the results of the processing of a high-resolution seismic dataset around a well for the injection of carbon dioxide (CO_2) in the subsurface. After obtaining a pre-stack migrated volume, we perform a seismic attribute analysis and an elastic impedance inversion. The results are of vital importance for the detection of low-permeability clay-layers which function as seals of the CO_2. The outcomes helped develop a dynamic model for CO_2 storage.

In second publication, I demonstrate the effectiveness of a comprehensive velocity building method that integrates velocity information from borehole measurements, modified first arrival times of seismic data and multiple iterations of seismic tomography. I investigate challenges and benefits of high-resolution seismic applied to a complex hard rock environment, in search for a suitable implementation of depth migration and velocity model building process. The method proposed in the paper is of interest for anyone facing challenges with the processing of hard rock seismic data and requires at the same time accurate imaging.

Lastly, in third publication, I evaluate cost-effective alternatives to a conventional high-resolution acquisition strategy, by introducing a distributed acoustic sensing (DAS) technology. The results of the world's first 3D DAS surface seismic survey, including multiple 2D DAS seismic profiles recorded in harsh surface conditions of salt lakes, are demonstrated and analysed in a detail in comparison to images obtained with conventional seismic sensors.

From CO_2 storage to the hard rock imaging, I propose solutions to various seismic exploration challenges, with the aim to improve the success rate of investigated projects. As new technologies are advancing, so are our instruments and the computing power, making it possible to collect and process seismic data in new and innovative ways. DAS technology has the potential to reduce the cost and complexity of seismic surveys and may even revolutionise the field of seismic exploration. By solving a wide range of seismic challenges, these technologies can help improve the efficiency, effectiveness, and sustainability of the exploration industry, as well as other industries that rely on seismic data.

Keywords:
Reflection Seismic, Depth Imaging, Velocity Model, Seismic Resolution, Hard Rock, Mineral Exploration, Distributed Acoustic Sensing

Acknowledgements

I would like to acknowledge financial assistance provided through Australian National Low Emissions Coal Research and Development (ANLEC R&D). ANLEC R&D is supported by Australian Coal Association Low Emissions Technology Limited and the Australian Government through the Clean Energy Initiative. The South West Hub project is managed by the Carbon Strategy Group of the Western Australia Department of Mines and Petroleum. It is supported through the Australian Commonwealth Government Flagship Program through the Department of Industry, Innovation and Science (DOIIS); the West Australian State Government through the Department of Mines and Petroleum; and the local community in the southwest of Western Australia.

The advances on depth imaging would not be possible without the support from Northern Star Limited and their permission to used use Carosue Dam data for the thesis.

I would like to thank Dave Felding and Camilo Guarin of Matsa Resource Company for providing key financial support, and equipment necessary field support and equipment for all DAS projects.

I acknowledge financial and technical support of the Mineral Research Institute of Western Australia (MRIWA) under the program M514, co-sponsored by Matsa Resources and HiSeis.

Special thanks to my supervisors Dr. Milovan Urosevic, Dr. Andrej Bona and Dr. Boris Gurevich for their support.

I would also like to thank Curtin University staff who made complex DAS data acquisition programs possible and HiSeis team for their ongoing support during Carosue Dam and DAS studies.

My thanks to Halliburton Company for their generous donation of Landmark processing software and to CGG for their donation of AVO and seismic inversion software.

Table of context

List of papers

1. Ziramov, S., Urosevic, M., Glubokovskikh, S., Pevzner, R., Tertyshnikov, K., Kepic, A., Gurevich, B., CO2 Storage Site Characterisation using Combined Regional and Detailed Seismic Data: Harvey, Western Australia*, Energy Procedia*, Volume **114**, 2017, Pages 2896-2905, ISSN 1876-6102, https://doi.org/10.1016/j.egypro.2017.03.1417.
(Chapter 2)

2. Ziramov, S., Young, C., Kinkela, J., Turner, G. & Urosevic, M. (2023) Pre-stack depth imaging techniques for the delineation of the Carosue Dam gold deposit, Western Australia, *Geophysical Prospecting*, **00**, 1– 19. https://doi.org/10.1111/1365-2478.13314.
(Chapter 2)

3. Ziramov, S. Bona, A., Tertyshnikov, K.,. Pevzner, R., Urosevic, M., Application of 3D Optical Fibre Reflection Seismic in Challenging Surface Conditions, *First Break*, Volume **40**, Issue 8, 2022, p. 79 – 89, https://doi.org/10.3997/1365-2397.fb2022071.
(Chapter 2)

---

4. Ziramov, S., Urosevic, M., Pevzner, R., Glubokovskikh, S., Gurevich, B., Carbon Storage Characterisation Using Pre-Stack Depth Migration in Harvey, Western Australia. *14th Greenhouse Gas Control Technologies Conference* Melbourne 21-26 October 2018 (GHGT-14), Available at SSRN: https://ssrn.com/abstract=3365598.
(Appendices)

List of figures in introductory material

List of abbreviations in introductory material

2D	Two-dimensional
3D	Three-dimensional
CDP	Common depth point
CIP	Common image point
DAS	Distributed acoustic sensing
PSTM	Pre-stack time migration
PSDM	Pre-stack depth migration
KDM	Kirchhoff depth migration
RTM	Reverse-time migration
RMO	Residual moveout
VMB	Velocity model building
OWEM	One-way wave-equation migration
SNR	Signal-to-noise ratio
FWI	Full waveform inversion
EI	Elastic impedance
CO_2	Carbon dioxide
QC	Quality control

1. Introduction and overview

Innovation has been the main driver of growth and prosperity throughout the human history. From the industrial revolution until modern days, new technologies have often been possible only after the discovery of new materials, methods, and energy sources (Mokyr and Strotz, 1998). Seismic exploration, which of all geophysical methods provides by far the highest spatial resolution, has undergone major developments in sensing, sources, efficiency and data processing and imaging (Waters et al., 2016). Extreme computing power required for depth imaging became reality only recently with developments in new technologies of materials and chip making, as well as rise in compute power.

Innovation in seismic exploration has been mainly led by the need to resolve various geological complexities in relation to exploration of natural resources. Hence, in this thesis I will focus on optimal utilisation of high-resolution seismic data acquired for the delineation of shallow underground targets in various geological settings, such as sediments, hard rocks and salt lakes. It should be emphasised that the hard rock environment is particularly challenging for the application of depth imaging technologies. These challenges involve complex geological settings such as steeply dipping reflectors, faults, fracture zones, thrusts, etc.; low signal-to-noise ratio; complex near-surface conditions (Brodic at al., 2021). Initial results are often elusive and may require further investigations and innovative solutions. In this chapter, I will describe the progress made in migration of such data to the present date and the most significant barriers to attaining accurate images of the interior of the Earth, with a special focus on imaging near surface.

Seismic depth imaging or migration is an important stage of seismic processing because it transforms acquired data into an image, considered to be an accurate structural description of the Earth. I will explore modern depth imaging techniques deployed in marine seismic, where seismic migration usually delivers adequate results. As the expectations of its accuracy, robustness, and reliability are high, I will incorporate these techniques into a depth imaging workflow for high-resolution, high-density land seismic data, that using relatively few assumptions, renders high-precision images of the underground.

Finally, I will present an economical alternative to a current high-resolution acquisition strategy, introducing distributed acoustic sensing (DAS) technology. This innovative acquisition strategy could deliver an order of magnitude saving, while substantially increasing the data density and hence allowing for the finest resolution.

1.1. Modern depth imaging methods

The current state of the art depth imaging techniques are mostly applied on high-quality, marine seismic data. Those techniques incorporate a comprehensive 3D pre-stack depth migration (PSDM) workflow, using one or more imaging methods with few assumptions (Furniss, 2000). The imaging process has two phases: to build a velocity model and to produce an image that ideally gives an interpreter evidence about structures, rock and fluid properties. Using seismic migration to estimate the velocity model needed for migration presents a nonlinear problem (Furniss, 2000). In depth imaging, a seismic tomography is the current popular solution to this nonlinear velocity/imaging problem. It is an iterative process, using a succession of depth migration iterations in combination with an optimisation routine to build and refine the velocity model (Furniss, 2000).

There are two main approaches to seismic migration: ray-based methods and wave-equation-based methods. Because all migration methods, including ray-based migrations, are based on the wave equation, the term "wave-equation migration" is often used for non-ray-based migration methods (Etgen et al., 2009). Ray-based methods, such as Kirchhoff and beam migrations, are the simplest and most efficient migration methods. They use a ray approximation, which is a high-frequency approximation to the wave equation (Yilmaz, 2019). Wave-equation-based methods are better at imaging complex geological structures and low-frequency seismic waves than ray-based methods, but they are also more computationally expensive. Wave-equation methods fall into one-way and two-way classes. Over time, many different wave-equation methods have been developed, but all of them can be described in terms of wavefield extrapolation followed by the application of an imaging condition (Yilmaz, 2019).

Kirchhoff migration is the most well-known of the ray-based methods. This method was published by French (1975) and then Schneider (1978), who proposed the kinematic process of diffraction stack as an asymptotically correct solution to the imaging problem. The method is further developed by Beylkin (1985) and Bleistein (1987), which led to a true-amplitude Kirchhoff migration. During 1980s and 1990s, Kirchhoff migration was the preferred depth imaging method. Its formulation as an integral solution to the wave equation was introduced by Schneider (1978):

$$I(X;X_s) = \int dX_r \int W \frac{\partial P_u(X_r,X_s,t)}{\partial t} \delta[t-(t_s+t_r)]dt, \quad (1)$$

where X is the image point location,
X_s is location of the source,
X_r location of the receiver,
t_s and t_r are the times it takes for seismic waves to travel from the source and receiver locations to the image point,
W is a weight function,
P_u represents recorded wavefield,
δ is Dirac function.

Equation 1 demonstrates the flexibility of Kirchhoff migration in imaging seismic data. It allows the user to control the sampling of the migrated image at location X, (Yilmaz, 2001). If the traveltimes, t_s and t_r for Kirchhoff migration are calculated using ray tracing, the method can be restricted to only include seismic waves with a certain range of incidence angles at the

recording surface (migration aperture). This is useful for imaging very steep dips. However, using ray tracing to calculate traveltimes can limit the accuracy of the migration, because wavefields at image locations may not be accurately represented by a single amplitude arriving at a particular time implied by equation 1 (Etgen et al., 2009).

Nowadays in oil exploration industry, most depth migration projects use methods other than Kirchhoff migration to produce the final image (Yilmaz, 2019). Imaging methods based on wave-equation and beam approximations tend to produce clearer and more accurate images than Kirchhoff migration. However, Kirchhoff migration is still commonly used to build velocity models because it is efficient and can output migrated common-image-point (CIP) gathers, which can be easily used by seismic tomography (Malinowski, 2022).

Beam migrations, which were first described by Sun et al. (2000) and Hill (2001), are a type of Kirchhoff migration that is performed on small sections of the recorded seismic data. This allows beam migrations to image areas of the subsurface with complex traveltimes, which is a limitation of standard Kirchhoff migration. As a result, beam migrations are typically more accurate than Kirchhoff migrations (Etgen et al., 2009). In addition, beam migrations have no limit on how steeply dipping geological formations they can image, giving them an advantage over migrations based on the one-way wave equation. However, most beam migrations rely on rays, which can limit their accuracy in areas with complex geological structures (Etgen et al., 2009).

One-way wave-equation methods (OWEM) apply Green's identity to the recorded wavefield and the wavefield coming from the source locations, using a wavefield extrapolator, that allows for downward or upward propagation. The first step of OWEM is to propagate the waves generated by the source (source wavefield, D) and the waves recorded at the surface (recorded wavefield, U) from the surface down into the subsurface. This is done by solving the one-way wave equations (Etgen et al., 2009):

$$\left(\frac{\partial}{\partial z}+i\frac{\omega}{V}\sqrt{1+\frac{V^2}{\omega^2}\left(\frac{\partial^2}{\partial x^2}+\frac{\partial^2}{\partial y^2}\right)}\right)U=0, \tag{2}$$

$$\left(\frac{\partial}{\partial z}+i\frac{\omega}{V}\sqrt{1+\frac{V^2}{\omega^2}\left(\frac{\partial^2}{\partial x^2}+\frac{\partial^2}{\partial y^2}\right)}\right)D=0. \tag{3}$$

Once we have propagated the seismic waves from the surface to the subsurface, we need to apply an imaging condition to generate an image of the subsurface (Claerbout,1971).

The initial OWEM began with low-dip approximation to the wave equation presented by Claerbout, (1971). This work is important because it was one of the first papers to discuss the challenges of imaging steep-dip geological formations. Over the years, a number of methods have been developed to improve the steep dip performance of one-way extrapolators (Etgen et al., 2009): (i) Implicit finite-difference algorithms (Berkhout, 1979; Ma, 1982; Lee and Suh, 1985; Zhang et al., 1988), (ii) Stabilized explicit extrapolation methods (Holberg, 1988; Hale, 1991a, 1991b; Soubaras, 1996), (iii) Phase-shift propagation with multireference velocities (Margrave and Ferguson, 1999; Gazdag, 1978) and (iv) Dual-space x-k methods (Stoffa et al., 1990; Ristow and Ruhl, 1994; Huang and Wu, 1996; Le Rousseau and de Hoop, 2001; Zhang et al., 2003; Chen and Liu, 2006).

The first full two-way wave equation was used on post-stack 2D data in the late 1970s (Loewenthal and Mufti, 1983; Baysal et al., 1983; McMechan, 1983; Whitmore, 1983). The method works by propagating the recorded seismic waves backward in time from the surface of the Earth into the subsurface (Zhang and McMechan, 2017), hence the name reverse-time migration (RTM). The method uses the full wave equation, not Green's identity, and requires computation of snapshots of the entire wavefield at all times from the latest to time zero.

Pre-stack RTM additionally involves propagation of source wavefield forward in time, so the method in essence comprises forward and reverse time migration, making RTM propagation engine the most accurate there is (Zhang and McMechan, 2017). The method directly solves the two-way acoustic wave equation:

$$\left(\frac{1}{V^2}\frac{\partial^2}{\partial t^2} - \frac{\partial^2}{\partial x^2} - \frac{\partial^2}{\partial y^2} - \frac{\partial^2}{\partial z^2}\right) p(x;t) = 0. \quad (4)$$

Unlike in ray-based migrations, there is no high-frequency assumption in equation 4, and unlike in OWEM, there are no approximations to the wave equation that limit propagation angle or the ability to handle strong lateral velocity variations (Etgen et al., 2009). RTM can easily handle any spatial velocity variation and has ability to image dips up to 180° which is an advantage over other methods.

Following Tsvankin (2001) and Alkhalifah (2000), RTM method has been modified to further improve the image quality, clarity, and positioning (Zhou et al., 2006; Zhang and Zhang, 2008; Fletcher et al., 2008). The history and development of modern seismic imaging methods has been well summarised by Malinowski, (2022).

RTM requires greater computation time and memory requirement compared to other methods. The memory requirements for Kirchhoff and beam migration can be minimal, which is the main reason they are still widely used (Zhang and McMechan, 2017). However, for a 3D RTM to work, we need memory allocation for several 3D wavefield snapshots at each time steps and the velocity model, which was a luxury requirement for computers in the past and remains a challenge today with large 3D projects. This is the reason why the industry settled for improvements in OWEM in the past, which has similar accuracy for moderate dips, and ray-based migration, which produced useful steep dip images.

Efficiency remains an issue for RTM, but computational advances have mitigated this problem to a large degree (Tang et al., 2021). Nowadays, cloud computing gains popularity with its ability to economically run computationally intense processes. With the cloud scalability of almost unlimited resources, for many imaging projects RTM is now considered indispensable.

As ray methods represent an asymptotic solution to the wave equation, there is an expectation that the wave-equation methods, especially RTM, are more accurate and without exception produce better images of the Earth's subsurface. This is not necessarily correct, as ray method can be a more robust with respect to errors in the velocity model, as well as in irregular seismic designs with limitations in source-receiver azimuth, and offset distribution (Zhang and McMechan, 2006). Generally, RTM is more accurate than most ray-based methods within their range of applicability, which can be limited.

The question remains how will RTM perform in an environment of complex overburden and high noise levels, typical for hard rocks? High-resolution surveys for mineral exploration

exhibit various problems and challenges but do require a high-precision imaging for delineation of small size structures and mineralisation. In this study, I will explore and assess performance of both Kirchhoff depth migration and RTM and create suitable workflow that will render reliable and accurate pictures of Earth's architecture.

1.2. Difficulty of direct transfer of imaging techniques to the mineral sector

Most of high-resolution 3D seismic surveys in mineral exploration have discreet, shallow imaging targets, which is the reason they are acquired with high spatial density and usually with a limitation in size and offset range (Sheriff, 2002). They are specifically designed to image small-size structures or mineralisation at depths that can be economically extracted. Although it is tempting to draw a similar optimism regarding effectiveness of depth migration as in the sedimentary environment, that conclusion is not automatically justified, primarily because this environment has a nontrivial near surface that needs to be imaged. In particular, when near-surface conditions vary rapidly, a common-depth-point (CDP) gather of input traces can bear only a small relationship with corresponding information from nearby gathers. This kind of ambiguity can be reduced by acquiring high-resolution, high spatial density seismic data. Larger size 3D surveys often use low spatial density of receivers. Hence so-called nested 3D of smaller extent but with much higher data density are often recorded directly above the prospective target or geological model of interest (Urosevic and Kepic, 2012).

Another problem arising particularly in the mineral sector is that seismic surveys often cover active mining sites, consequently resulting in high noise levels, limited access with often large source and receiver exclusion zones. This can result in irregular distribution of near-offset traces in places, reducing the early-time information. Some other challenges for imaging of hard rock seismic include: geological settings are rather complex, with steeply dipping geology, multiple complex shear zones, excessive heterogeneities involving strong alterations, change of fabric, small size mineral bodies, faults, fracture zones, thrusts (Eaton, et al., 2003; Ziramov et al., 2016.; Milkereit et al., 1992; Urosevic et al., 2012). Moreover, a hard rock environment is typically characterised by low intrinsic SNR and near surface conditions are often complicated and require a large static correction (Singh et al., 2019).

All these issues pose problems for the accurate velocity assessment in near surface, needed for depth migration. The velocity estimation processes must change considerably from standard velocity model building (VMB) methods largely driven and the past by oil exploration industry and adapt to the challenges of hardrock seismic exploration. In this thesis, I will investigate impact of these limitations on seismic imaging of hard rocks and explain why I had to introduce a specific depth imaging workflow using a combination of high-precision Kirchhoff and RTM techniques.

1.3. Hard rocks seismic – is it hard to image?

The history of the application of high-resolution seismic reflection surveys in mineral sector is characterised the successions of high and lows, stops and restarts, pessimism, and great promise. From the very beginning, various researchers realised that seismic could be utilised not only for prospecting but also for site characterizations, mine planning, and mine development. Seismic studies were attempted on many sites for exploration of numerous minerals such as iron, gold, silver, nickel, copper, starting in early 50's, (Berson 1957; Schmidt 1959; Gendzwill 1990; Juhlin et al., 1991; Friedel et al., 1995; Friedel et al., 1996; Urosevic and Evans 1998; Urosevic and Evans 2000; Perron et al., 2003; Chen et al., 2004). Various seismic acquisition techniques and survey designs have also been evaluated to optimize efficiency and improve the exploitation of mineral resources (Gupta, 1972; Ruskey, 1981; Gladwin 1982; Maxwell and Young,1992; Frappa and Molinier 1993; Bierbaum and Greenhalgh 1998; Duweke et al., 2002).

The breakthrough in seismic for mineral exploration came with the (3D) seismic designs recorded in South Africa in late 1980s and early 1990s (De Wet and Hall, 1994; Manzi et al., 2012). Afterwards, studies by Eaton et al. (1997) and Pretorius et al. (1997) demonstrated that the complexity of the hard rock environment is best assessed and delineated by 3D reflection seismic. The history and expansion of modern seismic methods for the exploration of mineral resources across the world has been well summarised in Malehmir et al. (2012). Since then, a steady rise in the use of 3D reflection seismic for exploration in brown fields, to extend the existing mine life and discover new resources at a greater depth has occurred (Urosevic, 2013; Urosevic et al., 2017; Gil, et al., 2022).

The potential for high sensor density designs for imaging the complex geometry of salt domes was hinted at in 1990 in the oil industry (McDonald and Lawton, 1990). However, both in oil exploration traditionally and mineral exploration nowadays, the main novelty driving the high-density 3D seismic surveys comes from cable-free nodal systems. Although first (primitive) nodal systems referred to as distributed cable recordings date back to the 1970-ies (Dean et al., 2018), the expansion in the production and utilisation of modern nodal systems is only recorded in middle of the last decade primarily in the oil sector. Another major driver is related with the seismic sources and primarily the utilization of broad bandwidth sweeps (Cordery, 2020). Modern vibroseis and electromagnetic vibrating sources provide broad band seismic signal that is required for the utilisation of novel inversion and imaging techniques (Naghizadeh et al., 2019; Pertuz et al., 2022; Singh et all., 2022). A combination of a large number of sensors (high spatial data density) and broad-band seismic sources enables the successful implementation of novel processing (signal enhancements, interpolations, etc), imaging techniques such as reverse time migration and inversions such as full waveform inversion. This led to early investigations into the potential of full waveform inversion (FWI) in hard rock environments (Adamczyk et al., 2014; 2015), while investigations into imaging techniques were documented by several authors (Hloušek et al., 2015; Broüning et al., 2020; Brodic et al., 2021; Singh et al., 2022).

The successful application of the seismic reflection method is to the first degree controlled by the contrast and the distribution of elastic properties of the geological environment (Eaton et al., 2003; Bohlen et al., 2003). However, mineral composition and more elusive rock characteristics such as alteration and rock texture also play an important role in recorded reflectivity (Schetselaar et al., 2019). Our ability to delineate reflectivity also depends on its geometry and volume, as well as the presence of fractures and joints, grain alignment and crystal symmetry, etc. Therefore, reflectivity in hard rock is controlled by many factors and it

is not readily predictable even in well explored mine sites (Milkereit et al., 1992). This, possibly peculiar reflectivity pattern of hard rocks is further exacerbated by high structural complexities. In terms of gold exploration in Western Australia, both the reflectivity patterns and excessively complex underground structures are commonplace (Stolz et al., 2004). The necessity to utilise high precision imaging techniques, such as Kirchhoff PSDM to delineate complex underground structures was recognised early in the application of seismic for gold exploration across Yilgarn craton of Western Australia (Urosevic et al., 2007a; Urosevic and Evans, 2007b). The application of seismic for gold exploration in Western Australia must be carefully staged in terms of both acquisition and data processing. Hence, seismic data acquisition is typically proceeded by a seismic feasibility study, that investigates the spatial distribution of seismic rock properties. The feasibility study incorporates forward modelling of seismic response and physical rock properties measured in boreholes for survey design to optimize the possibility of recording the seismic energy originating from the targets (Ayarza et al., 2000; Malehmir et al., 2013; White and Malinowski, 2012). Positive results would grant project continuation. After acquisition, data processing and analysis should adopt an optimal approach for imaging complex geological structures at all scales with maximum possible precision.

Since these early studies, many 3D seismic surveys have been acquired over gold prospects across the world to resolve such structurally-hosted mineralisation (Urosevic et al., 2017), including several 3D seismic surveys of exceptional quality acquired across hyper-saline lake Lefroy in Western Australia. Despite their significant exploration value (Urosevic et al., 2012), common equipment loss and corrosion in the harsh salt lake operating environment has meant such surveys entail high risk of writing off valuable electronic hardware. Whether we use a conventional cable to connect all the sensors on a seismic array, or a nodal seismic system that uses a network of wireless sensors to communicate with a central recording unit, the equipment is susceptible to damage from such environmental factors, and expensive to install and maintain (Issa et al., 2020). This has resulted in many highly prospective areas under salt lakes in WA remaining underexplored, creating a potential value case for more appropriate exploration concepts and technologies suited to work in these challenging environments (Urosevic et al., 2019).

A solution to this challenge was DAS, where the sensitivity to a highly invasive hyper-saline environment is only on the data receiving end: the recording unit known as interrogator. The interrogator is an electronic device that generates and analyses the light pulses used to probe the fibre optic cable (Hartog, 2018). The technology works by sending a laser pulse along a fibre optic cable. The seismic wave interacts with the fibre optic cable and the surrounding material, causing the fibre optic cable to stretch or compress slightly (Willis, 2022). This change in cable length is captured by changes in backscattered light and recorded by a DAS interrogator, which uses a variety of signal processing algorithms to convert this information into acoustic data (Hartog, 2018).

The sensitivity of DAS measurements to the direction of a seismic P-wave depends on how the measurements are made. For systems that measure strain or strain change rate directly (like Fotech or Silixa interrogators), the signal strength decreases as the cosine squared of the angle of incidence and for systems that measure deformation (like Terra15 interrogator), the signal strength decreases as the cosine of the angle of incidence (Sidenko et al., 2020). This means that in either case, the signal is the strongest when the wave is traveling directly along the fibre, and the weakest when it is traveling perpendicular to the fibre. As this sensing direction is not favourable for surface seismic, we have tested different options of winding the cable around

central support. A 60^0 pitch angle (cable helicity) will produce close to omnidirectional fibre optic sensitivity.

Once the helical cable is laid out on surface (or preferably buried), securing the interrogator from the harmful environment is trivial, while on the sensor side, DAS technology is corrosion-proof, easy to deploy, and several orders of magnitude cheaper than equivalent geophone seismic acquisition systems. Considering that salt lakes of Australia are often hosting mineral deposits, DAS technology is of a particular importance for advancing mineral exploration in such environments.

1.4. The potential of high resolution, high-density seismic data for creating accurate underground pictures

"High resolution" is a constant request from interpreters of geophysical data at all scales. It is a key attribute of interest when designing seismic surveys and it is usually requested in terms of temporal resolution (Egan et al., 2012). Thus, survey design strategies often focus on what temporal frequencies can be put into the Earth, for example, what maximum frequency should a vibrator sweep? This is often calculated by a simple rule that thickness of the bed model is resolvable if it is equal or greater than wavelength/4 (Kallweit and Wood, 1982).

The fact is, that extraordinary efforts for putting high-frequency energy into the ground can be wasted if the spatial resolution is not brought into harmony with the temporal. Therefore, spatial resolution and temporal resolution are very much intertwined (Egan et al., 2012). However spatial sampling is one of the key factors affecting survey cost, and hence most surveys utilise sparser receiver options. This is likely the principal reason for suboptimal imaging results and even quite poor result, particularly in the shallow (several hundreds of meters) subsurface, which is of critical importance for mineral exploration. In contrast, the high-resolution surveys presented in this thesis all have dense spatial sampling. This refers to small source point and sensor spacing and short line intervals, small source array dimensions, a single sensor per location, and a higher source frequency.

Extensive structural complexity typically encountered in a hard rock environment requires high spatial and temporal resolution as recognised in early seismic works by Stolz et al. (2004). High spatial density of sensors is of a key importance for imaging structurally controlled mineralisation (Urosevic et al., 2012). To avoid expensive investigations by deploying substantial number of sensors over large territory, it is possible, based on reciprocity, to partially compensate for a small sensor count by introducing additional source positions or repeating specific shooting patterns. Indeed, such an approach characterised hard rock 3D seismic surveys in the previous decade (Urosevic et al., 2017; Ziramov et al., 2015; 2016). One to two thousand receivers were typically deployed for 3D surveys at the time using moving, overlapping source-receiver templates. While this approach made 3D seismic more accessible and affordable to the mineral industry, it suffered from several drawbacks, related mainly to the size of aperture and target illumination consistency.

High-resolution seismic exploration is typically, and one may say necessarily, used in mineral exploration, and for hydrogeological and geotechnical investigations. However, while in this study I have mainly focused on the application of high-resolution seismic method in a hard rock environment, I also show and discuss the importance of having high data density for Carbon dioxide (CO_2) sequestration objectives.

Geological sequestration of CO_2 is relatively new idea and new technology aimed to reduce greenhouse effect (re-emission of the solar radiation by CO_2), which results in global warming (Hitchon, 1996). Until new technologies can oust the necessity of fossil fuel use, it is believed that the process of global warming could be slowed down by sequestering greenhouse gases such is CO_2 in the subsurface. Many options were proposed for CO_2 sequestration, but the most effective storage is eventually found in saline aquifers or depleted oil and gas reservoirs (Bachu et al., 1996; Ivanova and Luth, 2015). The storage is certainly a geological problem and seismic method can be used to verify if the selected site is suitable for the challenge. We use seismic for site characterisation, delineation of the target reservoir and monitoring of the sequestration process for safety purposes.

Indeed, at the Harvey area, a potential hub for CO_2 sequestration in Western Australia, the studies conducted demonstrate the importance of seismic for site characterization. A detailed study presented in this thesis, conducted with the nested, high-resolution 3D seismic survey demonstrates the importance of such data for delineation of subtle structures and faults in the near surface that can present risk for CO_2 sequestration in much deeper formation. Just as in hard rocks, the imaging precision is of paramount importance to CO_2 sequestration studies (Urosevic and Pevzner, 2015). Hence, my efforts in this field were directed towards imaging issues and image quality analysis, with the objective of delineation of subtle structural features of interest to CO_2 monitoring studies.

1.5. The Quest

My research aimed to address various challenges encountered in exploration of shallow complex targets. Hence, it was design towards optimal utilisation of high-density seismic data to precisely delineate shallow targets, through specific depth imaging approach. The study assesses seismic imaging of complex targets situated in different geological settings. The approach proposed is shown to be very effective in all of the cases analysed.

Specific tasks conducted in this study are summarised below:

- Investigate benefits of high-resolution, nested 3D seismic surveys.
- Image regolith with refraction tomography inversion.
- Devise an optimum workflow for the application of pre-stack depth migration algorithms in high-resolution 3D seismic surveys for mineral exploration;
- Construct an efficient workflow for integration of different velocity measurements and calculations into the appropriate velocity model for hard rock depth imaging;
- Conduct a cost-effective near surface seismic field survey in harsh environment using a novel DAS technology.

1.6. Summary of thesis publications and their relation to thesis topic

The thesis is compiled of three journal papers and one additional paper placed in the appendix, for further reading on depth imaging results in a carbon sequestration study. This chapter summarises the journal publications achievements relevant to the thesis topic.

Publication I

Ziramov, S., Urosevic, M., Glubokovskikh, S., Pevzner, R., Tertyshnikov, K., Kepic, A., Gurevich, B., CO2 Storage Site Characterisation using Combined Regional and Detailed

Seismic Data: Harvey, Western Australia, *Energy Procedia*, Volume **114**, 2017, Pages 2896-2905, ISSN 1876-6102, https://doi.org/10.1016/j.egypro.2017.03.1417.

This manuscript is a peer-reviewed publication that demonstrates benefits of a small (2 km^2), low-cost 3D seismic survey recorded with spatially high data density. It introduces a high resolution "nested" survey positioned at the location of Harvey-4 well. The survey is specifically designed for near surface imaging (i), delineation of small-size structures (ii) and implementation of seismic stratigraphy and quantitative interpretation (iii), as a part of a CO_2 monitoring project in Harvey, Western Australia.

Prior to acquisition of the nested 3D survey, some 115 km^2 of regional 3D seismic data were recorded in the investigated area. That large survey proved to be of significant importance for a regional characterisation of the reservoir, identification of large structures and key geological interfaces. However, small to medium size structures of interest for the development of the static and dynamic models were poorly imaged in this survey as the recording geometry was adjusted for the greater depths, which was between 2 km and 3 km.

The results of high-resolution 3D survey demonstrate that high-density surveys are important even at the characterisation stage and are crucial for development of a detailed static model. High-definition, crisp, images of nested data, when compared against the regional one, are demonstrated in Figure 1.

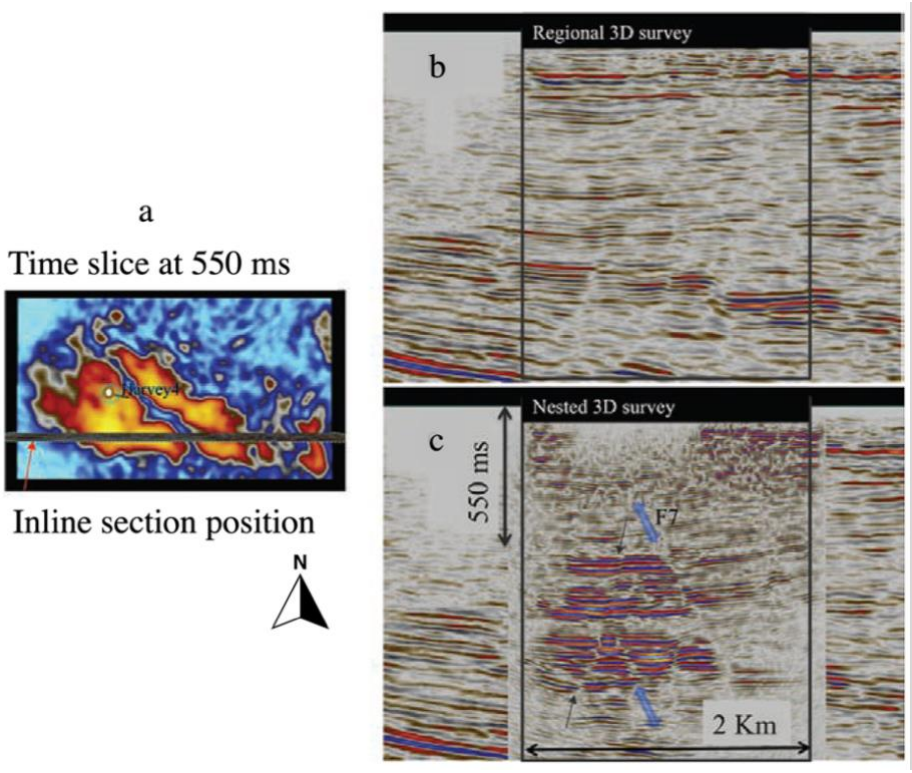

Figure 1: (a) Time slice through similarity section with the location of the in-line section under investigation and Harvey 4 borehole shown as a green circle, (b) regional Harvey 3D and (c) nested 3D PSTM stacked section inserted into the rectangular area. The blue transparent double arrow is used to denote fault images that are clearer in nested 3D volume, such as Fault 7. The black arrow denotes where fault is expressed with much better clarity in the nested 3D. Vertical scale is in time.

A pre-stack time migrated (PSTM) high-resolution volume and the attribute derived from it, such as coherency and acoustic impedance, enabled improved structural and stratigraphic

analysis around the Harvey 4 well. The results shown were of a crucial importance for the containment studies, development of the dynamic model and establishment of the injection intervals.

Both post and pre-stack inversions of these data were utilised to model distribution of paleosols, lenses of high clay content, which are assumed to serve as baffles for CO_2 upward migration. A good correlation was established between very low elastic impedance (EI) values and increased percentage of paleosols and on the other end of the scale, very high impedance values and low porosity sandstones, Figure 2.

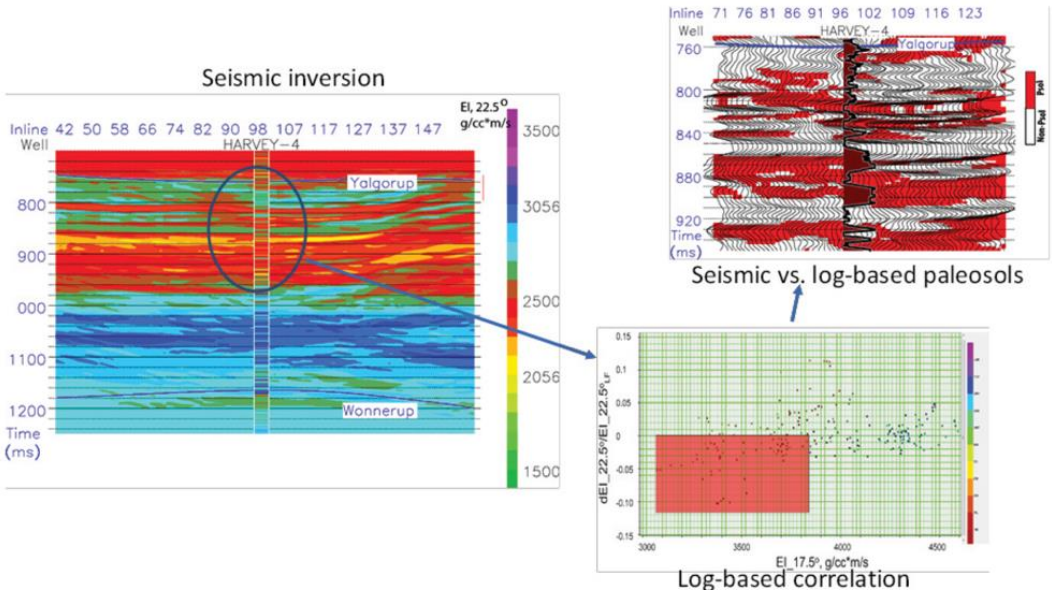

Figure 2: Elastic impedance inversion flow aimed at the paleosol mapping. Impedance section after well tie (left), cross-plot of the elastic impedance and selection of low values that are expected to be characteristic for paleosols (lower right) and mapping low EI values onto the seismic data (upper right) and comparing it to the log-derived paleosol intervals.

Considering all the additional structural and stratigraphic information obtained from the nested 3D seismic, it is evident that such surveys can be very valuable for site characterisation. Moreover, such data can be also used to optimise well position through better fault location prediction. The cost of the nested survey conducted is only a fraction of the drilling cost, but the impact can be significant in terms of borehole relocation, fault correlation, derivation of static model and subsequent dynamic simulations.

Publication II

Ziramov, S., Young, C., Kinkela, J., Turner, G. & Urosevic, M. (2023) Pre-stack depth imaging techniques for the delineation of the Carosue Dam gold deposit, Western Australia. *Geophysical Prospecting*, **00**, 1– 19. https://doi.org/10.1111/1365-2478.13314

In this peer-reviewed paper, we investigate and address various issues in relation to the imaging techniques for high-resolution, high density 3D seismic surveys for mineral exploration. The study focuses on the extraction of maximum value from the seismic dataset recorded for gold exploration by optimisation of acquisition parameters, processing flow, imaging and velocity model building algorithms. High-precision subsurface imaging utilises the full depth imaging workflow, which respects shallow lateral velocity variations in the overburden and fully implements seismic tomography. By using a unique depth imaging workflow, we were able to

delineate shallow gold hosting structures and render an accurate picture of the interior of an excessively complex hard rock area of Yilgarn craton in Western Australia.
As mentioned in the Introduction, hard rock seismic processing faces a unique set of challenges relative to sedimentary environments. They often consist of complex geological settings comprising steeply dipping interfaces and heterogeneities (stratigraphy, faults, fracture and shear zones etc.), low intrinsic signal to noise ratio and complex near surface conditions (strongly contrasting weathered overburden relative to bedrock). These complexities require innovative imaging approaches to accurately reposition the seismic energy back to its true spatial location. In this paper we have demonstrated how the latest generation of seismic imaging algorithms (migration) that have been successful in the oil and gas environment can be adapted to overcome the unique challenges often encountered in mineralised terrains.

The seismic survey was aimed to improve the geological understanding and aid in the discovery of additional gold resources within the Carosue Basin. High-density reflection seismic is particularly effective in resolving complex structures (Stolz et al., 2004; Urosevic et al., 2005, 2012, 2017; Ziramov et al., 2015, 2016), and is becoming more commonly used in exploration for structurally controlled gold mineralisation.

In this study, I have assessed performance of pre-stack Kirchhoff depth migration (KDM) and RTM in a complex hard rock environment. Since the success of depth imaging methods largely depends on the accuracy of estimated velocities, building a depth imaging workflow (Figure 3) that incorporates comprehensive velocity model building, was the main objective of the study.

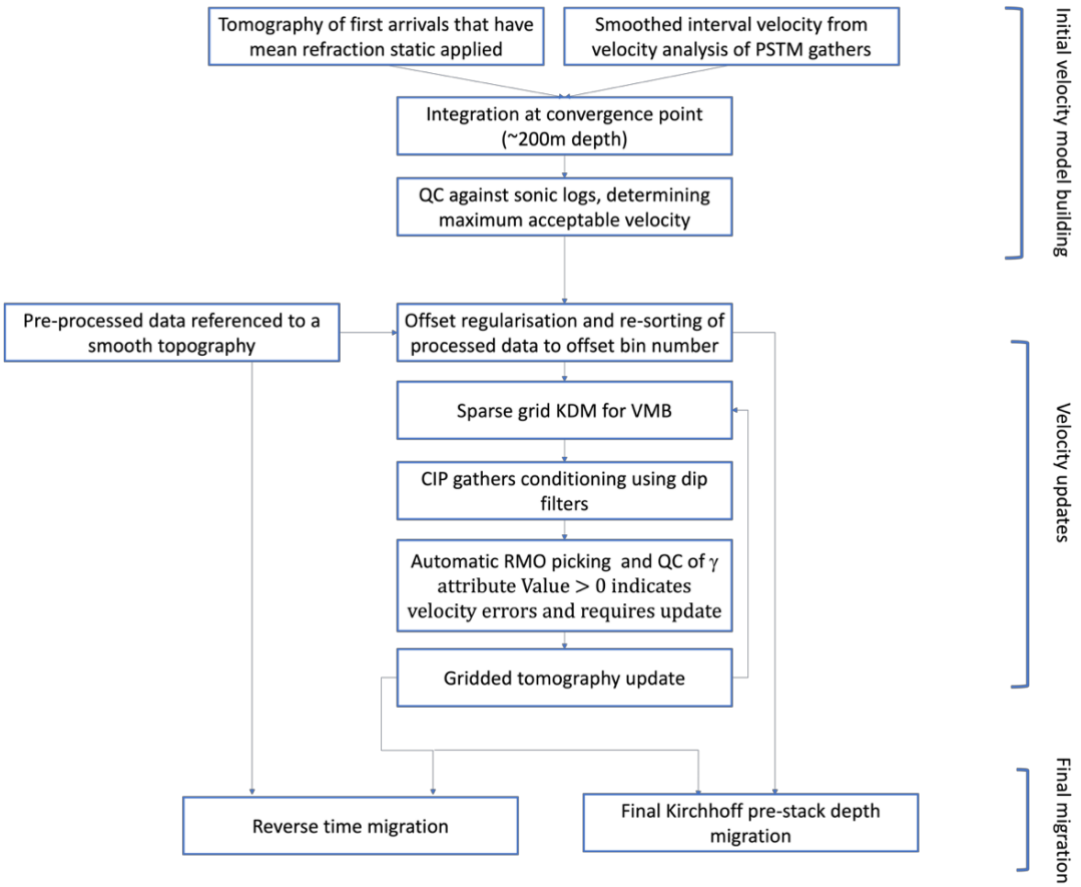

Figure 3: A block diagram of VMB and depth imaging workflow. The initial velocity model obtained from refraction tomography and PSTM velocities is refined using iterative Kirchhoff depth migration and residual moveout (RMO) process followed by reflection tomography.

One of the critical issues the seismic method faces in a hard rock environment is the effect of the low velocity zone associated with weathering and its consequences on imaging quality. In many hard rock seismic projects, the velocity change from overburden to the fresh rock is drastic and happens over such small distances that even depth imaging cannot fully resolve this problem. In this study the near surface component of velocity model was built using the approach also investigated by Singh et al. (2022). The method involves applying refraction statics to first arrival times, which are then used in refraction tomography to compute a velocity model for imaging. The near surface velocity model was then combined with a velocity estimated from pre-stack time migration converted to depth to get an initial velocity model. The process was guided by sonic velocities from wireline measurements. The initial velocity model has been further refined by computing several iterations of reflection tomography from imaged gathers. An illustration of velocities from refraction tomography, initial velocity model, final velocity model and their comparison with sonic logs is demonstrated in Figure 4.

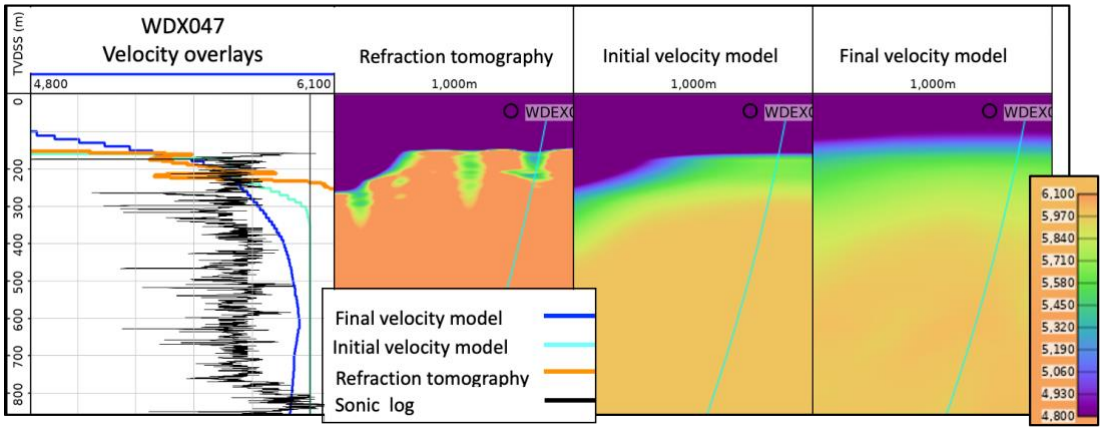

Figure 4: Displays of V_p sonic log, refraction tomography, initial and final velocity model surrounding the borehole location. Highlighted is the zone where all velocities converge.

Pre-stack depth migration algorithms coupled with appropriate velocity model building show significant uplift when compared to the time imaging, especially in the top 1 km of depth, critical to mining exploration. In Figure 5, pre-stack time and depth imaging (RTM) are compared. Comparison of depth slices with wireframes in the Karari mine area show that faults that disrupt an earlier-formed shear responsible for the emplacement of gold mineralisation are accurately imaged using RTM migration, when compared against pre-stack time migration.

.

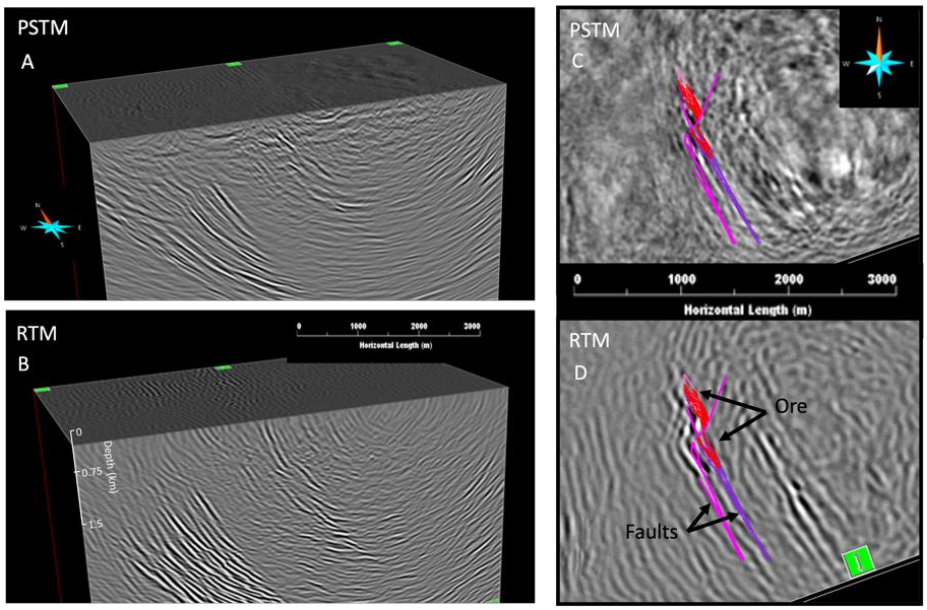

Figure 5: Comparison of time (A) and depth (B) imaging (RTM) at the Karari deposit. Depth slice at 300 m below the surface of PSTM (C) and RTM (D) volume are compared against wireframes modelled from drillhole measurements.

It is becoming clear that depth imaging will play a crucial role in the mineral sector due to its precision and reliability. Specific challenges associated with each new hard rock project mean that some site-specific parameterisation may still be needed to achieve maximum imaging accuracy.

Publication III

Ziramov, S. Bona, A., Tertyshnikov, K.,. Pevzner, R., Urosevic, M., Application of 3D Optical Fibre Reflection Seismic in Challenging Surface Conditions, *First Break*, Volume **40**, Issue 8, 2022, p. 79 – 89, https://doi.org/10.3997/1365-2397.fb2022071.

This publication is a contribution invited by the publisher. It demonstrates never-used-before DAS (distributed acoustic sensing) cable deployment method and world's first published 3D surface seismic survey, using DAS as a continuous receiver line. This method introduces a cheaper alternative to acquiring seismic in harsh conditions, where hazard of equipment damage exists, such as a hypersaline lakes environment.

The introduction of DAS technology into seismic surveying practice in the mineral sector could deliver an order of magnitude saving, while substantially increasing the data density and hence allowing optimum performance of modern seismic imaging algorithms. DAS systems utilise interferometry of backscattered laser light through distributed optical fibre sensors approach to identify fibre strain changes caused impinging seismic or acoustic wave by comparing sequential back-scattered laser pulses (e.g., Hartog, 2018). Because of the high rate of information transfer involved, fibre strain is measured through optical interferometry (Hartog, 2018; Issa et al., 2020).

In this study, I demonstrate the application of DAS sensing technology to 2D and 3D seismic reflection imaging of complex underground structures in a mineral exploration context. An evaluation of DAS technology against current seismic exploration practices is discussed briefly, omitting the long-term ominous efforts conducted in the background that led to the seismic experiments and the results present in this study. The field studies were of the key importance

in evaluating DAS technology and enabled us to develop an efficient methodology based on the new generation of sensors in combination with a specific type of acquisition geometry, combined with portable, efficient sources of seismic energy.

The ultimate evaluation stage involved implementation of 3D reflection seismic survey across the hyper-saline surface of Lake Carey, close to the existing mine site, covering approximately 1.5 km^2. The geometry of the DAS survey and the acquisition strategy is illustrated in Figure 6. Two interrogators by Terra15 were utilised to interrogate 7 km of fibre optic cable each. These interrogators record deformation rate rather than the strain or strain rate as do the other interrogators used in this study.

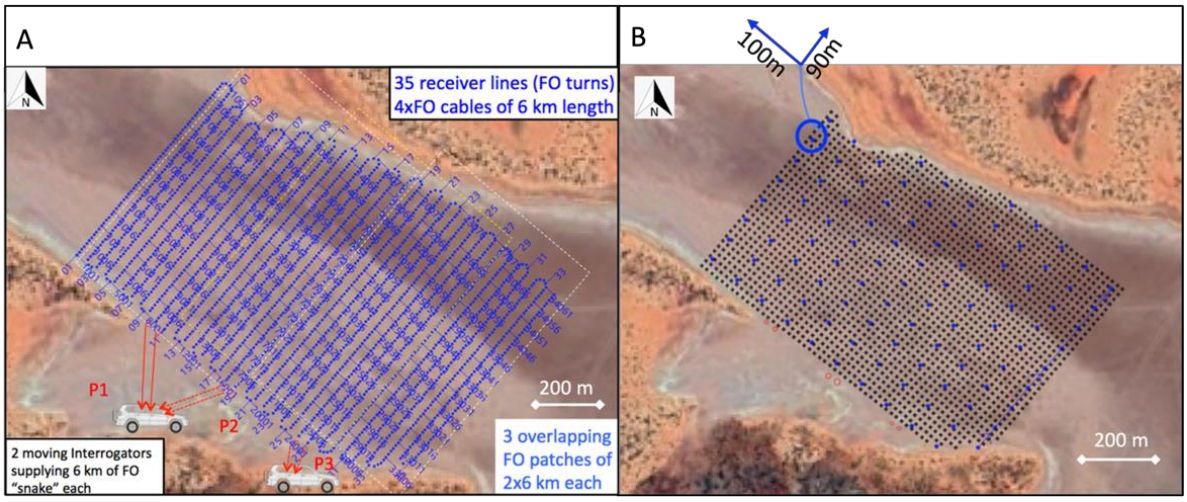

Figure 6: 3D survey layout. (A) Source array and geophone receiver distribution. Betsy gun shots were delivered in a rectangular pattern on a 20x20m spacing. Geophones are arrayed in 90x100m grid using 100 Unite 3-component units and 200 extension cables to minimise use of electronic equipment. (B) Optical cables were distributed in four patches of 6 km length each in a "snake-like" pattern. Two patches at a time are connected to the two active interrogators. As shooting progresses from NW-SE the two, interrogators are shifted one patch down at the time. Lake Carey, WA, 29° 13' 10"S, 122° 26' 46"W, Eye alt 5 km. http://www.earth.google.com

Two Betsy guns were also utilised for shooting along 20x20 m grid pattern (Figure 6B). As the shooting progressed, the two interrogators were shifted by one cable of 7,000 m length. In total three DAS patters were utilised to complete the survey. 103 Sercel Unite channels (with geophone extensions) were positioned in a 90x100 m grid pattern (Figure 6B). Utilisation of such sparse geophone grid enabled both refraction and reflection data analysis, provided support to DAS data processing and eventually allow for a direct comparison between the two data sets. Comparing the stacked sections, it is clear that even sparse geophones produced superior result over DAS, however, after migration DAS data appears to have improved SNR and are comparable to geophone images (Figure 7). This is attributed to higher density of DAS data, an equivalent of 32,000 sensors 0.8 m apart.

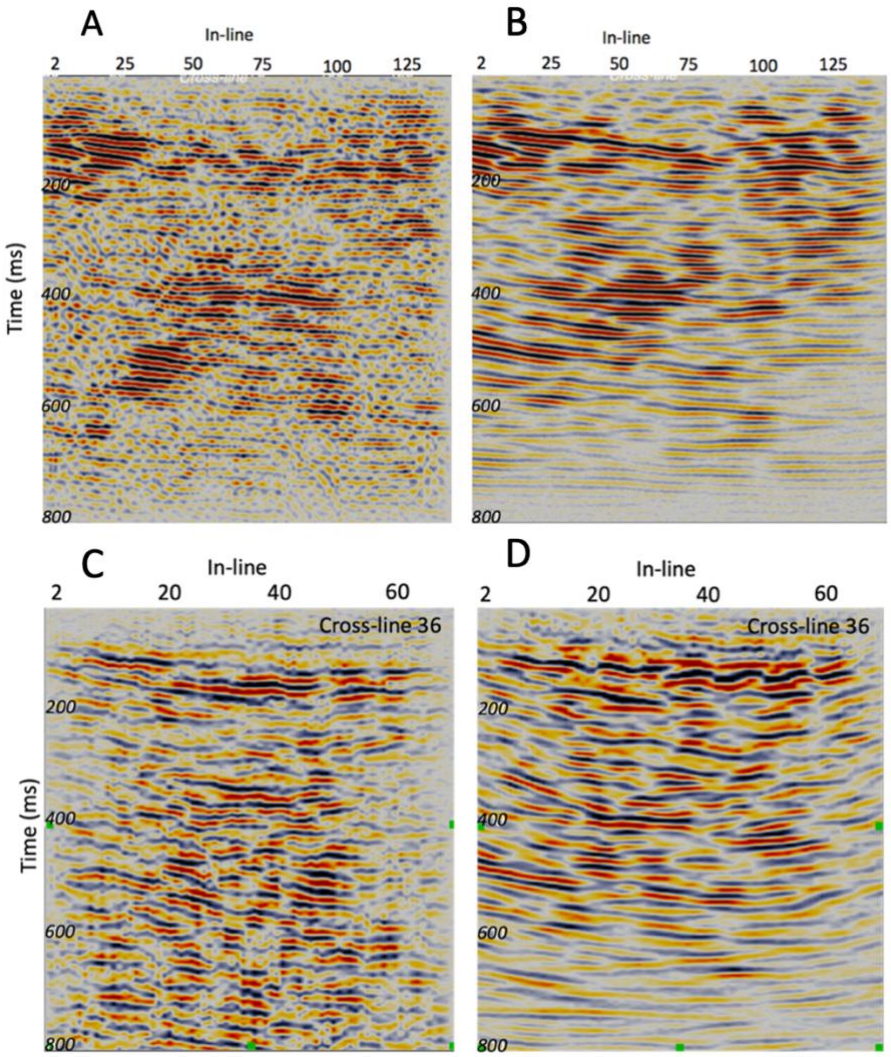

Figure 7: Cross-line section from DAS volume before migration (A), after migration (B). Note significant SNR improvement after migration. Geophone section in the same position, before migration (C), and after migration (D).

Many lessons were learnt in the utilisation of DAS technology for the objectives of seismic reflection prospecting of mineral resources. While the learning continues, it is becoming clear that DAS technology will play a crucial role in the mineral sector due to its efficacy, low cost and exceptional spatial data density that allows for new thinking in data processing and interpretation.

1.7. Conclusions and outlook

1.7.1 Conclusions

In this thesis I have explored and analysed the benefits of high-resolution, high data density surveys. I first analysed a high-resolution 3D "nested" survey introduced specifically to delineate subtle geological features of interest for CO_2 sequestration objectives. In contrast to the regional 3D, the nested 3D survey has enabled me to produce sharper images of key structures in the near surface. Indeed, a detailed delineation of the subsurface geology, particularly subtle structural features, can only be achieved with a high-resolution survey.

Seismic method has been routinely used in oil and gas exploration, so it is not surprising that the most sophisticated imaging methods have been developed to target exploration of these commodities. My quest for an optimum imaging approach of shallow structures using high resolution, spatially dense data sets embarked me into the journey through the seismic exploration of the hard rocks. I've realised that a generalised depth imaging workflows developed in oil and gas exploration cannot be blindly applied in any geological environment, rather it may require a significant adaptation, depending on the specific case analysed. During the final stages of my dissertation, it came to my attention recently published work by Singh et al. (2022), whose research has also explored approaches to obtaining a near surface velocity model. It is encouraging to see similar concepts demonstrated across a range of different surface and underground conditions.

I investigated high-precision imaging technique, utilised the full depth imaging workflow, that respects shallow lateral velocity variations in overburden and fully implements both refraction and reflection tomography. With relatively few assumptions about the velocity model, the workflow was able to render high-precision images of the interior of the Earth. This approach was subsequently utilised in much more complex geological setting of hard rocks with a great success. Hence the depth imaging workflow I adopted, appears to be of a wider importance as it could be implemented in both hard and soft rock environment, yielding accurate images and making geological interpretation much easier and more trustworthy.

Computation time of depth imaging algorithms varies greatly. This is an important factor to consider when choosing the imaging algorithm for a specific purpose. Kirchhoff's integral has always been preferred method for velocity estimates, due to its flexibility in producing subsets of output volumes. In my experience, it is beneficial to have more than one technique utilised. One then can critically analyse their performance against available geological facts. In the less controlled zone that is zone with no ground truth, having both images enable us to propose a geological model with a greater certainty.

Data analysis and imaging tests I conducted on numerous data sets suggest that in a high-resolution land survey, we should not aim to determine subsurface velocity using purely migration process. In near surface areas where data have low signal-to-noise ratio, we should employ refraction tomographic inversion or if data allows it, FWI. Where data are more challenging, the results can seem elusive. It is essential to validate the imaging against all available borehole data and it is also important to analyse the consistency of different migration algorithms in both situations when geological information is abundant and when it is not.

Finally, I presented the world first published 3D reflection survey using DAS technology. A cost-effective alternative to conventional seismic, in harsh surface conditions such as sault

lakes. This was preceded by several 2D experimental DAS surveys that utilised different cable types, mode of deployment, cable geometry and interrogator type. This study sets a foundation for the future application of cost-efficient DAS seismic technology for exploration of mineral resources. While the learning continues, it is becoming clear that DAS technology will play a crucial role in the mineral sector due to its efficacy, low cost and exceptional spatial data density that allows for new thinking in data processing and interpretation.

1.7.2 Outlook

I've demonstrated a cost-effective, high-density 3D survey, nested around a borehole with existing wireline measurements. The wireline measurements were used to accurately image reflectors at depth and to map paleosols into a 3D rock probability volume. This was possible due to a uniquely low EI of paleosols in comparison to surrounding rock types. In situations where acoustic or elastic impedance is not unique, rock probability extraction is not possible. It is recommended that a feasibility study is conducted before committing to a quantitative interpretation of a seismic dataset.

The "nested" method cannot be routinely applied to every case study. The limitation of this approach is the geology of the area in combination with a 3D seismic survey size. If geology consists of steeply dipping reflectors, such is often the case in hard rocks, we need large enough seismic survey to both record reflections and migrate them into reflectors of appropriate dip. This can significantly increase the survey cost.

After a review of Carosue Dam results, it is becoming clear that depth imaging will play a crucial role in the mineral sector due to its precision and reliability. However, there are specific challenges associated with each new hard rock project, such as high noise level, sub-optimal design parameters, geology of fresh rock, complexity of regolith. Depth imaging workflow that I demonstrated will often need some site-specific parameterisation to achieve maximum imaging accuracy.

All imaging techniques continually improve as they compete in imaging accuracy of complex geological targets. Different techniques and approaches always have some common elements, so one particular technique may never dominate. Despite the success of RTM in structural imaging of Carosue Dam, we have not reached the point where one depth imaging technique is superior in every way. Depending on the survey design, and geological environment either ray-based or wave equation-based algorithms, or both could be useful and be selected to image underground.

The seismic method's ability to provide high resolution information at depths, has caught the mining industry's attention in last couple of decades and long-held view that seismic is too expensive for mining applications is quickly changing. As technology advances in the area of acquisition hardware and computing facilities, the overall price of seismic exploration projects is continually decreasing.

My study of optic fibre cable application in mineral exploration shows that the new technology, smarter survey geometries and specialised small sized seismic crews can accomplish suitable and cost-effective seismic surveys.

The application DAS technology in down hole seismic is rapidly attracting attention of the industry; however, the prospect in surface seismic is not as clear. The directivity issues and

high noise level associated with optic fibres are a challenge hard to overcome. I recognise and sincerely hope that further progress in DAS reflection seismology and processing is likely to be made in the years ahead. I expect that the extraordinary data density provided by optical cables will further advance the imaging technology and overcome present limitations.

The research covered in this thesis is of importance to the future of seismic surveying not only within investigated case studies, but the exploration worldwide. Encouraging results from various methods prove that the surface seismic reflection technique is a viable exploration tool even in challenging conditions of mineralised terrains. Depth imaging in combination with appropriate velocity model building technique can improve ore identification, fault delineation, which enables determination of an improved geological model that will guide drilling for future mine expansion.

1.8. References

Adamczyk, A., Malinowski, M., and Melehmir, A., 2014, High-resolution near-surface velocity model building using full-waveform inversion – a case study from southwest Sweden: *Geophys. J. Int.,* **197**, 1693–1704.

Adamczyk, A., Malinowski, M., and Górszczyk, A., 2015, Full-waveform inversion of conventional Vibroseis data recorded along a regional profile from southeast Poland: *Geophys. J. Int.,* **203**, 351– 365

Alkhalifah, T., 2000, An acoustic wave equation for anisotropic media: *Geophysics*, **65**, 1239–1250.

Ayarza, P., C. Juhlin, D. Brown, M. Beckholmen, G. Kimbell, R. Pechnig, L. Pevzner, R. Pevzner, C. Ayala, M. Bliznetsov, and A. Glushkov, 2000, Integrated geological and geophysical studies in the SG4 borehole area, Tagil Volcanic Arc, Middle Urals: Location of seismic reflectors and source of the reflectivity: Journal of Geophysical Research, Solid Earth, **105**, 21333–21352, doi: 10.1029/2000JB900137.

Bachu, S., Gunter, W.D. and Perkins, E.H., 1996, Carbon dioxide disposal, in Hitchon, B., Eds, Aquifer Disposal Of Carbon Dioxide: Geoscience Publishing, Alberta, Canada.

Baysal, E., D. D. Kosloff, and J. W. C. Sherwood, 1983, Reverse time migra-tion: Geophysics, **48**, 1514–1524., 1984, A two-way nonreflecting wave equation: *Geophysics*, **49**, 132–141.

Berkhout, A. J., 1979, Steep dip finite-difference migration: *Geophysics*, **27**, 196–213., 2008, Changing the mindset in seismic data acquisition: *The Leading Edge*, **27**, 924–938.

Beylkin, G., 1985, Imaging of discontinuities in the inverse scattering prob-lem by inversion of a generalized Radon transform: *Journal of Mathematical Physics,* **26**, 99–108.

Bierbaum S. and Greenhalgh S., 1998, A high-frequency downhole sparker sound source for crosswell seismic surveying: *Exploration Geophysics* **29** (3/4), 280-283.

Bleistein, N., 1987, On the imaging of reflectors in the earth: *Geophysics*, **52**, 931–942.

Bohlen, T., Mueller, C., Milkereit, B., 2003, 5. Elastic Seismic-Wave Scattering from Massive Sulfide Orebodies: On the Role of Composition and Shape. 10.1190/1.9781560802396.ch5.

Brodic, B., Malehmir, A., Pacheco, N., Juhlin, C., Carvalho, J., Dynesius, L., van den Berg, J., de Kunder, R., Donoso, G., Sjölund, T., and Araujo, V., 2021, Innovative seismic imaging of volcanogenic massive sulphide deposits, Neves-Corvo, Portugal – Part 1: In-mine array: *Geophysics*, **86**, 165–179.

Broüning, L., Buske, S., Malehmir, A., Backström, E., Schön, M., and Marsden, P., 2020, Seismic depth imaging of iron-oxide deposits and their host rocks in the Ludvika mining area of central Sweden: *Geophysical Prospecting*, **68**, 24–43.

Chen G., Liang G., Xu D., Zeng Q., Fu S., Wei X., He Z. and Fu G., 2004, Application of a shallow seismic reflection method to the exploration of a gold deposit: *Journal of Geophysics and Engineering 1* (1), **12-16.**

Chen, J., and H. Liu, 2006, Two kinds of separable approximations for the one-way wave operator: *Geophysics*, **71**, no. 1, T1–T5.

Claerbout, J. F. 1971, "Toward a unified theory of reflection mapping". In: *Geophysics* vol. **36**, no. 3, pp. 467–481.

Cordery, S., 2020, An effective data processing workflow for broadband single-sensor single-source land seismic data: The Leading Edge, **39**, 401–410, doi: 10.1190/tle39060401.1.

Dean, T., Tulett, J., Barnwell, R., 2018, Nodal land seismic acquisition: The next generation**:** *First Break*, **36**, 47-52.

De Wet, J. A. J., and D. A. Hall, 1994, Interpretation of the Oryx 3-D seismic survey, in C. R. Anhaeusser, ed., Proceedings XV CMMI Congress: *SAIMM Symposium Series*, S14, **3**, 259–270.

Duweke W., Trickett J., Tootal K. and Slabbert M., 2002, Three-dimensional reflection seismics as a tool to optimise mine design, planning and development in the Bushveld Igneous Complex: *64th Conference and Exhibition, EAGE,* Mining and Best of SAGA, Extended Abstracts, 1-6.

Egan, M.S., Seissiger, J., Salama, A., El-Kaseeh, G., 2012, The influence of spatial sampling on resolution: *CSEG Recorder*, March 2010.

Etgen, J., Gray, S. and Zhang, Y., 2009, An overview of depth imaging in exploration geophysics: *Geophysics*, **74**, WCA5-WCA17.

Eaton D. W., Milkereit B. and Adam E., 1997, 3-D seismic exploration: *Proceedings of Exploration*, 65-78.

Eaton, D. W., Milkereit, B., & Salisbury, M. H., 2003, Hardrock seismic exploration: Society of Exploration Geophysicists.

Fletcher, R., X. Du, and P. J. Fowler, 2008, A new pseudo-acoustic wave equation for TI media: *78th Annual International Meeting*, SEG, Expand-ed Abstracts, 2082–2086.

Furniss, A., 2000, An Integrated Prestack Depth Migration Work Flow using Model Based Velocity Estimation and Refinement, Geohorizon.

French, W. S., 1975, Computer migration of oblique seismic reflection profiles. Geophysics, **40** (6), 961-980.

Friedel M. J., Jackson M. J., Scott D. F., Williams T. J. and Olson M. S., 1995, 3-D tomographic imaging of anomalous conditions in a deep silver mine: *Journal of Applied Geophysics* **34** (1), 1-21.

Friedel M. J., Scott D. F., Jackson M. J., Williams T. J. and Killen S. M., 1996, 3-D tomographic imaging of anomalous stress conditions in a deep US gold mine*: Journal of Applied Geophysics* **36** (1), 1-17.

Frappa M. and Molinier C., 1993. Shallow seismic reflection in a mine gallery*: Engineering Geology* **33** (3), 201-208.

Gazdag, J., 1978, Wave equation migration with the phase-shift method: Geophysics, **43**, 1342–1351.

Gendzwill D., 1990. High-resolution seismic reflections in an underground mine: 60th Annual International Meeting, SEG, 397-398.

Gil, A., Malehmir, A., Ayarza, P., Buske, S., Carbonell, R., Orlowsky, D., Carriedo, J., & Hagerud, A., 2022, 3D reflection seismic imaging of the Zinkgruvan mineral-bearing structures in the south-eastern Bergslagen mineral district (Sweden): Geophysical Prospecting, **70** (8), 1544-1561.

Gladwin M. T., 1982. Ultrasonic stress monitoring in underground mining*: International Journal of Rock Mechanics and Mining Sciences &Geomechanics Abstracts* **19** (5), 221-228.

Gupta R., 1972. Seismic determination of geological discontinuities ahead of rapid excavation: Semi Annual Report No. 6311, *Bendix Research Laboratory* **40**, 90 p.

Hale, D., 1991a, Stable explicit depth extrapolation of seismic wavefields: Geophysics, **56**, 1770–1777.

Hale, D., 1991b, 3-D depth migration by McClellen transformations: Geophysics, **56**, 1778–1785.

Hitchon, B., 1996, Sedimentary basins as sequesters of carbon dioxide, *in* Hitchon, B., Ed., Aquifer disposal of carbon dioxide: Geochemical Services Ltd., 1-10.

Hill, N. R., 2001, Prestack Gaussian-beam depth migration. Geophysics, **66** (5), 1240-1250.

Hloušek F., Hellwig O. and Buske S. 2015, Improved structural characterization of the Earth's crust at the German Continental Deep Drilling Site using advanced seismic imaging techniques. Journal of Geophysical Research: *Solid Earth* **120**, 6943–6959.

Holberg, O., 1988, Toward optimum one-way wave propagation: *Geophysical Prospecting,* **36**, 99–114.

Huang, L.-J., and R.-S. Wu, 1996, Prestack depth migration with acoustic screen propagators: *66th Annual International Meeting*, SEG, Expanded Abstracts, 415–418.

Hartog, A., 2018, An introduction to distributed optical fibre sensors, series in fiber optic sensors. FL, USA: *CRC Press Taylor & Francis Group*. ISBN 9781138082694.

Ivanova, A., and Luth, S., 2015, Geophysical monitoring at the Ketzin pilot site for CO2 storage: International Journal of Greenhouse Gas Control, **40**, 314-334.

Issa, N., Roelens, M. A. F., and Frisken, S. J., 2020, Distributed optical sensing systems and methods, *US Pattent App*. 16/633,706.

Juhlin C., Lindgren J. and Collini B., 1991, Interpretation of seismic reflection and borehole data from Precambrian rocks in the Dala Sandstone area, central Sweden: *First Break* **9** (1), 24-36.

Kallweit, R., and Wood, L., 1982, The limits of resolution of acoustic imaging in two and three dimensions: Geophysical Prospecting, **30** (1), 232-247.

Le Rousseau, J. H., and M. V. de Hoop, 2001, Modeling and imaging with the scalar generalized-screen algorithms in isotropic media: *Geophysics*, **66**, 1551–1568.

Lee, M., and S. Suh, 1985, Optimization of one-way equation: *Geophysics*, **50**, 1634–1637.

Loewenthal, D., and I. R. Mufti, 1983, Reverse-time migration in spatial frequency domain: *Geophysics*, **48**, 627–635.

Ma, Z., 1982, Steep dip finite difference migration: *Oil Geophysical Prospecting*, **1**, 6–15 in Chinese.

Margrave, G. F., and Ferguson, R. J., 1999, Wavefield extrapolation by nonstationary phase shift: Geophysics, **64**, 1077-1088.

Malehmir, A., Urosevic, M., Bellefleur, G., Juhlin, C. and Milkereit, B., 2012, Seismic methods in mineral exploration and mine planning. Geophysics77, WC1–WC2.

Malehmir, A., E. Lundberg, P. Dahlin, C. Juhlin, H. Sjöström, and K. Högdahl, 2013, Reflection seismic imaging and petrophysical investigations of the Dannemora iron ore bodies, central Sweden: Proceedings of the 12th Biennial SGA Meeting, 134–139.

Manzi, M., Gibson, M., Hein, K., King, N., Durrheim, R., 2012, Application of 3D seismic techniques to evaluate ore resources in the West Wits Line goldfield and portions of the West Rand goldfield, South Africa, Geophysics, **77**, 163-. 10.1190/geo2012-0133.1.

Malinowski, 2022, Seismic Imaging of Mineral Exploration Targets: Evaluation of Ray- vs. Wave-Equation-Based Pre-Stack Depth Migrations for Crooked 2D Profiles. Minerals 2023, **13** (2), 264.

McDonald, J.A., and Lawton, D.C., 1990, High-resolution seismic imaging of salt domes using high-density geophones: The Leading Edge, **9** (11), 12-18.

Milkereit, B., E. Adam, A. Barnes, C. Beaudry, R. Pineault, and A. Cinq- Mars, 1992, An application of reflection seismology to mineral exploration in the Matagami area, Abitibi Belt, Quebec: Current Research, Part C, 13–18.

Maxwell S. C. and Young R. P., 1992, Sequential velocity imaging and microseismic monitoring of mining-induced stress change: *Pure and Applied Geophysics* **139** (3-4), 421-447.

McMechan, G. A., 1983, Migration by extrapolation of time-dependent boundary values: *Geophysical Prospecting*, **31**, 413–420.

Mokyr, J., and Strotz R., H., 1998, The second industrial revolution, 1870-1914., *Storia dell'economia Mondiale* 21945, no. 1.

Perron G., Eaton D. W., Elliot B. and Schmitt D., 2003. 13. Application of Downhole Seismic Imaging to Map Near-Vertical Structures: *Normetal* (Abitibi Greenstone Belt), Quebec.

Pertuz, T., Melehmir, A., Bos, J., Brodic, B., Ding., Y., Kunder, R., and Marsden, P., 2022, Broadband seismic source data acquisition and processing to delineate iron oxide deposits in the Blötberget mine-central Sweden: *Geophysical Prospecting,* **70**, 79-94.

Ristow, D., and T. Ruhl, 1994, Fourier finite-difference migration: *Geophysics*, **59**, 1882–1893., 1997, 3-D implicit finite-difference migration by multiway splitting: Geophysics, **62**, 554–567.

Ruskey F., 1981. High resolution seismic methods for hard rock mining, Premining investigations for hardrock mines: Proceedings: Bureau of Mines Technology Transfer Seminar, 4–28.

Schetselaar E, Bellefleur G, Hunt P., 2019, Elucidating the Effects of Hydrothermal Alteration on Seismic Reflectivity in the Footwall of the Lalor Volcanogenic Massive Sulfide Deposit, Snow Lake, Manitoba, Canada: Minerals, **9**, (6):384. https://doi.org/10.3390/min9060384.

Schmidt G., 1959, Results of Underground-Seismic Reflection Investigations in the Siderite District of the Siegerland: *Geophysical Prospecting*, **7**, (3), 287-290.

Sheriff, S.E., 2002, 3D seismic exploration for mineral deposits: The Leading Edge, **21** (11), 1134-1140.

Singh, B., Malinowski, M., Hloušek, F., Koivisto, E., Heinonen, S., Hellwig, O. et al., 2019., 3D seismic imaging in the Kylylahti mine area, Eastern Finland: comparison of time versus depth approach. Minerals, **9** (5), 305. https://doi.org/10.3390/min9050305.

Singh, B., Malinowski, M., Górszczyk, A., Melehmir, A., Buske, S., Sito, Ł., and Marsden, P., 2022, 3D high-resolution seismic imaging of the iron oxide deposits in Ludvika (Sweden) using full-waveform inversion and reverse time migration: *Solid Earth*, **13**, 1065–1085.

Schneider, W. A., 1978, Integral formulation for migration in two and three dimensions. Geophysics, **43** (1), 49-76.

Soubaras, R., 1996, Explicit 3-D migration using equiripple polynomial expansion and Laplacian synthesis: *Geophysics*, **61**, 1386–1393.

Stoffa, P. L., J. T. Fokkema, R. M. de Luna Freire, and W. P. Kessinger, 1990, Split-step Fourier migration: *Geophysics*, **55**, 410–421.

Stolz, E., Urosevic, M., and Connors, K., 2004, Reflection seismic surveys at St. Ives gold mine, WA: *Preview*, **111**, 79.

Sun, Y., F. Qin, S. Checkles, and J. P. Leveille, 2000, 3-D prestack Kirchhoff beam migration for depth imaging: *Geophysics*, **65**, 1592–1603.

Tang, Y., Zhang, Y., Yan, H., and Huang, X., 2021, A review of recent advances in reverse-time migration: Progress in Geophysics, **36**, 159-213.

Tsvankin, I., 2001, Seismic signatures and analysis of reflection data in an- isotropic media: *Elsevier Science Publ*. Co., Inc.

Urosevic M., 2013. What can seismic in hard rocks do for you?: ASEG-PESA 2013, *23rd International Geophysical Conference and Exhibition*, CSIRO, 1-4.

Urosevic, M, Bona, A., Ziramov, S., Pevzner, R., Kepic, A., Egorov, A., Kinkela, J., Pridmore, D. Dwyer, J., 2017, Seismic for mineral resources – a mainstream method of the future: *Proceedings of Exploration* **17**.

Urosevic, M., Bhat, G., and Grochau M. H., 2012, Targeting nickel sulfide deposits from 3D seismic reflection data at Kambalda, Australia: *Geophysics*, **77**,123-132.

Urosevic, M., Stolz, E., and S. Massey, 2005, Seismic exploration of complex mineral deposits - Yilgarn Craton, Western Australia: *67th Conf. of European Assoc. of Explor. Geophys.*, Madrid, Spain, Z-99.

Urosevic, M., Kepic, A., Stolz E., & C. Juhlin, 2007a, Seismic exploration of mineral deposits in Yilgarn Craton, Western Australia: *Exploration' 07*, Toronto, Canada.

Urosevic and Evans, 2007b, Feasibility of seismic methods for imaging gold deposits in Western Australia, M363 project, Report No. 267, Minerals and Energy Research Institute of Western Australia, Report No. 267, 1-99.

Urosevic M. and Evans B., 1998. Seismic methods for the detection of kimberlite pipes: *Exploration Geophysics* **29** (3/4), 632-635.

Urosevic M. and Evans B. J., 2000, Surface and borehole seismic methods to delineate kimberlite pipes in Australia: *The Leading Edg*e **19** (7), 756-758.

Urosevic, M., and Kepic, A., 2012, Nested 3D seismic surveys for mineral exploration: The Leading Edge, **31** (11), 1326-1332.

Urosevic, M., and Pevzner, R., 2015, Geologically Storing Carbon: Learning from the Otway Project Experience, Editor Peter Cook, CSIRO, Publisher.

Urosevic, M., Bona, A., Ziramov, S., Martin, R., Dwyer, J., Felding, D., and Foley, A., 2019, Seismic prospecting of mineral reserves with DAS*: 16th SAGA Biennial Conference and Exhibition*, Durban, South Africa.

Waters, K.H., and Kendall, C.H., 2016, Seismic exploration: A century of innovation: The Leading Edge, **35** (12), 1052-1059.

White, D., and M. Malinowski, 2012, Interpretation of 2D seismic profiles in complex geological terrains: Examples from the Flin Flon mining camp, Canada: Geophysics, **77**, no. 5, WC37–WC46.

Whitmore, N. D., 1983, Iterative depth migration by backward time propagation*: 53rd Annual International Meeting,* SEG, Expanded Abstracts, 382– 385., 1995, An imaging hierarchy for common angle plane-wave seismograms: *Ph.D. dissertation*, The University of Tulsa.

Willis, M. E., 2022, Distributed acoustic sensing for seismic measurements: What geophysicists and engineers need to know, SEG DISC Series.

Yilmaz, Ö., 2001, Kirchhoff migration for imaging 3D seismic data. Society of Exploration Geophysicists.

Yilmaz, Ö., 2019, Seismic imaging: A modern approach. Society of Exploration Geophysicists.

Ziramov, S., Dzunic, A. and Urosevic, M., 2015, Kevitsa Ni-Cu-PGE deposit, North Finland? A seismic case study: *ASEG Extended Abstracts* 2015.1, 1-4.

Ziramov, S., Kinkela, J., and Urosevic, M., 2016, Neves-Corvo 3D- A High-resolution Seismic Survey at a Mine Camp Scale: Near Surface Geoscience 2016, *22nd European Meeting of Environmental and Engineering Geophysics*, Barcelona, Spain, 4–8 September 2016, cp-495-00188.

Zhang, G., S. Zhang, Y. Wang, and C. Liu, 1988, A new algorithm for finite-difference migration of steep dips: *Geophysics*, **53**, 167–175.

Zhang, Y., and McMechan, G. A., 2006, Ray-based seismic migration in the presence of velocity model errors and irregular acquisition geometries: Geophysics, **71**, S213-S226.

Zhang, H., and Y. Zhang, 2008, Reverse time migration in 3D heterogeneous TTI media: *78th Annual International Meeting*, SEG, Expanded Abstracts, 2196–2200.

Zhang, Y., C. Notfors, and Y. Xie, 2003, Stable *x-k* wavefield extrapolation in *v x,y,z* medium: *73rd Annual International Meeting*, SEG, Expanded Abstracts, 1083–1086.

Zhang, Y., and McMechan, G. A., 2017, Reverse time migration: Principles and applications: Geophysics, **82**, SM3-SM18

Zhou, H., G. Zhang, and R. Bloor, 2006, An anisotropic acoustic wave equa-tion for modeling and migration in 2D TTI media: *76th Annual International Meeting*, SEG, Expanded Abstracts, 194–198.

2. *Published papers*

2.1. CO_2 storage site characterisation using combined regional and detailed seismic data: Harvey, Western Australia

Available online at www.sciencedirect.com

ScienceDirect

Energy Procedia 114 (2017) 2896 – 2905

Energy Procedia

13th International Conference on Greenhouse Gas Control Technologies, GHGT-13, 14-18 November 2016, Lausanne, Switzerland

CO_2 storage site characterisation using combined regional and detailed seismic data: Harvey, Western Australia

Ziramov, S., Urosevic, M., Glubokovskikh, S., Pevzner, R., Tertyshnikov, K., Kepic, A., Gurevich, B.

Curtin University and National Geosequestration Laboratory, 26 Dick Perry Ave, Kensington WA 6151, Australia

Abstract

Some 115 km^2 of regional 3D seismic data were acquired in the first quarter of 2014 near Harvey, Western Australia, for the needs of the South West CO2 Hub project. The survey proved to be of great importance for a regional characterisation of the reservoir, identification of the large structures and key geological interfaces. However, small to medium size structures of interest for the development of the static and dynamic models were poorly imaged in this survey as the recording geometry was adjusted for the greater depths, which was between 2 km and 3 km. To improve the imaging of the shallow structures, a high-resolution (nested) 3D survey centered at Harvey 4 well was undertaken in 2015 (Urosevic et al., 2015). This survey utilised a single geophone and single, 24 s long, broadband (6–150 Hz) sweep combined with high data density to improve signal to noise ratio that was initially lowered by not employing high-power sources and geophone arrays. The results of this high-resolution 3D survey demonstrate that high-density surveys are important even at the characterisation stage and are crucial for development of a detailed static model. For that purpose, both post and pre-stack inversions of these data were utilised to model distribution of paleosols, lenses of high clay content, which are assumed to serve as baffles for CO_2 upward migration. A good correlation was established between very low impedance values and increased percentage of paleosols and on the other end of the scale very high impedance values and low porosity sandstones. A pre-stack migrated high-resolution cube and the attribute derived from it, such as coherency and impedance, enabled improved structural and stratigraphic analysis around Harvey 4 well. The results shown were of a crucial importance for the containment studies, development of the dynamic model and establishment of the injection intervals.

Peer-review under responsibility of the organizing committee of GHGT-13.

Keywords: Geological storage; geosequestration; leakage; carbon dioxide; high-resolution seismic; fault;

Peer-review under responsibility of the organizing committee of GHGT-13.
doi:10.1016/j.egypro.2017.03.1417

1. Introduction

In 2013, a first-order assessment of the CO_2 containment for the South West Hub (SWH) suggested possible migration pathways across faults with potential for improving reservoir connectivity but also bypassing the primary and secondary seals (Langhi et al., 2013). The assessment was based on a geological model built upon sparse 2D seismic data with locally high uncertainties specifically regarding the structural architecture. The next stage of the site characterisation involved integration of the regional 3D seismic dataset acquired in 2014 with the available Harvey-2 and Harvey-4 wells data. This vastly improved the initial assessment of the CO_2 containment. Regional 3D seismic shed new light onto the structural architecture of the SWH site and provided an initial assessment of the potential for lateral and vertical circulation of CO_2 through the Wonnerup and Yalgorup Members (Pevzner et al., 2015). The relationship between the modelled faults and the present-day stress field is investigated to analyse the stress field changes on fault kinematic behaviour and to define which critically stressed fault segments are most likely to be forced into failure with pore-pressure build-up. Areas of fault reactivation are associated with an increase in structural permeability and therefore with the potential for the fault flow (Morris et al., 1999, Mildren et al., 2005, Bretan et al., 2011).

The regional Harvey 3D seismic survey provided good information of the large-scale subsurface structures and main stratigraphic units. The survey is officially known as DMPWA 2013 Harvey-Waroona 3D seismic survey. For simplicity, in this paper we refer to it as the regional Harvey 3D seismic survey or simply Harvey 3DR. This survey, as it is typical for most of regional land 3D surveys, suffers from low data density, which limits the imaging. Hence, the spatial distribution and orientation of shallow fractures and faults remained unresolved. These geological features were targeted by an additional high-resolution 3D survey, acquired in December 2014. It was hoped that this nested high-resolution 3D survey, would produce a crisp image of the structures surrounding the Harvey-4 well, define fault tips and the termination points in the shallow and provide sufficiently high data quality that could be utilised for quantitative interpretation.

The primary objective of the nested 3D survey at the Harvey-4 well was to obtain a better image of the shallow fault zones and to assess the risk for the CO2 storage complex. The opportunity to use the latest state-of-the-art seismic data acquisition equipment enabled us to design a high-density, high-resolution 3D survey. The application of powerful 3D processing technologies was expected to produce:

- A high-definition seismic image of the shallow subsurface geology around Harvey-4 well.
- Detailed characterisation of the near-surface structures around Harvey-4 well.
- Information on the location of the new shallow wells through the identification of additional, smaller scale faults associated to the larger faults observed in the regional 3D survey. Possible presence of a more complex fault system was suggested by (Lenghi et al., 2012, 2013).
- Validation of the “infill approach” where conventional and high-resolution seismic methods are combined to produce high-quality images for all depths. The high data density utilised in the nested 3D survey provides geological information of the shallow structures that are not recorded with sparse regional 3D seismic survey geometry. This approach is rarely utilised in the seismic exploration practice. In the case of SWH investigations at Harvey, the “high-resolution infill approach” is of a particular interest due to difficulties associated with obtaining the permission for seismic survey execution.
- Validation of the effectiveness of high-resolution data acquisition and processing techniques.
- Investigation into the potential use of converted shear waves for an improved fault characterisation workflow.

The integration of the processed seismic datasets and well data, allows us to interpret the data in terms of subsurface distribution of petrophysical properties. This information can be used to constrain static and dynamic models, which form a core value for feasibility studies of CO_2 sequestration at the SWH area.

2. Regional and nested 3D seismic designs

A Harvey 3DR seismic reflection survey was acquired by the Department of Mines and Petroleum, Western Australia in February−April 2014 (Figure 1a). The seismic survey was carried out by Geokinetics (Australasia) Pty. Ltd. in the Shires of Harvey and Wroona, 140 km South from Perth. It covered 114.81 km^2 of land in total (Pevzner et al., 2015).

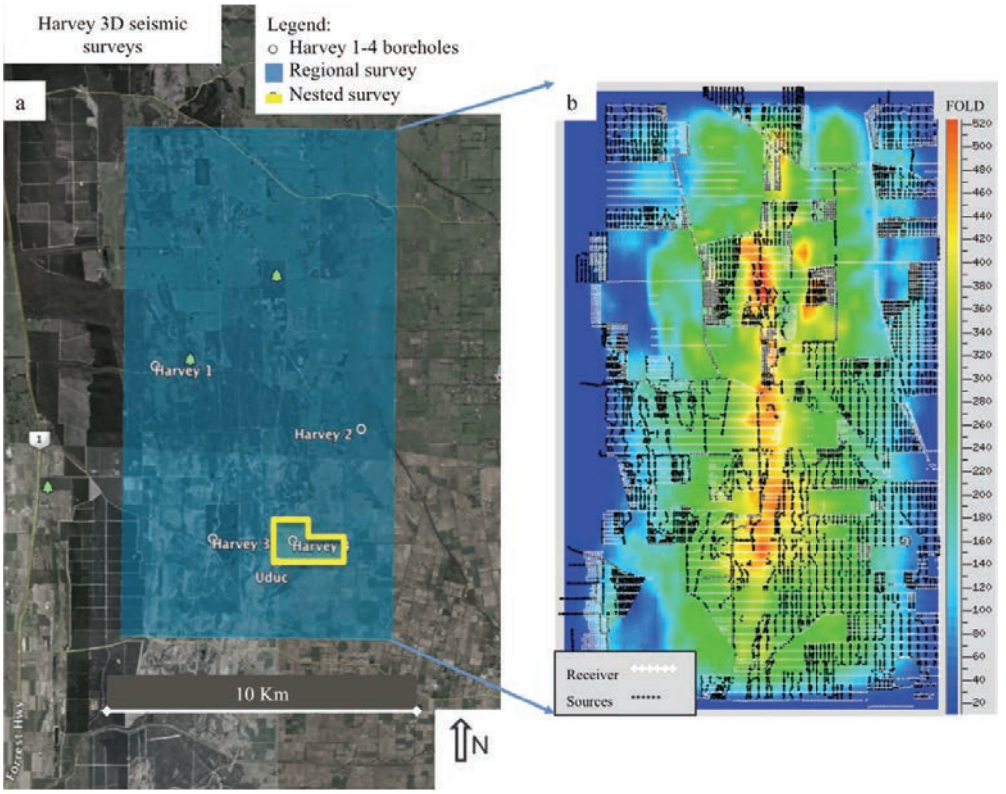

Fig. 1. (a) Harvey 3D seismic surveys location. Apart from Harvey-1, other three boreholes were drilled after 3D survey took place. The area of the high-resolution nested 3D survey is shown in yellow; (b) Harvey 3DR survey layout and fold coverage.

The survey covered many small farms, which are often owned/operated by the multiple individual landowners. The permission across a number of farms was not granted in time. This resulted in long total duration of the survey, patchy data coverage and uneven fold of the survey (Figure 1b). The uneven fold distribution in the regional seismic survey made the processing and particularly imaging difficult. Also data was not suitable for the quantitative analysis. Following the acquisition of the Harvey 3DR data, several wells were drilled (Harvey-2, 3 and 4). Subsequently, a new study was approved. In 2015, a small (2.12 km^2) high-resolution 3D seismic survey was designed and acquired by the National Geosequestration Laboratory (NGL) and Curtin University crew (Urosevic et al., 2015). Location of the nested 3D surveys is shown in Figure 1a.

The principal difference between two surveys was in the data density, that is the number of vibrating points (VP) and live receivers per km^2. Details of the data acquisition parameters for both regional and nested 3D survey are provided in Table 1. The high data density of nested 3D provided a much higher fold, particularly in the shallow and hence much improved the signal to noise ratio (SNR). Since SNR is proportional to square root of fold, the resultant nested data images proved to be superior. Moreover, the high data density and broad band sweep resulted in much improved vertical and horizontal resolving power.

Table 1. Regional and nested Harvey 3D seismic survey parameters.

Design parameters	Regional Harvey 3D	Nested Harvey 3D
Receiver spacing	50 m	15 m
Source spacing	50 m	15 m
Receiver line interval	200 m	50 m
Source line interval	200 m	90 m
Bin size	25 m x 25 m	7.5 m x 7.5 m
Maximum fold	~440	~150
Survey area	130 km^2	2.12 km^2
Near offset	25 m	8 m
Far offset	8218 m	2340 m
Sweep parameters	12 s 5–100 Hz linear upsweep with 350 ms tapers; 2 sweeps per VP	24 s 6–150 Hz linear upsweep with 500 ms tapers; 1 sweeps per VP

The advantage of the nested 3D design for imaging of shallow targets can be illustrated by choosing 550 ms of two-way-travel time (TWT), which can be recorded by maximum 1100 m offset, assuming that events are sub-horizontal and the mute is 40% stretch (Figure 2). Fold coverage limited by 1100 m offset of regional survey drops to only 20, while in nested survey it is at 100. This is the reason why noise suppression in a nested survey is expected to be more successful.

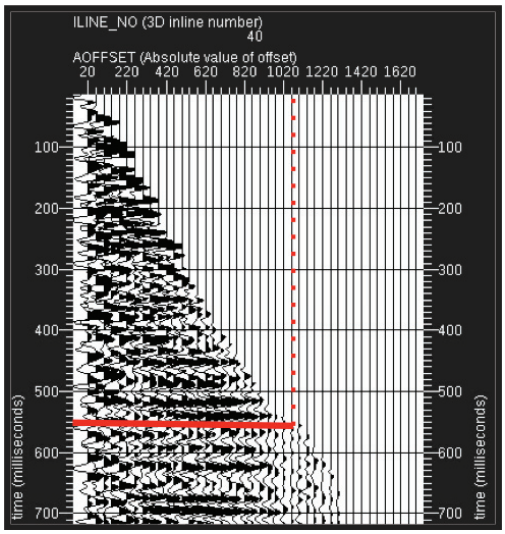

Fig. 2. Image gathers showing useable offsets to record event of 550 ms TWT.

It worth noting that, if a location for shallow release of gas is identified, then the initial results indicated that a set of high-density electrical resistivity profiles should be able to map, in detail, the continuity and distribution of shallow clays. The resistivity is surprisingly heterogeneous over the site, suggesting that the shallow geology is complex. The continuity and distribution of the shallow clays may be of considerable importance. If for example, a shallow release of CO_2 into faulted sediments is to be completed, final migration pathways may be strongly influenced by distribution of shallow clays.

Clearly, the nested 3D survey design was built to improve the lateral resolution. The receiver/source density is an order of magnitude higher that Harvey 3DR, while bin size of the nested survey is reduced to 7.5 m, approximately by a factor of 3 (Table 1). It was also hoped that broadband sweep (6–150 Hz) would inject high frequencies at shallow depths, which would improve the vertical resolution as well. The new broadband seismic vibrating source also proved to be quite powerful. It generates enough energy to clearly record events from depths of at least 1500 m, as verified in the nested survey data. The equipment and the approach used in this project provide a low footprint, low impact option for acquiring seismic data in areas that have public concern regarding the surface environmental disturbance, yet still have the capacity to obtain high-resolution images to reservoir depth. A small crew size of only eight people, operating some 3000 channels completed shooting this survey in less than five days. Such surveys may get a wider acceptance for CO_2 monitoring programs and also public approval in Harvey area.

3. Seismic data processing and imaging

For both the regional and nested survey, the processing was structured around two flows. The first flow utilised robust scaling, 3D dip moveout (DMO) and post-stack migration. The second flow utilised an amplitude preservation approach and pre-stack time migration (PSTM). The aim of the first flow was just to produce a "baseline" image against which further processing improvements are measured. It became apparent that a conventional DMO correction followed by post-stack migration was insufficient to handle the lateral changes in velocity field. Therefore, pre-stack time migration based on Kirchhoff integral solution was attempted to aid in handling the complex velocity field. The goal of pre-stack time migration was to derive a velocity model appropriate for the geologic setting, to place events at the proper position, to avoid introduction of a false structure and to flatten the image gathers.

The processing flow for the final imaging is shown in Table 2 and 3.

Table 2. Processing parameters.

Processing procedure	Parameters
Data conversion	SEG-D data Input and conversion to Seispace internal format
Geometry and binning	Nested 7.5 m x 7.5 m, Regional 25 m x 25 m
Gain recovery	Surface consistent amplitude recovery and spherical divergence correction
Static correction	Application of elevation and residual statics
Deconvolution	Minimum phase predictive
Band-pass filter	Sweep frequencies inclusive
Surface wave noise attenuation	Velocity 1200 m/s, frequencies 4–40 Hz
Automatic gain control (display purposes)	500 ms

Table 3. Imaging algorithm.

Imaging procedure	Parameters
Data input	Pre-processed dataset
PSTM Iteration I	PSTM velocity field I
Velocity analysis	Compute PSTM velocity field II
PSTM Iteration II	PSTM velocity field II
60% stretch mute	Post-NMO top mute
3D stack	Normalisation scalar 0.5
FXY deconvolution	Window 200/800 ms
SEGY output	Standard SEG Rev1

4. Regional and nested 3D surveys

The main objective of the nested 3D survey was to produce high-resolution images of the shallow structures (0–1000 m). One way of verifying that the objective was achieved is through a direct comparison of migrated nested 3D imagines with those of the Harvey 3DR survey. Initial comparison was made using a chair display. One such example is shown in Figure 3. A brief inspection of images shown clearly demonstrates that the objectives were achieved and that the nested 3D survey contains new geological details, not observable in the previous regional survey. Further investigation and comparison utilised 2D images planes, which are easier to comprehend and observe in detail. One of the objectives was compare fault expression in the two data sets. For that purpose we first enhanced the faults through the computation of a so-called minimum similarity cube.

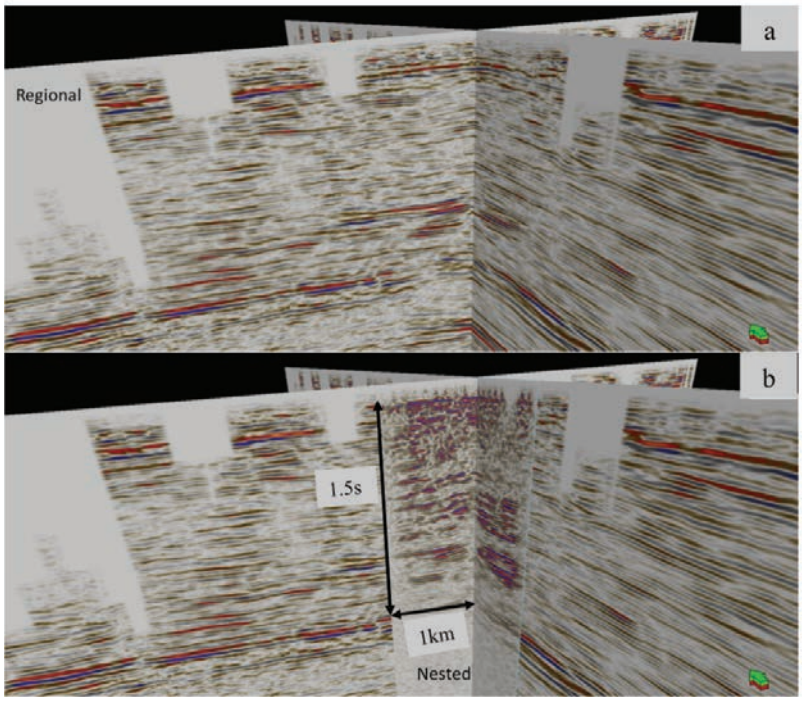

Fig. 3. (a) Regional Harvey 3D survey (b) regional survey with nested survey inserted. Nested 3D survey demonstrated higher resolution and better overall expression of shallow geology. Vertical scale is in time.

Firstly, time slices showing clear fault expression were selected. Then the in-line and cross-line passing through the fault trace were used for comparison. This is demonstrated in Figure 4. It is clear that the nested high-resolution 3D has provided new information about the shallow structures, not seen in the regional data. It is also clear that the dense survey grid has provided more fidelity of fault traces down to an approximately 1.5 km depth and possibly deeper.

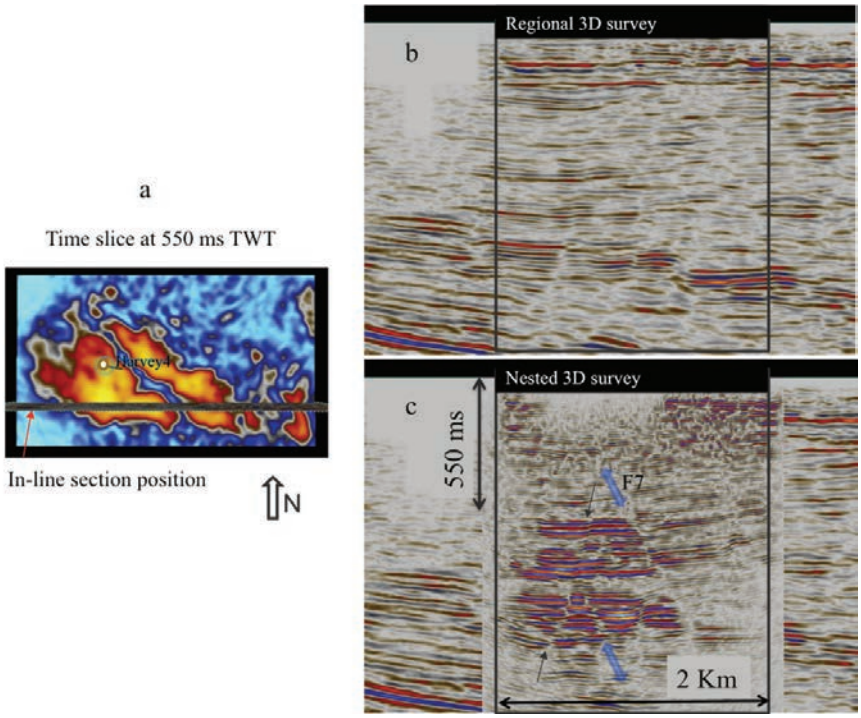

Fig. 4. (a) Time slice through similarity section with the location of the in-line section under investigation and Harvey 4 borehole shown as a green circle, (b) regional Harvey 3D and (c) nested 3D PSTM stacked section inserted into the rectangular area. The blue transparent double arrow is used to denote fault images that are clearer in nested 3D volume, such as Fault 7. The black arrow denotes where fault is expressed with much better clarity in the nested 3D. Vertical scale is in time.

A number of fault expressions were analysed in time slice domain. Additional information and improved fault trace identification was achieved with so-called similarity cube. Such an example is shown in Figure 5 where horizontal intersections through amplitude and similarity cubes area compared. Faults of different scales or orders can be seen in these two displays. Both displays should be used concurrently as some faults are better expressed in one domain rather than the other.

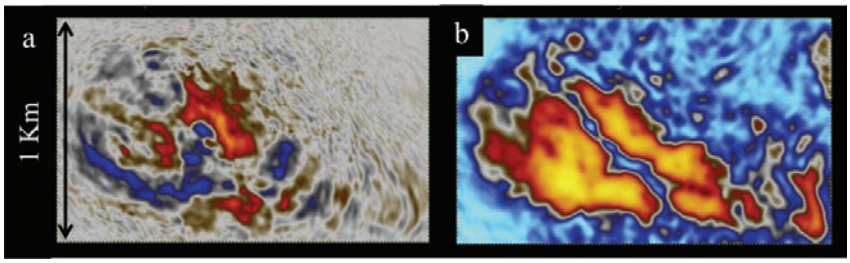

Fig. 5. (a) Time slice from the amplitude cube; (b) time slice from similarity cube. Main faults can be seen tracking from top left to bottom right as a blue linear trend with the orange area of the similarity time slice.

5. Seismic quantitative interpretation

Having the processed seismic datasets along with analysed well data, we can start 3D quantitative interpretation to integrate these pieces of information into 3D reservoir models. The aim is to interpret the data in terms of subsurface distribution of petrophysical properties, relevant for the CO_2 sequestration modeling: porosity, permeability etc. Derived petrophysical cubes are then used to constrain static and dynamic models.

To tie well data to the seismic, one needs to compute a synthetic seismic trace using a logs-based 1D model of elastic impedance:

$$EI = V_P^{\left(1+\tan^2\theta\right)} V_S^{\left(-8K\sin^2\theta\right)} \rho^{\left(1-4K\sin^2\theta\right)} \quad (1)$$

where $K=(V_S/V_P)^2$; θ - angle of wave incidence at the boundary. At the normal incidence EI reduces to the acoustic impedance [$Z_P=\rho V_P$]. Well tie requires log data conditioning, but other challenges surrounding each well in the area (Figure 6). Some are listed below:

- Harvey-1 corresponds to the area of reliable seismic amplitudes, but almost vanishes in the Wonnerup member; moreover the logs were acquired only at the bottom of the Yalgorup member;
- Harvey-2 penetrates Fault 10 which causes intense scattering of the seismic energy, thus a complex wavefield is present close to the borehole;
- Harvey-3 is surrounded by the forest, prohibiting deployment of receivers and shot points; this results in a blank vertical zone in the seismic image along the borehole;
- Harvey-4 trajectory is intersected by the oblique Fault 7 and possibly another fault going in parallel to the Fault 7, which are not clearly visible in the commercial seismic but obvious in the nested seismic (Figure 4). As a result, intensity of the seismic varies significantly above and below the faults.

The features listed above limit significantly the reliability of the amplitude-based inversion of both 3D seismic surveys. It also affects correlation of the logs interpretation to the seismic. Even improved processing of the large seismic did not lead to a significant improvement of the correlation to the wells. However we were able to obtain meaningful elastic impedance cube from the nested 3D seismic data after correlation to Harvey-4 well. The main objective of inversion was to utilise inverted impedance data for characterisation of the Yalgorup member. Of particular interest was to define paleosols, as they are potential barrier to upward migration of CO_2. Their limited lateral extent and small thickness makes them difficult target for analysis, particularly from seismic amplitudes. Preserved relative amplitude seismic data and edited logs were used in correlation process. First, we extracted seismic wavelet from the data based on the highest log-derived synthetic to seismic correlation of 75%. Subsequent stages included acoustic and elastic inversion.

We established that the highest SNR corresponds to the mid-offset range of seismic data that correspond to 15^o–25^o angle stack. After series of cross-plots it was determined that the intervals of low values of $EI(20^o)$ and negative deviation from this trend correlate with paleosol facies derived form well data (Figure 7). At the right part of the figure we see the comparison of the detected paleosol bodies against the paleosol effective thickness interpreted from the well logs (micro-imagers, gamma-ray and density logs). The agreement is rather good.

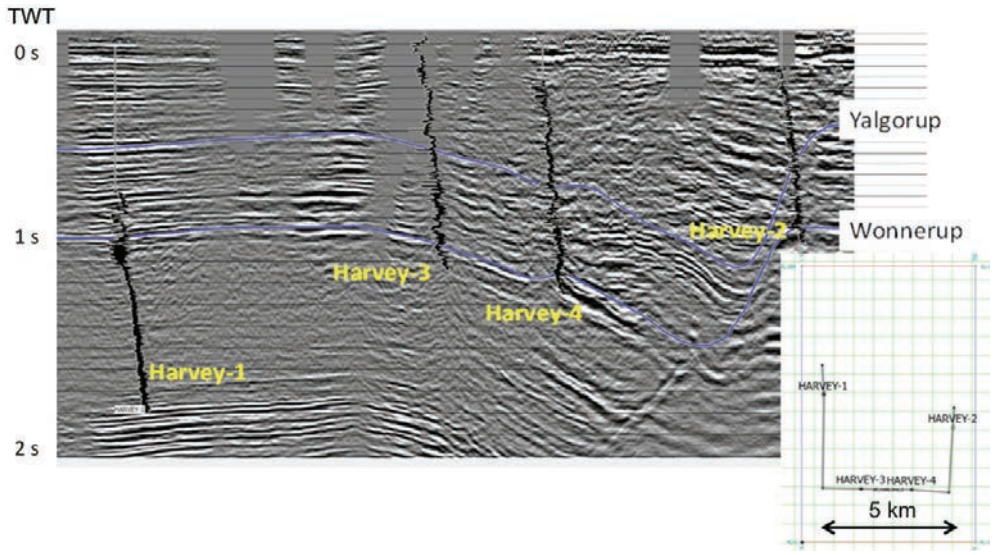

Fig.6. Arbitrary line (shown in the inset) extracted from the large commercial seismic overlaid by V_P from logs.

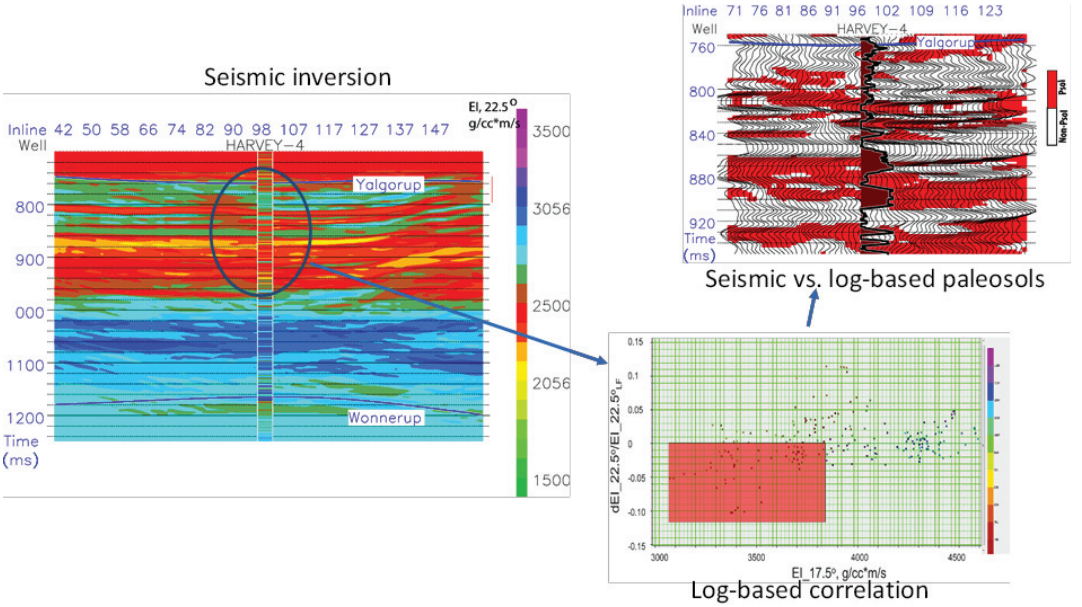

Fig.7. Elastic impedance inversion flow aimed at the paleosol mapping: Impedance section after well tie (left), cross-plot of the elastic impedance and selection of low values that are expected to be characteristic for paleosols (lower right) and mapping low EI values onto the seismic data (upper right) and comparing it to the log-derived paleosol intervals.

6. Conclusion

The high-resolution Harvey nested 3D seismic data has been acquired with the NGL using a state-of-the-art hybrid recording system. Two light NGL vibrator trucks (UNIVIB) with extra-wide tires were deployed in a "flip-flop" shooting pattern. No footprint was left in the ground by this seismic source vehicle. A small seismic crew

comprised of eight people managed the deployment of 2,300 channels with ease and fired close to 1600 shots in 4.5 days. A single long-duration sweep and a single sensor, combined with the achievements of a high fold produced very good quality data of envious SNR. Preserved amplitude processing and pre-stack imaging proved to be a very effective processing approach for both structural and stratigraphic analysis. Very good quality images enabled qualitative studies involving acoustic and elastic inversions.

By inserting the nested 3D data cube into the regional 3D data we show that:

- Several new faults, not seen in the regional data, were identified in nested 3D data;
- All discontinuities (large and small) are much better imaged in nested 3D survey;
- The extent of some fault tips close to the surface was mapped from the nested data;
- Faulting in the area has a high complexity than previously thought;
- The Harvey 4 well was drilled through a fault of a large throw (several tens of metes).

The fault density and their complexity cannot be fully realised with the low-resolution seismic data even at greater depths. Low-resolution data are also not appropriate for the implementation of seismic stratigraphy and quantitative interpretation. The new nested high-resolution seismic data after appropriate processing and imaging were of sufficient quality to produce good correlation with well data and permit the process of seismic inversion. After low values of the elastic impedance were related to paleosols it was the matter of mapping these intervals onto seismic section. Very good agreement achieved stimulates further work along this path.

Considering all the additional structural and stratigraphic information obtained from the nested 3D seismic it is that such surveys can be very valuable for site characterisation. Moreover, such data can be also used to optimise well position through better fault location prediction. The cost of the nested survey conducted is only a fraction of the drilling cost but the impact can be significant in terms of borehole relocation, fault correlation, derivation of static model and subsequent dynamic simulations.

Acknowledgements

The South West Hub project is managed by the Carbon Strategy Group of the Western Australia Department of Mines and Petroleum. It is supported through the Australian Commonwealth Government Flagship Program through the Department of Industry, Innovation and Science (DOIIS); the West Australian State Government through the Department of Mines and Petroleum; the Australian National Low Emissions Coal R&D Program and the local community in the south west of Western Australia.

We are grateful to Halliburton Company for their generous donation of Landmark processing software and to CGG for their donation of seismic inversion software.

References

[1] Bretan, P., Yielding, G., Jones, H. (2003) Using calibrated shale gouge ratio to estimate hydrocarbon column heights, AAPG bulletin, 87, 397–413.

[2] Langhi, L., Ciftci, B., Strand, J. (2013) Fault seal first-order analysis – SW Hub, CSIRO report EP13879, pp. 50.

[3] Langhi, L. , Zhang, Y. , Nicholson, C., , Bernardel, G., Rollet, N., Schaubs, P., Kempton, R., and Kennard, J. (2012) Geomechanical modelling of trap integrity in the northern offshore Perth basin, CSIRO Open file report: EP 12425.

[4] Morris, A., Ferrill, D.A., Henderson, D.B. (1996) Slip tendency analysis and fault reactivation, Geology 24 (3), 275–278.

[5] Mildren, S.D., Hillis, R.R., Dewhurst, D.N., Lyon, P.J., Meyer, J.J., Boult, P.J. (2005) Fast: a new technique for geomechanical assessment of the risk of reactivation-related breach of fault seals, Boult, P. & Kaldi, J. (eds) Evaluating fault and cap rock seals. AAPG hedberg series, 2, 73–85.

[6] Pevzner, R., Lumley, D., Urosevic, M., Gurevich, B., Bóna, A., Alajmi, M.A., Shragge, J., Pervukhina, M., Mueller, T., Shulakova, V. (2013) Advanced geophysical data analysis at Harvey-1: storage site characterization and stability assessment, ANLEC R&D project number 7-1111-0198.

[7] Urosevic, M., Ziramov, S., Pevzner, R. (2015) Acquisition of the Nested 3D seismic survey at Harvey, ANLEC R&D Project 7-1213-0224 Final report, Curtin University, 36 pp.

[8] Urosevic, M., Ziramov, S., Pevzner R. and Kepic, A. (2014) Harvey 2D test seismic survey-issues and optimisation: ANLEC R&D Project 7-1213-0223.

2.2. Pre-stack depth imaging techniques for the delineation of the Carosue Dam gold deposit, Western Australia.

Received: 30 May 2022 | Accepted: 23 December 2022

DOI: 10.1111/1365-2478.13314

Geophysical Prospecting | EAGE EUROPEAN ASSOCIATION OF GEOSCIENTISTS & ENGINEERS

ORIGINAL ARTICLE

Pre-stack depth imaging techniques for the delineation of the Carosue Dam gold deposit, Western Australia

Sasha Ziramov[1,3] | **Carl Young**[2] | **Jai Kinkela**[1] | **Greg Turner**[1] | **Milovan Urosevic**[1,3]

[1]Hiseis Pty. Ltd., Subiaco, Western Australia, Australia

[2]Northern Star Resources Ltd., Subiaco, Western Australia, Australia

[3]Curtin University, Kensington, Western Australia, Australia

Correspondence
Sasha Ziramov, Hiseis Pty. Ltd., 140 Hay St, Subiaco 6008, Western Australia, Australia.
Email: s.ziramov@hiseis.com

Abstract

In this study, we explore the latest generation of seismic imaging algorithms (migration) that have been successful in the oil and gas exploration industry and apply them in the more challenging hard rock environment. Seismic migration is a crucial processing step required to build an accurate image of the Earth's subsurface. The seismic method applied in a hard rock environment has a specific set of challenges: complex geological settings often comprised of steeply dipping interfaces and heterogeneities (faults, fracture zones, thrusts, etc.); spatially variable zones of alteration, low intrinsic signal-to-noise ratio; complex near-surface conditions (the weathered overburden has a very high contrast in seismic properties with base formations). Here, we present how a dense source–receiver 3D grid in combination with the latest pre-stack depth imaging techniques can image the geology with a remarkable level of detail and to depths as shallow as the top of fresh rock. We also propose a comprehensive velocity model building strategy applied specifically to the Carosue Dam deposit, Western Australia, which is mainly characterized by volcaniclastic and volcanic rocks within the Carosue Basin disrupted by a complex system of gold-bearing faults. To arrive at an optimized velocity model for pre-stack depth imaging, we combine drillhole data with tomographic refinement. Excellent correlation between resultant seismic images and refraction tomography, vertical seismic profiling and drillholes can be attributed to the integrated velocity model building workflow used for depth migration.

KEYWORDS

depth migration, high-resolution seismic, reverse time migration, seismic tomography, seismic velocities

INTRODUCTION

The golden era of geophysical discoveries of shallow, rich mineral deposits has well passed. Exploration targets have now moved to a much greater depth window. In general, depths below 500 m are difficult to investigate with precision by any other geophysical method except the seismic reflection technique (Malehmir et al., 2012). The exploration value of the seismic reflection method is well established and documented by the oil industry. In the minerals industry, despite very early seismic work that can be dated back to 1927 (Karaev & Rabinovich, 2000), subsequent regular and continuous utilization of this technology for mineral exploration purposes has not been carried out. From the early

1950s when the first high-resolution seismic study was conducted by Berson (1957), numerous and valuable seismic studies followed, demonstrating the high penetration, resolution and precision of reflection seismic in detecting complex geological underground forms at all depths. The history, development and application of modern seismic methods for the exploration of mineral resources across all continents have been well summarized by Malehmir et al. (2012). While the potential of seismic was clearly demonstrated through several early field studies (Durrheim & Maccelari, 1991; Milkereit et al., 1992; Pretorius et al., 1989), the mining industry was reluctant to embrace it on a larger scale, certainly incomparable to the utilization of potential field and electromagnetic methods. Until 1994, seismic for mineral exploration was exclusively conducted along a profile (2D). The first breakthrough came with the areal (3D) seismic design recorded in South Africa (De Wet & Hall, 1994). Subsequently, Eaton et al. (1997) used 3D seismic for the delineation of a deep ore deposit in Canada, while Pretorius et al. (1997) conducted the first 3D survey for the purpose of underground mine planning and development. These early works demonstrated that the complexity of the hard rock environment is best assessed and delineated by 3D reflection seismic. Instead of flourishing, a significant downturn in the application of 3D seismic followed until 2011–2012. Since then, a slow but steady rise in the use of 3D reflection seismic for exploration in brown fields, to extend the existing mine life and discover new resources at a greater depth, has occurred (Urosevic, 2013; Urosevic et al., 2017).

Extensive structural complexity typically encountered in a hard rock environment requires high-precision measurements. In the case of seismic measurements that translate into requirements for high spatial and temporal resolution as recognized in early seismic works (Stolz et al., 2004; Urosevic et al., 2005). The high spatial density of sensors is of key importance for imaging structurally controlled mineralization (Urosevic et al., 2012). Unfortunately, a high-resolution, high-fidelity seismic approach requires a large number of sensors to be simultaneously deployed over a large territory which makes such investigations very expensive. It is possible, based on reciprocity, to partially compensate for a small sensor count by introducing additional source positions or repeating specific shooting patterns. Indeed, such an approach characterized hard rock 3D seismic surveys in the previous decade (Urosevic et al., 2017; Ziramov et al., 2015, 2016). One to two thousand receivers were typically deployed for 3D surveys at the time using moving, overlapping source–receiver templates. While this approach made 3D seismic more accessible and affordable to the mineral industry, it suffered from several drawbacks. Insufficient offset range is probably the most important issue that in some limited cases could have affected the imaging of steep dips at depth, perhaps outside of the mining window but still of interest to structural geologists.

The potential for high sensor density designs for imaging the complex geometry of salt domes was hinted at in 1990 in the oil industry, while the first (primitive) nodal systems referred to distributed cable recordings dating back to the 1970s (Dean et al., 2018). The real 'explosion' in the production and utilization of modern nodal systems is recorded only in the middle of the last decade in the oil sector. The benefit of a high receiver count for imaging complex structures in a hard rock environment at all depths was quickly realized in the minerals industry and deployed even for 2D surveys (Naghizadeh et al., 2019). Similarly, modern vibroseis and electro-kinetic vibrating sources provide a broad-band seismic signal that is required for the utilization of novel inversion and imaging techniques (Naghizadeh et al., 2019; Pertuz et al., 2022; Singh et al., 2022). A combination of a large number of sensors (high data density) and broad-band seismic sources enables the successful implementation of novel processing (signal enhancements, interpolations, etc.), imaging techniques such as reverse time migration (RTM) and inversions such as full-waveform inversion (FWI). This led to early investigations into the potential of FWI in hard rock environments (Adamczyk et al., 2014, 2015), while investigations into imaging techniques were documented by several authors (Brodic et al., 2021; Broüning et al., 2020; Ding & Malehmir, 2021; Hloušek et al., 2015; Singh et al., 2022).

The successful application of the seismic reflection method is to the first degree controlled by the contrast and the distribution of elastic properties of the geological environment (Bohlen et al., 2003). However, mineral composition and more elusive rock characteristics such as alteration and rock texture play an important role in recorded reflectivity (Schetselaar et al., 2019). Our ability to delineate reflectivity also depends on its geometry and volume, as well as the presence of fractures and joints, grain alignment and crystal symmetry, etc. Therefore, reflectivity in hard rock is controlled by many factors and it is not readily predictable even in well explored mine sites. This possibly peculiar reflectivity pattern of hard rocks is further exacerbated by high structural complexities. In terms of gold exploration in Western Australia, both the reflectivity patterns and excessively complex underground structures are commonplace (Stolz et al., 2004). The necessity to utilize high-precision imaging techniques, such as Kirchhoff pre-stack depth migration (PSDM) to delineate complex undergraduate structures, was recognized early in the application of seismic for gold exploration across Yilgarn craton of Western Australia (Urosevic et al., 2007; Urosevic & Evans, 2007a). Consequently, the application of seismic for gold exploration in Western Australia must be carefully staged. Hence, seismic data acquisition is typically proceeded by a seismic feasibility study looking into the seismic rock properties. Positive results will grant project continuation. After the acquisition, data processing and analysis should adopt the best approach for imaging complex

geological structures at all scales with the maximum possible precision.

Such an approach was carried out at the Carosue Dam site. Extensive rock property measurements were conducted prior to 3D data acquisition. As the primary objective of the survey was to refine the existing geological model needed for the discovery of additional gold resources within the Carosue Dam Operations, maximum precision seismic imaging was required. That included the delineation of numerous small-sized, steeply dipping brittle-ductile faults that facilitate the emplacement of gold mineralization at this site.

To accomplish such a task, we evaluated several approaches to velocity model building, composed of refraction and iterative reflection tomography, to construct high-precision seismic images using concurrently pre-stack Kirchhoff depth migration and reverse time migration. We describe a complete depth imaging workflow rooted in the standard oil and gas industry to depth imaging tailored to a hard rock environment. This workflow is applied to a high-density, high-quality, large (50 km^2) 3D seismic survey shot over the complex gold mineralization target in WA (Carouse Dam). The resultant images correlated very well with the existing downhole logs, vertical seismic profiling (VSP) and drillhole information that provide validation of the results. High-quality seismic images obtained in this study gave rise to high-quality geological analysis and interpretation that are hoped to define new drilling targets soon.

Geological background

The northwest-trending Carosue Basin is located in the Kurnalpi Terrane of Swager (1997) and the Murrin Murrin domain of Cassidy et al. (2006) in Western Australia. The Carosue Basin contains intermediate volcaniclastic sedimentary rocks, intermediate volcanic rocks, epiclastic sedimentary rocks, felsic to intermediate intrusions and minor lamprophyre intrusions that generally dip to the northeast. Rocks are weakly foliated and metamorphosed to mid-greenschist facies. The concealed western margin of the Carosue Basin is an interpreted nonconformity between the Carosue Basin rocks and the older Menangina domain rocks (Cassidy et al., 2006). The Menangina domain mostly comprises mafic volcanic and intrusive rocks, ultramafic intrusions, felsic volcanic rocks and minor fine-grain sedimentary rocks. East of the Carosue Basin is the older Murrin Murrin domain (Cassidy et al., 2006) that comprises mafic and ultramafic volcanic and subvolcanic rocks with minor epiclastic sedimentary rocks. The contact between the Carosue Basin and the Murrin Murrin domain is obscured locally by sandstone, siltstone and polymictic conglomerate of the younger Yilgangi Basin, which is intruded by ca. 2.66 Ga syenite and monzodiorite (Nelson, 1996). The eastern part of the Carosue Basin and isolated remnants of the Yilgangi Basin in the Carosue Dam area are strongly deformed with tight folding and stretching fabrics.

The general architecture of the two largest gold deposits in the Carosue Basin, Karari and Whirling Dervish, is steep northeast-dipping tabular to lenticular beds that are moderately foliated with localized steeply northward-plunging transposition folds and associated shearing. The stratigraphic sequence (Figure 1) from west to east in the area covered by the 3D seismic survey is (i) mostly northeast-dipping Menangina mafic-ultramafic succession, (ii) a mostly northeast-dipping, quartz-bearing turbidite sequence with local disruption by folding and thrust faulting (iii) the informally termed central mineralized zoned (CMZ; Witt et al., 2009) comprising mostly volcaniclastic sandstones, minor andesite and minor conglomerate, (iv) a variably thick (50–250 m) sequence of andesite, intruded by monzonite, syenite and lamprophyre (the Eastern Intrusive Complex or EIC; Witt et al., 2009) that forms the hanging wall to most of the gold deposits in the Carosue Basin, (v) intercalated volcaniclastic sandstone, conglomerate and minor andesite and (vi) a thick sequence of fine- to medium-grained epiclastic sediments. The margin between the Carosue Basin and the Murrin Murrin rocks to the east is obscured by epiclastic sandstones and polymictic conglomerates of the Yilgangi Basin that are strongly foliated and folded. This zone of high strain is considered to be the likely trace of the regionally significant Keith Kilkenny Shear Zone.

Within the Karari and Whirling Dervish gold deposits, the EIC succession has undergone high shear strain and hydrothermal alteration. Across this structural domain, the reversal in younging directions (east-facing in the CMZ; overturned west-facing stratigraphy east of the EIC) demonstrates the deposits are sited on a district-scale, faulted-out fold closure with a shallow north plunge. Shearing in the CMZ is generally concentrated on the contacts between the mechanically weaker andesitic tuffaceous conglomerates or lamprophyre dykes and more competent sandstone or monzonite units. Gold mineralization is generally within these sheared domains and in the heavily fractured and pervasively altered zones in the competent units (see Witt et al., 2009, for further details on the gold mineralization). Numerous north-to-northeast trending, steeply dipping brittle-ductile faults dissect the Carosue Basin and offset mineralization. The Osman Fault has dextrally offset the Karari and Whirling Dervish deposits by around 1 km. Similar chloritic faults have developed as late reactivation of earlier-formed mineralized shear zones. The Resurrection fault and Young Fella fault, which in places includes cataclasite fault gouge, are such examples.

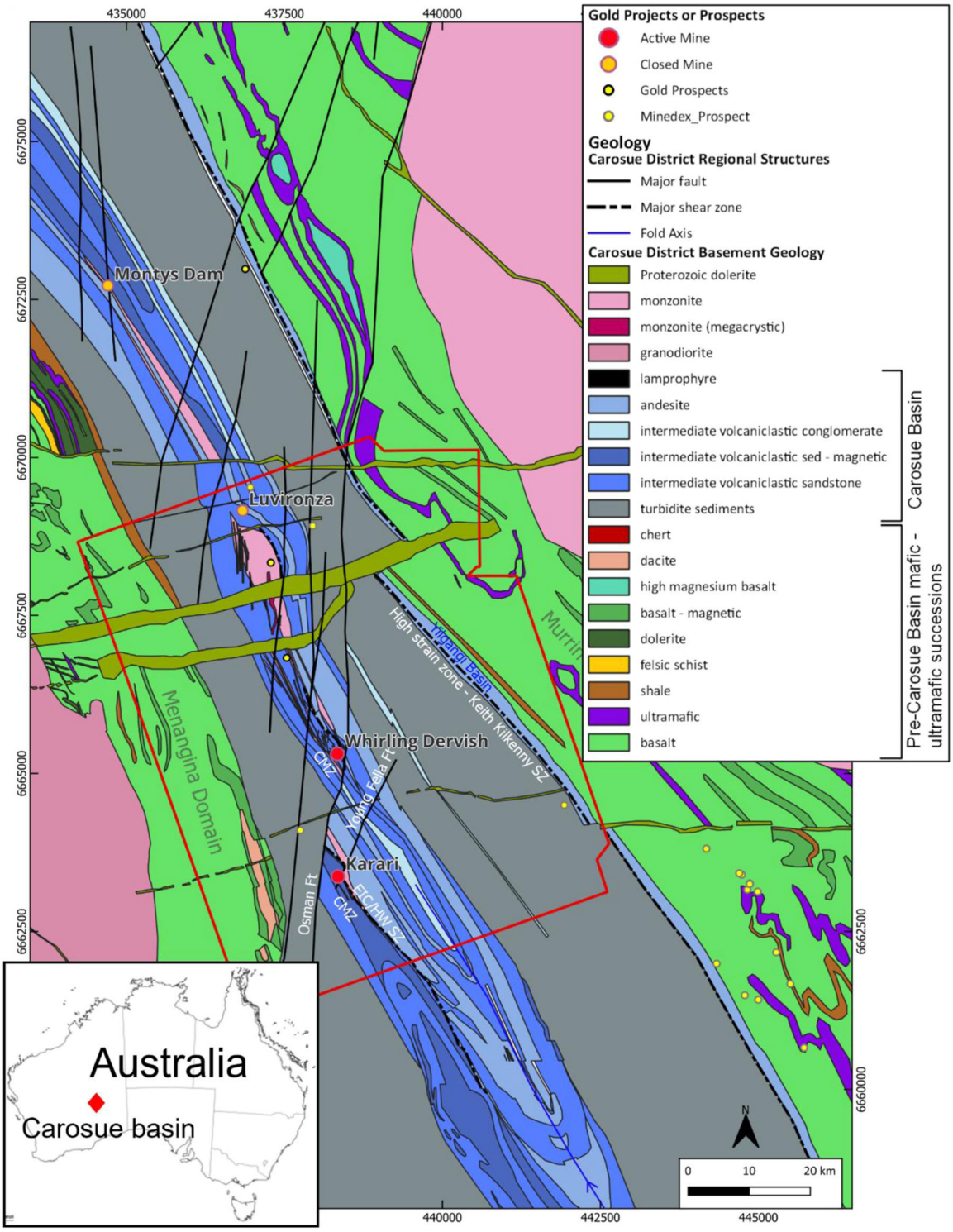

FIGURE 1 Carosue Basin geology with embedded 3D survey boundary in red

Rock properties: seismic feasibility study

The seismic exploration strategy for Carosue Dam utilized a 3-phased approach to determine whether the local geology was amenable to modern seismic reflection imaging. The first phase completed in 2017 involved the characterization of the rock properties and predicting seismic reflectivity via measurements of P-wave velocity (*Vp*) and specific gravity on the core samples. The second stage of seismic activity involved the acquisition of 2D and borehole seismic, which demonstrated excellent reflectivity from key lithologies and structures within the area of interest. This is illustrated in

Geophysical Prospecting EAGE EUROPEAN ASSOCIATION OF GEOSCIENTISTS & ENGINEERS

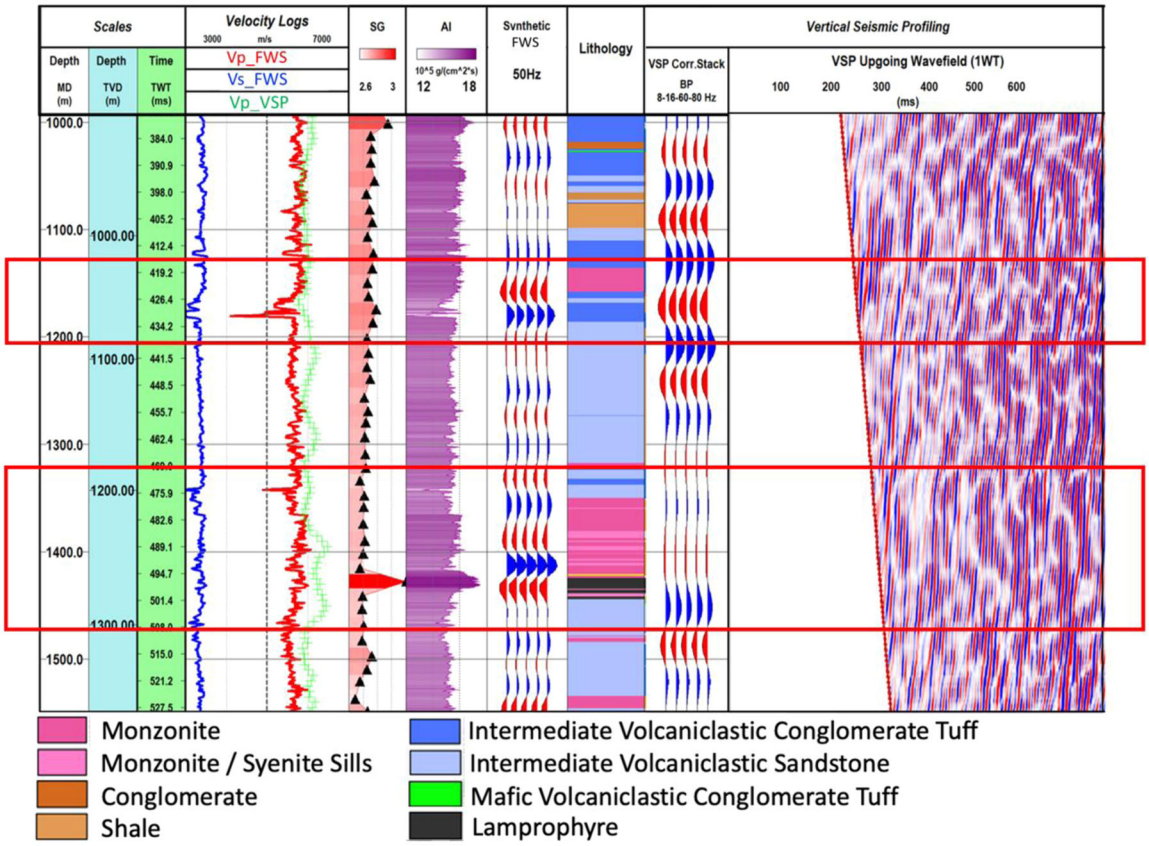

FIGURE 2 Rock property measurements in a mineralized zone associated with the Whirling Dervish orebody (borehole WDX047), with the highlighted area showing strong P-impedance changes from wireline and VSP measurements

Figure 2, by comparing wireline and VSP measurements against sampled mineralized zones. WDX047 is the deepest borehole acquired in the Whirling Dervish area, intercepting mineralization at 1.1–1.6 km of depths. Synthetic traces computed from P-impedance from wireline logging show high reflectivity in areas of gold-bearing monzonite dykes. Following the successful 2D and wireline programme, the HiSeis team proceeded with the third stage of the seismic investigation, whereby a 50-km^2 3D seismic survey was acquired over an area covering the Karari and Whirling Dervish deposits.

3D seismic data acquisition

Acquisition of 3D seismic utilized two vibroseis trucks, each having a mass of 27,200 kg, in flip flop shooting order. Data acquisition geometry utilized a rolling swath design using INOVA's Hawk wireless seismic acquisition system. Recording parameters are listed in Table 1.

The acquisition phase took place in early 2019 with the final survey design illustrated in Figure 3, showing the distribution of azimuths and offsets of the survey. The active shouting template highlights a maximum inline of 2.2 km and a maximum crossline offset of 1.2 km. It is a common occurrence to acquire hard rock seismic surveys through operating mine sites, with access constraints around key infrastructure, including the mining operations, pits, waste dumps and tailings storage facilities. To reduce acquisition footprint, offset regularization was applied prior to data imaging.

Seismic data were processed shortly after acquisition, and imaging was carried out using a Kirchhoff pre-stack time migration (PSTM). This initial volume showed encouraging results, which provided new insights into the geology of the area. In this study, we have revisited imaging of the data with the aim of trialling pre-stack depth migration algorithms, in order to improve the imaging of small complex structures that are known to exist in the target zone but were not fully resolved with time imaging. Our expectation was that depth imaging will not only increase the imaging accuracy but will provide better resolution and hence enable less ambiguous geologic interpretation. The re-processing of the Carosue Dam data was conducted through the following steps: seismic data processing, pre-stack depth imaging and velocity model building.

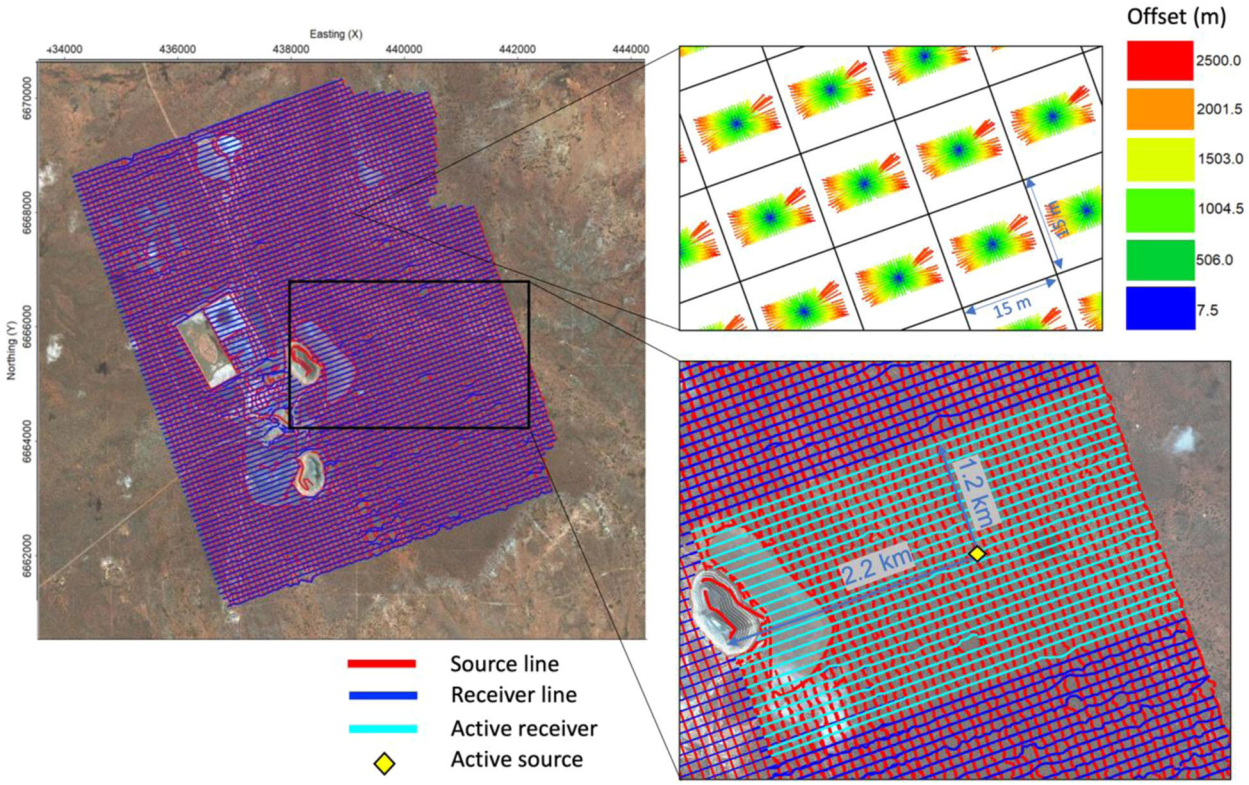

FIGURE 3 Survey design with spider plot showing the distribution of offsets and azimuths in the right top insert. Right bottom insert illustrates an active spread for a highlighted shot. Background image is from Google Earth (2017), Western Australia, 30° 09′ 56′′ S, 122° 20′ 58′′ E, eye alt 30 km. http://www.earth.google.com

Seismic data processing

The reflection seismic method faces many challenges in a hard rock geological environment. Often high noise levels due to mining activity, a complex overburden, overthrust zones, fracture zones and steeply dipping stratigraphy require us to constantly advance our approach to seismic processing and imaging. The Carosue Dam environment is known to exhibit all of these challenges. In order to address these, a tailored processing sequence was designed and is shown in Table 2. The seismic processing can be grouped into the following categories:

- Signal-to-noise (S/N) improvements
- Wavelet shaping and conditioning (deconvolution)
- Near-surface static corrections
- Corrections for positioning (imaging)

The higher data density characteristic of hard rock survey designs provided proper wavefield sampling in the spatial domain, which supported the effective application of source-generated noise removal techniques. Refraction statics were calculated using refraction tomography-based inversion. The process involves measuring the arrival times of refracted seismic energy. These travel times are then inverted for seismic velocities at each layer and their corresponding depths. This is because the angle of the refracted event directly depends on the ratio of velocities between the two layers (Snell's law). To improve the accuracy of the velocity-depth model, several iterations of tomographic updates were utilized. A refraction and residual static that corresponds to smooth topography (floating datum) has been applied to compensate for small-scale velocity anomalies in the near surface that imaging could not correct. This is one of the main differences relative to legacy processing, where a full static solution that shifts the data to a final flat datum has been applied prior to imaging. Shot gathers before and after data processing are illustrated in Figure 4. It can be observed that the conditioning steps have increased signal-to-noise ratio (SNR) and vertical resolution of the seismic records.

Seismic data imaging

Seismic imaging (migration) is the final step applied to the seismic data that moves reflection events to their true spatial location. Since migration is essentially an inverse process to seismic modelling, its natural computation region is depth.

Geophysical Prospecting EAGE EUROPEAN ASSOCIATION OF GEOSCIENTISTS & ENGINEERS

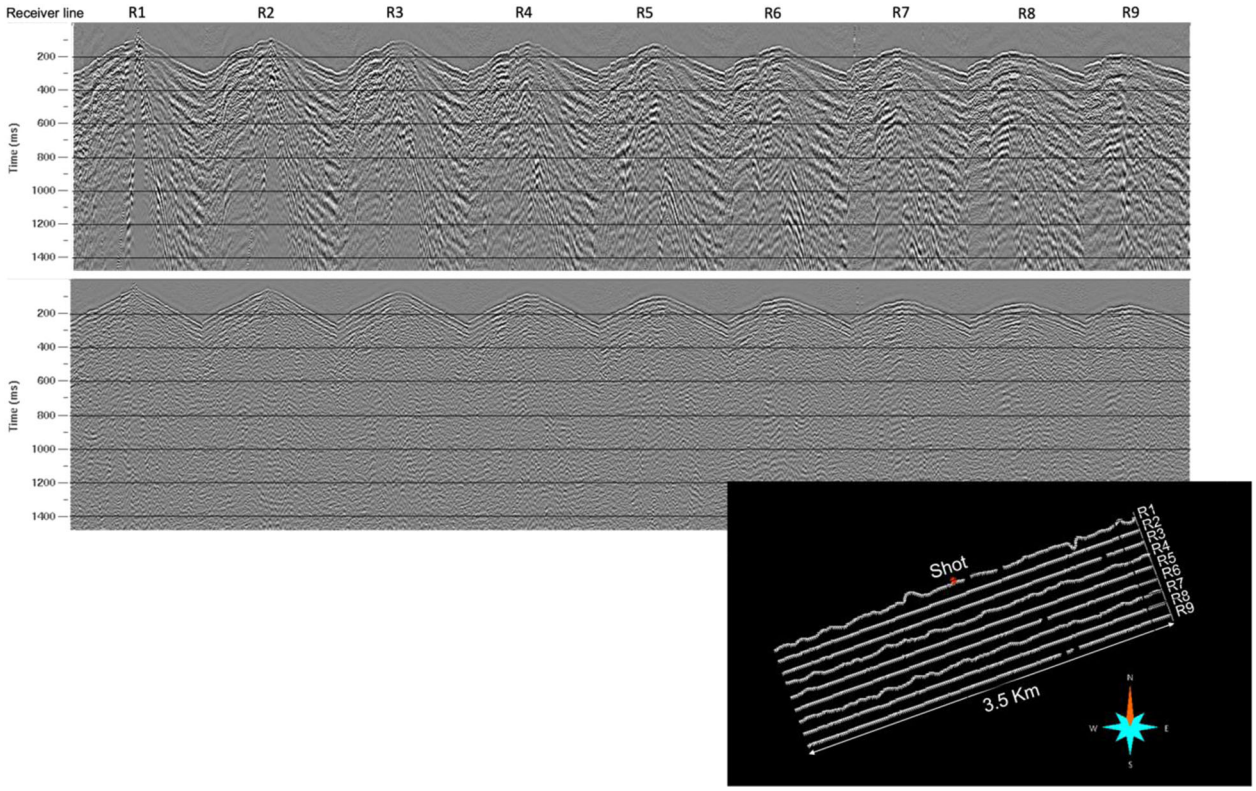

FIGURE 4 Sample of the raw shot (top) and processed data (bottom) with display automatic gain control (AGC) of 500 ms, with shot and receiver positions (insert)

TABLE 1 Recording parameters

Source type	Vibroseis INOVA AHV-IV
Electronics	Pelton VibPro HD
Sweep frequency range	6–120 Hz
Sweep duration	14 seconds
Sweep type	Linear
Tapers	300 ms (cosine)
Vibrator array	1 vibe active
Record length	3 seconds
Operating Force (terrain dependant)	70%
Total number of shots	41,773
Total number of receivers	70,628
Acquired number of receiver lines per patch	24
Acquired receivers per line	300
Acquired stations per patch	7200
In-line receiver interval	15 m
X-line receiver interval	90 m
In-line source interval	15 m
X-line source interval	90 m
Minimum offset	7.5 m
Maximum offset	2450 m

TABLE 2 Processing flow

1.	SGY input
2.	Geometry assignment and verification using a nominal bin size of 7.5 × 7.5 m
3.	First break picking and quality control
4.	Trace edits for anomalous traces
5.	Refraction tomography and refraction static application (to a floating datum)
6.	Multichannel filtering in time–frequency domain
7.	Zero-phase spike deconvolution (Wiener-Levinson, least square algorithm)
8.	Ormsby bandpass filter (8–18–90-120 Hz)
9.	Surface consistent amplitude compensation
10.	Coherent noise attenuation in frequency-space domain
11.	Application of residual statics calculated by maximizing CDP stack power
12.	Offset regularization (50-m offset bin size) for KDM only

In practice, however, migration can be applied in either time or depth, before or after CDP stacking. These processes are known as pre-stack and post-stack migrations, respectively. Time migration produces an image in two-way travel time, utilizing a simplified extrapolation of the wavefield. Because of that, it is a more robust process when it comes to imperfections or smaller errors in the velocity model. Depth imaging

directly outputs images in depth and accommodates for lateral velocity changes as it incorporates ray bending through a heterogeneous and anisotropic medium, mainly attributed to a more accurate wavefield extrapolation and imaging principle. In this study, we focused on pre-stack 3D depth migration techniques that in recent years have been successfully used in oil and gas exploration. The challenge in a hard rock environment is how to appropriately apply them in a complex geological environment that produces discontinuous reflections with low SNR, such as that experienced at Carosue Dam.

If the basic migration assumptions are met, the quality and accuracy of the migrated image largely depend upon the type of migration. The following are common basic migration assumptions (Dondurur, 2018):

- All reflection events are a result of primary reflections, and the data are devoid of noise components and S waves.
- Velocities at every sample location of the seismic event are known.
- There are no out-of-plane reflections (applicable for 2D migration).

Seismic migration is a reflection imaging process, and we must make sure that the input data only contain reflections. During the seismic data conditioning stage, all non-reflected waves such as surface, air-wave and diving waves are attenuated.

The second assumption is immensely more difficult to accomplish. Vertical velocity distribution can be obtained from a reliable sonic log or velocities from vertical seismic profiling (VSP). However, borehole velocities provide only a one-dimensional function and do not necessarily match with the migration velocity, which undergoes 3D wave propagation. The only way to assess a 3D velocity model is through the surface seismic method.

Imaging structural complexities in the near surface (top 1 km) of the Carosue Basin are of critical importance for exploration and, consequently, time imaging has to be replaced by depth imaging techniques to accommodate for the lateral velocity variations of the subsurface (Buzlukov & Landa, 2013). Lateral velocity variations are often associated with complex geology and the depth migration algorithm has the ability to accommodate such features, including steep dips (Yilmaz, 2001).

METHODS

Kirchhoff's integral migration is a ray-based migration method widely used in both time and depth domains due to its effectiveness and robustness. In the depth domain, it is based on solutions of the wave equation, assuming a high-frequency approximation. Thus, seismic waves approximate rays and ray paths, with the assumption that the scale of the structure is greater than the seismic wavelength (Etgen et al., 2009; Jones, 2003). However, ray-based migration methods rely on a gently varying smooth velocity field for calculating travel times, which make these less accurate than wavefield extrapolation-based methods such as reverse time migration (RTM).

The Kirchhoff depth migration (KDM) process is computed in two stages:

1. Travel time table calculation, using dynamic ray tracing or a solution to the Eikonal equation.
2. Collection of the associated data samples within the migration aperture and their summation.

Our application of the KDM algorithm utilized ray tracing in a 60 × 60 m grid. Offset bin increment was 50 m, with an anti-aliasing filter applied. The maximum migration aperture was 6 km, limited by an 80° migration angle.

Due to the efficiency of its implementation and computation, we use KDM to iteratively update the velocity model and RTM for the final imaging solution.

RTM is the most effective way to image complex structures and handle strong velocity variations. It uses the wave equation to model complete wavefronts. In general, the RTM method is based on two key steps:

1. Forward propagation of the source wavefield and backward propagation of the receiver (recorded) wavefield.
2. Construction of the image by applying the imaging condition.

RTM is able to solve most imaging challenges but is characterized by expensive computational costs and significant computer memory demands. An increase in maximum frequency causes the run times to increase exponentially. The concept of wavefield extrapolation migration was first proposed 50 years ago (Claerbout, 1971), and it was only in recent years, with the expansion of digital technology, that the RTM method became a widely used imaging method in oil and gas seismic exploration. With the advent of commercial cloud computing, these algorithms are now accessible on a broader scale.

RTM is a two-way wave extrapolation method and employs both the down-going and up-going wavefields. The imaging condition is obtained by cross-correlating the two wave fields at each time step (Claerbout, 1971). However, it is expected that due to differences in the amplitudes of up-going and down-going wavefields, the correlation can introduce long-period artefacts, especially in areas of strong velocity contrast

Geophysical Prospecting EAGE EUROPEAN ASSOCIATION OF GEOSCIENTISTS & ENGINEERS

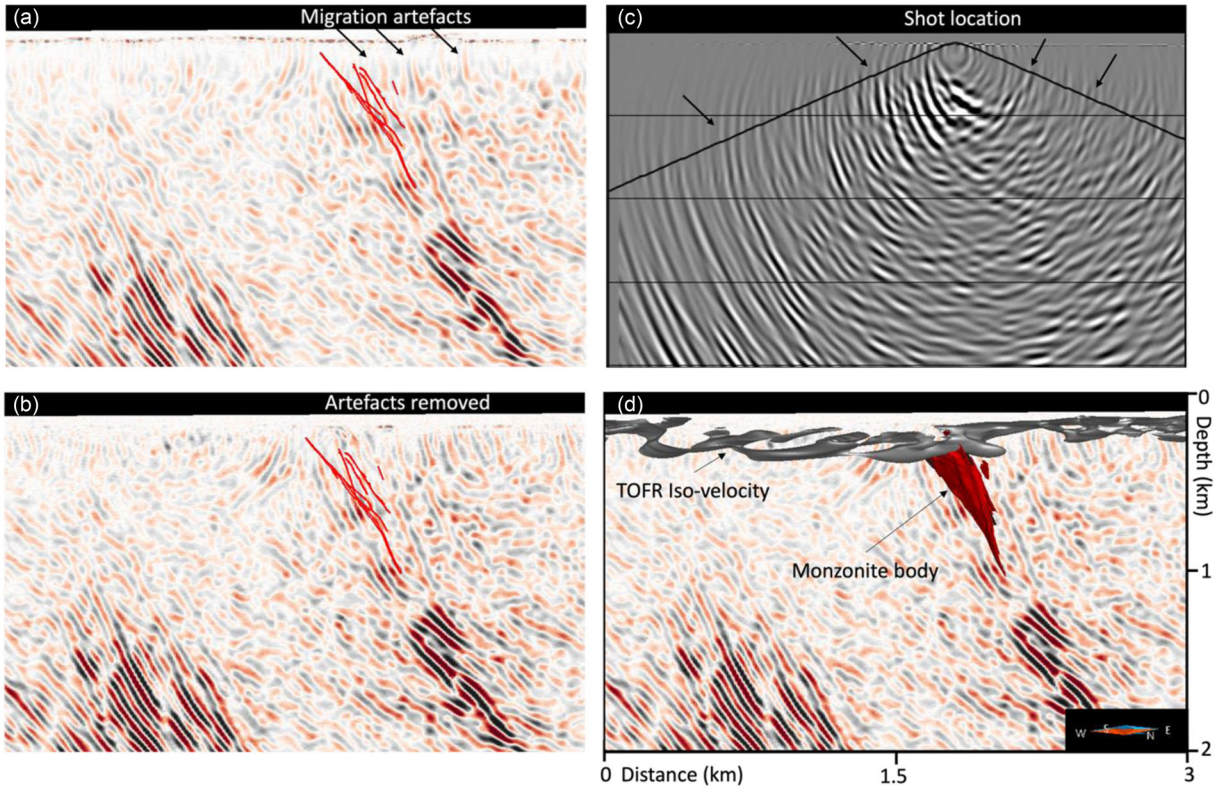

FIGURE 5 RTM artefact removal. Due to strong velocity contrast in the near surface, the reflectors in RTM stacked volume are curving beyond 90° (a). After the application of post-migration mute the artefact disappears (b), the reflectors extend to the TOFR, without curving. Straight and steeply dipping reflectors are verified by a monzonite wireframe from borehole measurements. The mute function is illustrated on a single migrated shot record (c), the iso-velocity of 5700 m/s that approximates TOFR, and a monzonite body is overlain on RTM stack with artefacts removed (d)

(Robein, 2010). We observe significant RTM noise in the shallow, near the top of fresh rock (TOFR). This was in turn mitigated through the application of a Laplacian filter and trace muting in the pre-summation process (Figure 5).

The algorithm is applied on processed shot gathers, producing a migrated volume for each shot. To test computation speed and the parameters for RTM, we migrated 2% of all shot records in the southern region of the survey. Figure 6 shows an assessment of the maximum frequency to be used for the final migration run. The final parameters were a maximum frequency of 60 Hz and an aperture of 6 km to match the KDM imaging distance. It was found that sorting the RTM data into common image point (CIP) gathers comes at a great computational cost as well. For this reason, we have run RTM on the full data set only once using the final velocity model and final choice of parameters.

Final depth migrations were computed using a depth interval of 6 m and a CDP binning grid of 7.5×7.5 m. Both algorithms migrate data from a smooth surface directly to the final flat datum. This excludes the need to use a static shift and an assumed replacement velocity to shift data to a final flat datum, reducing ambiguity caused by near-surface velocities.

Handling the near surface

The success of pre-stack depth migration methods largely depends on the accuracy of the velocity model. One of the critical issues the seismic method faces in a hard rock environment is the effect of the low-velocity zone associated with weathering and its consequences on imaging quality. In many hard rock seismic projects, the velocity change from overburden to the fresh rock is drastic and varies over such small distances that even depth imaging cannot fully resolve this problem. In this study, the near-surface velocity model was built using the approach introduced by Singh et al. (2019). The method involves applying a floating datum refraction static to first-arrival times, which are then used in refraction tomography to compute a velocity model for imaging.

A non-linear, first-arrival tomographic travel time inversion (Zhang & Toksöz, 1998) was run until convergence to a unique solution was achieved. Upon each iteration, ray tracing was used to compute synthetic travel times and minimize the difference between the measured times and synthetic first break picks. The process resulted in a detailed velocity model of the near surface (Figure 7) that was used to compute

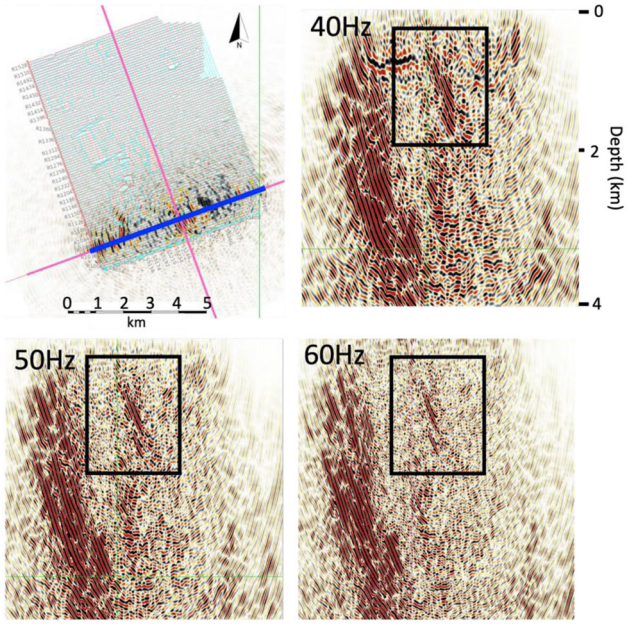

FIGURE 6 Maximum frequency test for RTM. Highlighted (blue) is the position of the section. Top left is a plan view of the stacked volume. A total of 2% of shot records have been migrated using 40, 50 and 60 Hz maximum frequency. Highlighted in the square is the Karari deposit zone with an expected east-dipping reflector. The reflector is best resolved with a maximum frequency of 60 Hz

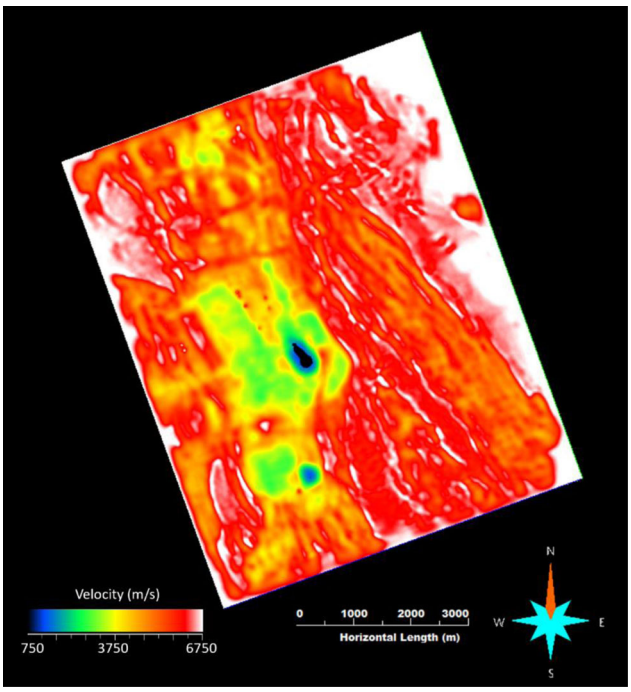

FIGURE 7 Velocity model from refraction tomography, confirming NW-SE trend of stratigraphic sequences illustrated in geology map. Velocity-depth slice at 300 m below surface. Low-velocity areas (blue to green) relate to mining infrastructure (pits, waste dumps or tailings dams)

refraction tomo-statics, as well as for the interpretation of the TOFR.

As refraction tomography provided velocities down to the TOFR, the initial velocity model has been extended using a pre-stack time migration (PSTM) velocity model converted to interval velocity and smoothed in a 600 × 600 × 600 m (*X, Y, Z*) grid. A large smoother was used to avoid the introduction of velocity errors in the initial velocity model for migration.

Velocity model building

Velocity updates using pre-stack reflection tomography have been widely used in the oil and gas seismic industry. It requires large enough source–receiver (S-R) offsets, good reflectivity and CIP gathers that have been migrated with an appropriate initial velocity model. The initial velocity model needs to be accurate in the near surface, because low trace fold and small S-R offsets mean the reflection tomography will not be able to update the velocity model.

In Figure 8 we are revisiting the deepest borehole WDX047, where we compare refraction topography using raw first arrivals, to the initial velocity model, final velocity model and the sonic log. We notice that due to different angles of wave propagation, the values of velocities show a substantial difference. Velocity overlays show that values vary from 4800 to 6100 m/s. All models converge at approximately 200 m of depth and a velocity value of 5700 m/s. This iso-velocity is extracted from refraction tomography and used for the interpretation of the TOFR (Figure 16). Down to 200 m depth our initial velocity model was built using the Singh et al. (2019) approach, which is consequently a smooth version of raw refraction tomography, while the deeper velocity is guided by interval velocities from PSTM with a maximum value set to 6100 m/s, based on the maximum velocity of sonic logs. This smoothed initial velocity model will be updated using several iterations of KDM followed by grid-based reflection tomography.

The pre-stack reflection tomography method uses multiple iterations of residual moveout (RMO) analysis on a sparse (60×60 m) grid and depth-migrated CIP gathers to update the initial model. The grid-based tomography method has been described by Woodward et al. (2008). The process is repeated until the velocity error between input and output model is minimized (Tanis et al., 2006). To QC velocity updates a γ attribute was computed. It is a unitless measure of the RMO depth error, represented as a fraction of the reference depth of the primary event on a CIP.

$$Z^2 = Z_0^2 + \left(\gamma^2 - 1\right) X^2, \tag{1}$$

where Z is the depth of the event, Z_0 is the depth at the referenced offset, γ is the gamma factor, and X is the offset.

Geophysical Prospecting EAGE EUROPEAN ASSOCIATION OF GEOSCIENTISTS & ENGINEERS

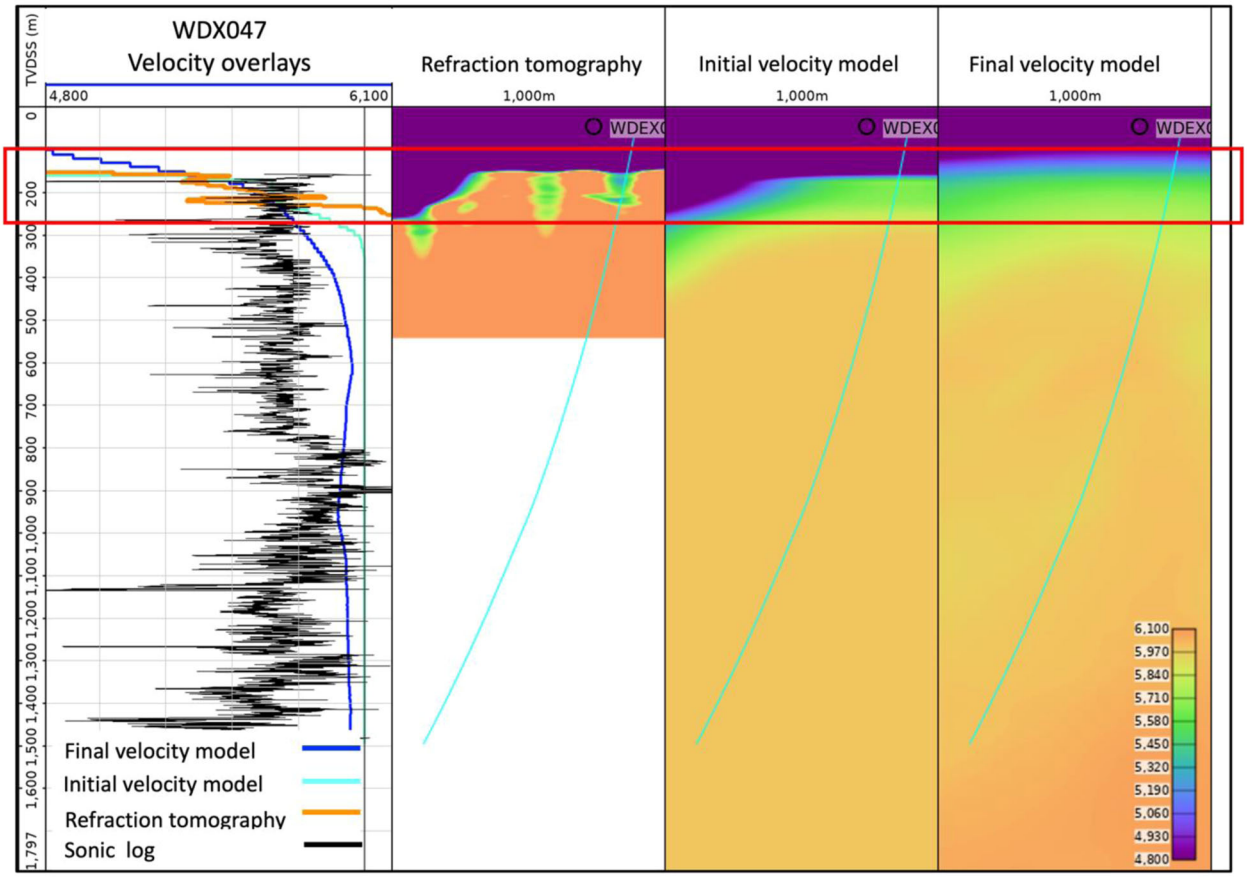

FIGURE 8 Displays of V_p sonic log, refraction tomography, initial and final velocity model surrounding the borehole location. Highlighted is the zone where all velocities converge

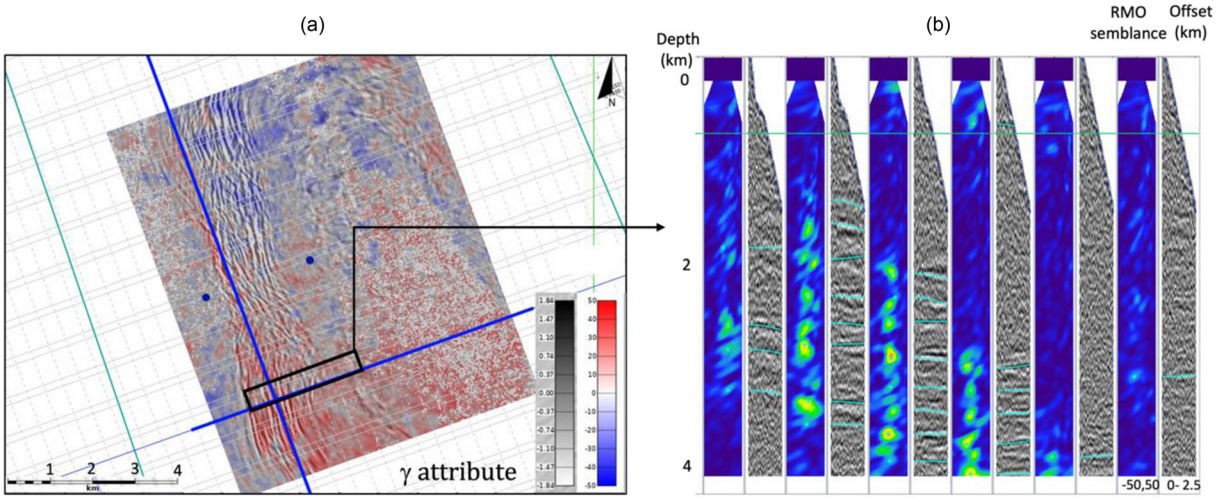

FIGURE 9 RMO used for γ attribute calculation is automatically estimated from conditioned CIP gathers. PSDM overlain with γ attribute, depth slice at 2.5 km indicates velocity errors in the initial model. Blue, gathers curving up; red, gathers curving down (a); CIP gathers with corresponding RMO semblance (b)

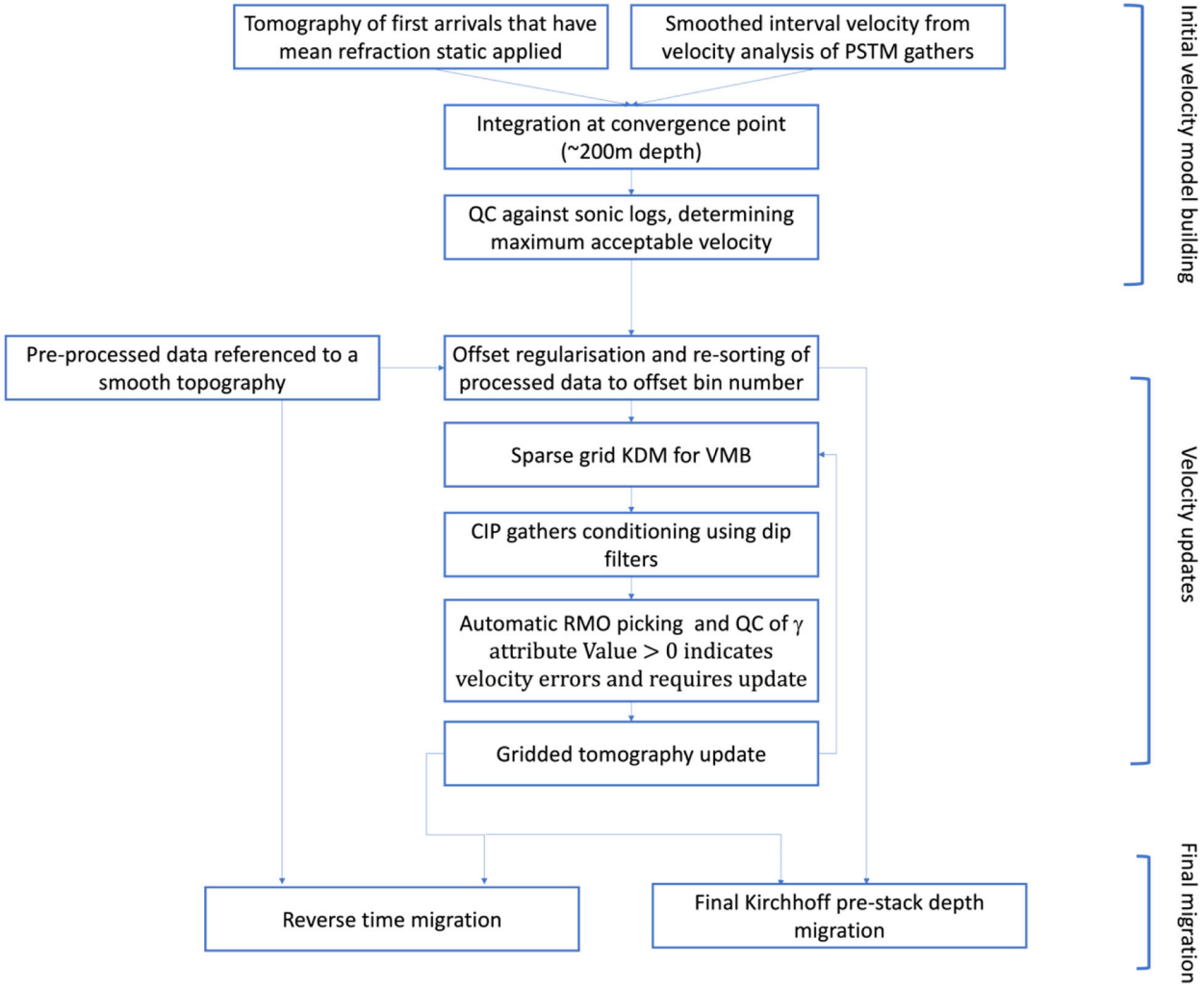

FIGURE 10 A block diagram of velocity model building (VMB) and depth imaging workflow

Figure 9 shows a γ attribute of the full survey at a depth slice of 2.5 km and sample of CIP gathers for the first iteration of velocity model building. Pre-conditioning of gathers involved dip filtering and coherency filters to remove remaining coherent noise and improve S/N ratio, respectively. A block diagram of the process is illustrated in Figure 10. Iterations were focused on correcting velocity discrepancies observed in shallow zones and then progressively worked deeper to update the entire velocity model.

Figure 11 shows a comparison of the final KDM stack and final velocity model. We can notice the correlation between reflectors and velocity anomalies. A comparison of CIP gathers shows that the final velocity model better flattens reflectors than the initial model (Figure 12).

RESULTS

One of the main aims of our analysis was to evaluate the effectiveness and accuracy of depth imaging solutions in a hard rock environment. For this purpose, we validated depth imaging results against the legacy pre-stack time migration (PSTM), refraction tomography, drillholes, modelled wireframes, magnetics and vertical seismic profiling (VSP)-migrated section.

In Figures 13 and 14, we compare the initial PSTM, Kirchhoff depth migration (KDM) and reverse time migration (RTM). The PSTM volume was processed shortly after acquisition of the seismic, independently of this study. Both depth-imaged sections have enhanced steep dips, better resolved the near surface and contained fewer migration artefacts when compared with the legacy PSTM. In comparison to KDM, the RTM results have better-defined steep dips, particularly in the near surface. The higher wavenumber of KDM is beneficial in resolving discreet contacts, while RTM has clearer reflector terminations and faults, such as the Young Fella fault highlighted in Figure 14. The monzonite wireframes modelled from drilling show a good correlation with KDM and RTM sections and confirm the steeper dips that depth imaging resolves well. This correlation is a testament

Geophysical Prospecting EAGE EUROPEAN ASSOCIATION OF GEOSCIENTISTS & ENGINEERS

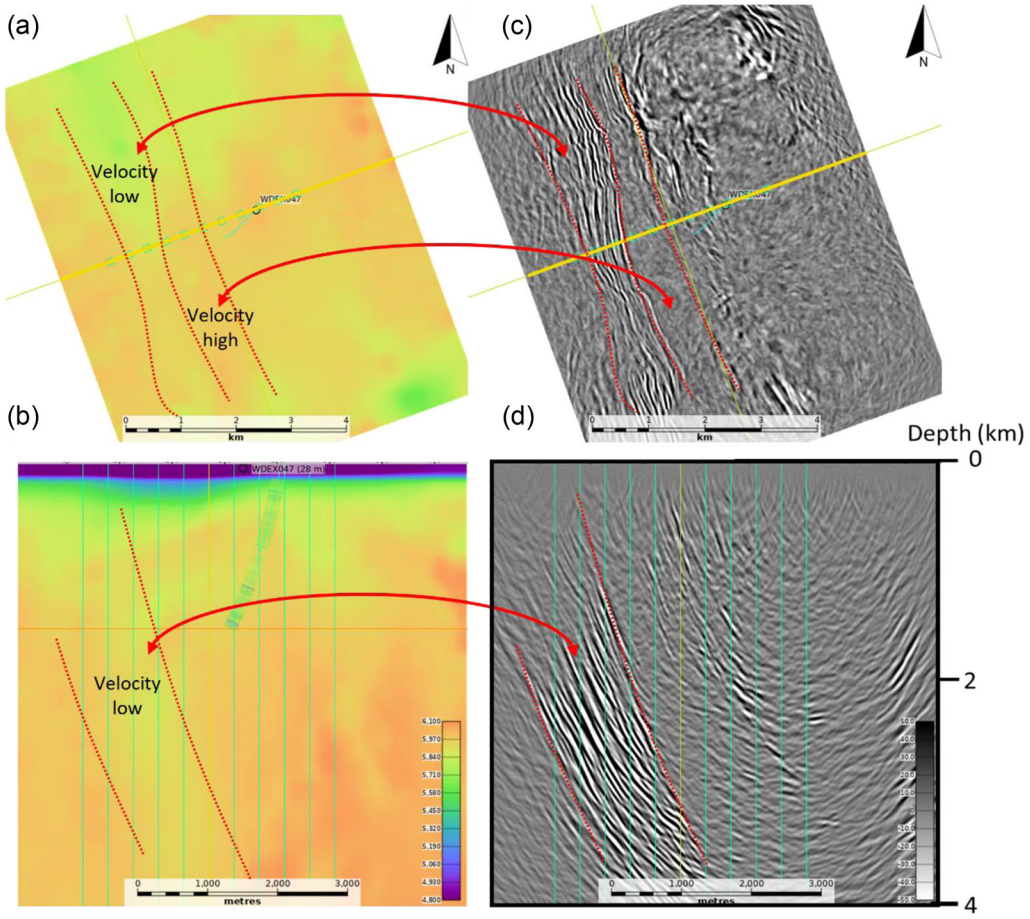

FIGURE 11 Final velocity model depth slice at 1.5 km (a) and W-E section view (b), with corresponding final KDM depth slice (c) and section view (d). The correlation between anomalies in the velocity model and KDM stack migrated with the final velocity model is highlighted with a red arrow

to an effective high-density seismic design and an appropriate depth imaging workflow being applied.

DATA INTERPRETATION AND DISCUSSION

To validate the depth imaging results, we compared them against other seismic outputs. Refraction tomography uses first-arrival measurements to compute a detailed near-surface velocity model. The correlation between steep dips observed in the depth imaging volumes and a depth slice from the velocity model shows an impressive correlation (Figure 15). The near surface is the hardest zone to image, and the match between these two seismic outputs is accurate to within a couple of metres.

In Figure 16, we compare a blended instantaneous phase and energy attribute from the reverse time migration (RTM) volume at a depth slice 778 m below surface with the Carosue Dam geological map as well as a top of fresh rock iso-surface extracted from the refraction tomography with airborne magnetics. The four geological domains – Footwall Sedimentary Sequence, Central Mineralized Zone, Eastern Intrusive Complex and an Andesite Sequence – are easily recognized in the seismic data sets.

An overlay of drillhole measurements and the depth imaging results is shown in Figure 17a. The 'shape' of the drillhole represents acoustic impedance (AI) while colour corresponds to lithology. A reflection on the seismic image is expected where a change in AI is present. We can observe that reflectors broadly correlate well to AI changes. In some instances, changes in AI are related to the presence of mineralized structures. The high reflectivity domain in the reverse time migration volume correlates with mineralized monzonite intrusions.

Next, we compare our results with vertical seismic profiling (VSP) data acquired during the preliminary de-risking stage of the project in borehole WDX047. Another good correlation between surface and VSP migrated sections was achieved, although the resolution of the VSP is much higher (Figure 17b). This is expected because of the one-way travel path through the attenuative overburden and altogether shorter

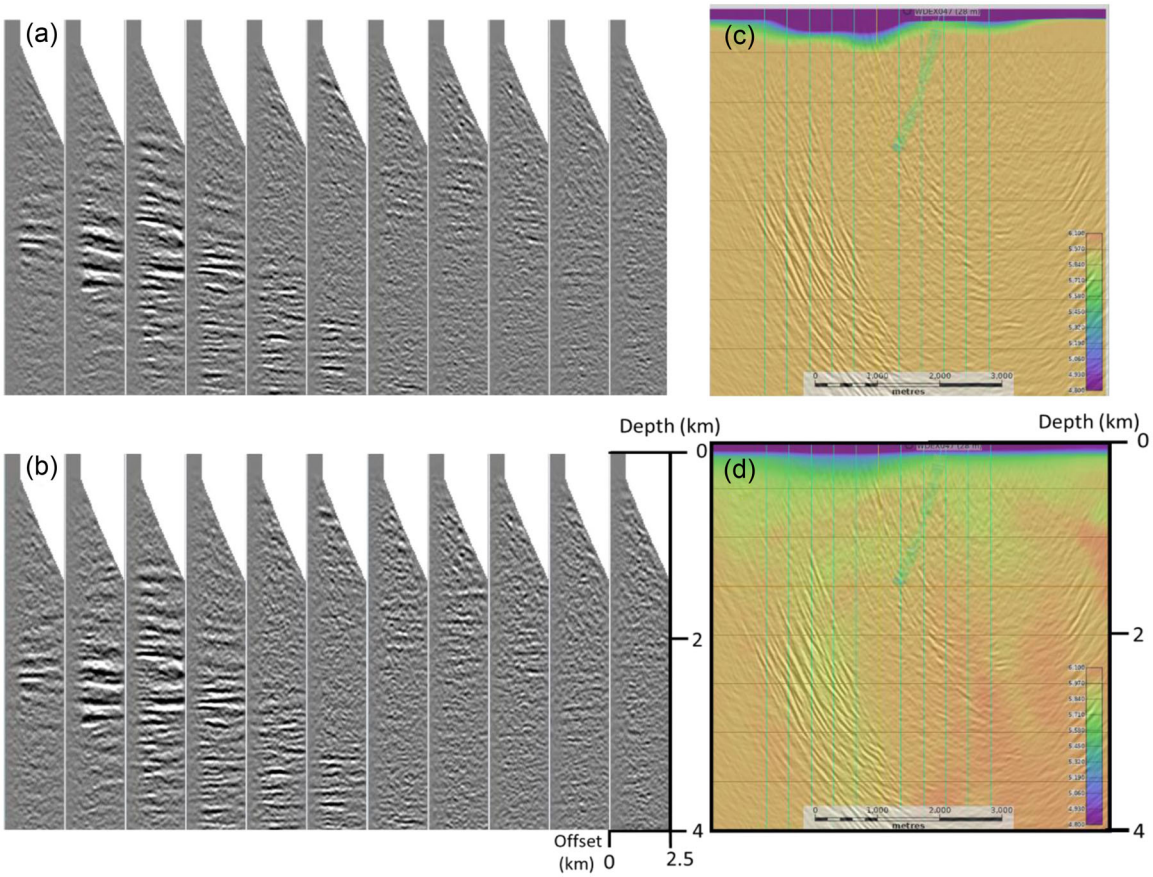

FIGURE 12 KDM gathers with the corresponding velocity model. CIP gathers migrated with the initial velocity model (a), using the final velocity model (b). Gathers are converted to time using migration velocities and scaled to depth using a final velocity model for comparison purposes. Initial velocity model with superimposed KDM stack and highlighted gather location, W-E section view (c). Final velocity model with final KDM stack (d)

propagation distance in VSP, which means less absorption of the higher frequencies. Overall, the match with drillhole data gives us confidence in the velocity model used for imaging as well as in the interpretation of this complex volume.

Several structures have been easily mapped in the RTM volume, with the most significant including the Osman Fault, the Resurrection fault and the reactivated Young Fella fault. By imaging these as well as other geological features, the 3D seismic survey was found to successfully verify, update and extend the current geological model, map key lithologies and generate new drill targets. These can then be used to accelerate subsurface characterization to inform decisions throughout the life of mine.

Finally, we compare the run time of fast-track pre-stack time migration (PSTM), Kirchhoff depth migration (KDM) and RTM in reference to the imaging uplift. We use cloud computing technology to efficiently run processing and imaging flows on a multi-node system. The advantage of cloud computing is in its scalability, as we can use a large number of nodes for most processes. For example, using 100 nodes for 1 h results in the same computing cost as using 1 node for 100 h, except the latter option is not nearly as time-efficient.

Before computing a full-depth imaging process, it is important to estimate node hours required for the job, which will reflect the run cost. PSTM and KDM node hours are estimated by running a single offset plane and multiplying the run time with the total number of offset planes. RTM run time is assessed from a single shot, or for better accuracy, a selection of shots belonging to the same swath. In Figure 6, we illustrated the RTM imaging outcome using only 2% of available shot records, with different maximum frequencies imaged. The estimated full run is extrapolated to be 50 times longer.

Our final PSTM, KDM and RTM runs, using 50 nodes, each node consisting of 30 cores, 256 Gb Random Access Memory (RAM), took 50, 70 and 100 h, respectively. This makes RTM ~50% more expensive to run, compared with KDM. Even so, considering the uplift in imaging steep reflectors and faults, we are encouraged to regularly run RTM on our 3D data.

The velocity model building process is what makes depth imaging a significantly longer to run technique compared

Geophysical Prospecting EAGE EUROPEAN ASSOCIATION OF GEOSCIENTISTS & ENGINEERS

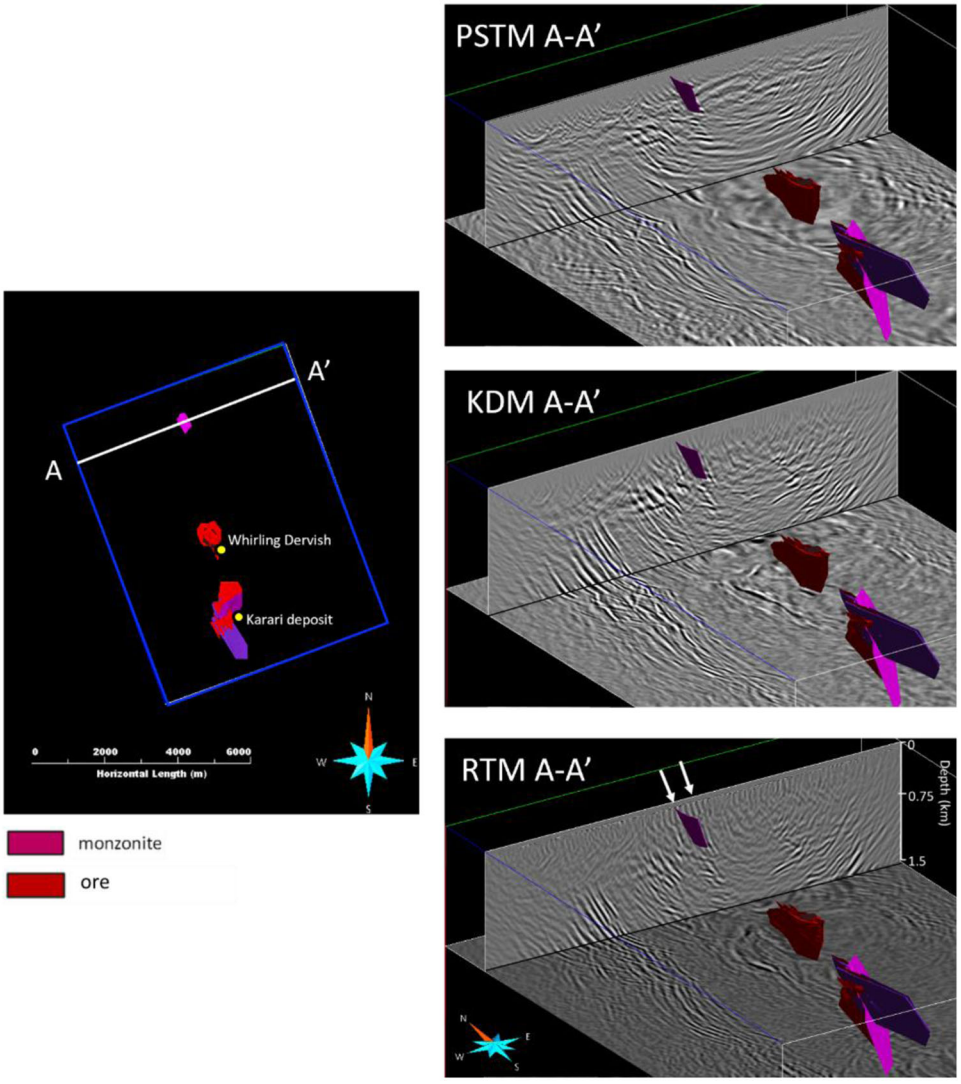

FIGURE 13 Comparison of imaging results in the north region of the survey. Inline A-A' section has no vertical exaggeration; depth slice is at 1.5 km from surface. Legacy PSTM is scaled to depth using smoothed velocity from depth imaging. KDM and RTM show improved imaging of steep dips particularly in near surface and better-resolved reflectors in depth slice. PSTM suffers from migration artefacts (migration swings) and unreliable near surface. Highlighted in white arrows are east-dipping reflectors indicating a good correlation with monzonite models measured from boreholes

with time imaging. It included 10 iterations of refraction tomography and four iterations of sparse KDM each followed by reflection tomography. It took us two months to achieve the final velocity model for depth imaging, twice as long as the time processing and fast-track PSTM. However, the imaging uplift from both KDM and RTM migrations, with respect to precision of reflector positioning in 3D space is of essence in the mining industry, therefore justifying the extended imaging timeline.

CONCLUSIONS

A tailored approach to the application of depth imaging techniques applied to seismic data recorded over a complex geological environment in a mineral exploration context is proposed and implemented in this study. Pre-stack depth imaging (Kirchhoff and reverse time migration (RTM)) achieved a high degree of correlation between depth migration solutions compared with drillhole data, magnetics, refraction tomography and VSP. This further highlights the importance and role of depth imaging for the delineation of complex hard rock environments. The proposed workflow for velocity model building was of key importance for the successful application of depth imaging techniques and ultimately in developing an efficient methodology for hard rock data imaging.

This study demonstrated that both PSDM algorithms when coupled with appropriate velocity model building showed significant uplift when compared with the initial time imaging, especially in the critical top 1 km and as shallow as the TOFR.

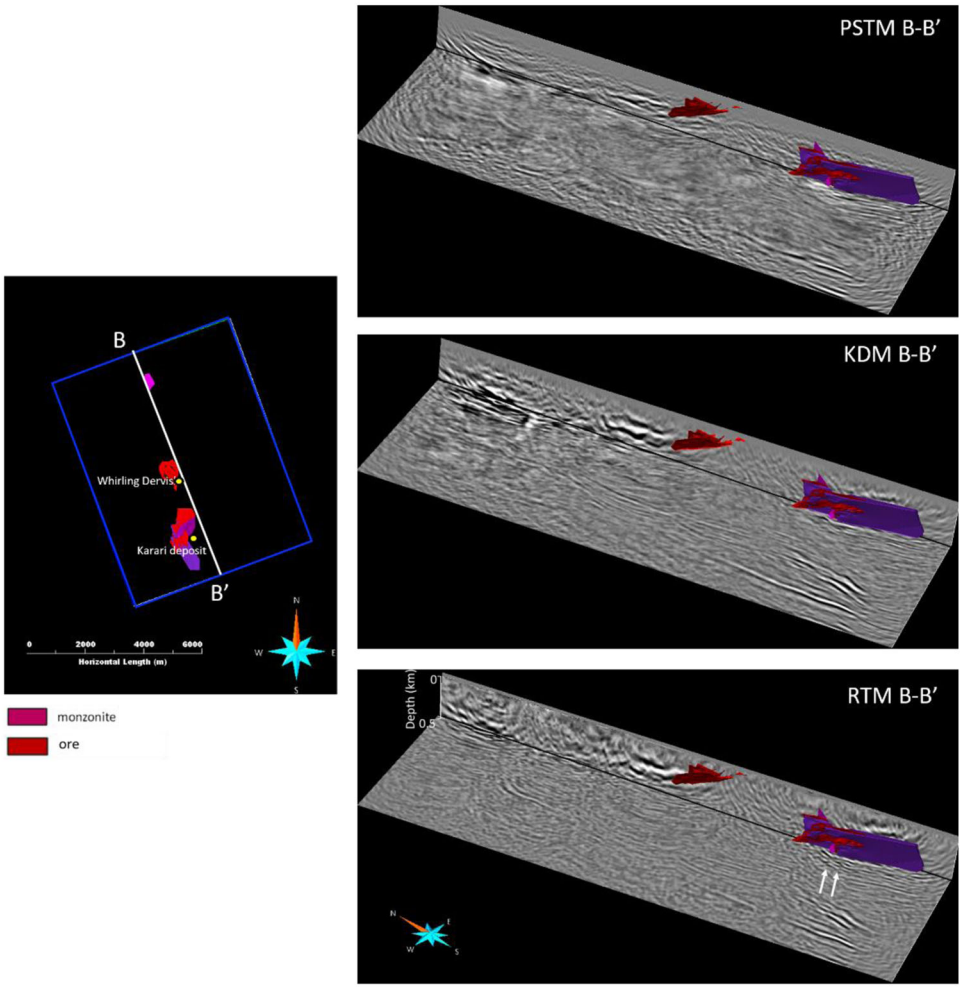

FIGURE 14 Comparison of imaging results across Whirling Dervish and Karari mine. Crossline B-B' section has no vertical exaggeration; depth slice is at 500 m from the surface. Legacy PSTM is scaled to depth using smoothed velocity from depth imaging. KDM and RTM show excellent correlation with existing ore and monzonite surfaces from drilling. Highlighted in white arrows are faults visible on RTM volume in the Karari basin

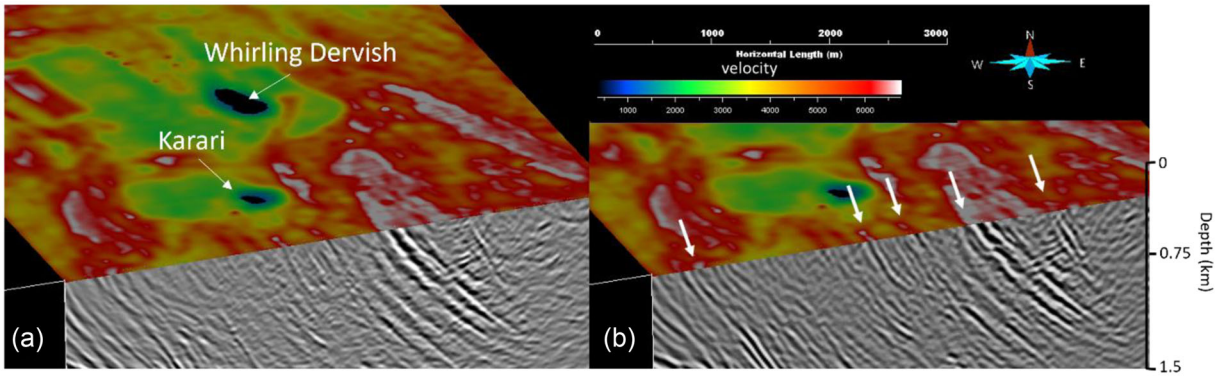

FIGURE 15 Comparison of KDM (a) and RTM (b) stacked volume in the area of the Karari deposit. Depth slice at 300 m below the surface corresponds to refraction tomography. Both volumes show a good correlation against velocity anomalies on refraction tomography. White arrows on RTM volume highlight the contact of steep reflectors with higher velocities on the depth slice

Geophysical Prospecting EAGE EUROPEAN ASSOCIATION OF GEOSCIENTISTS & ENGINEERS

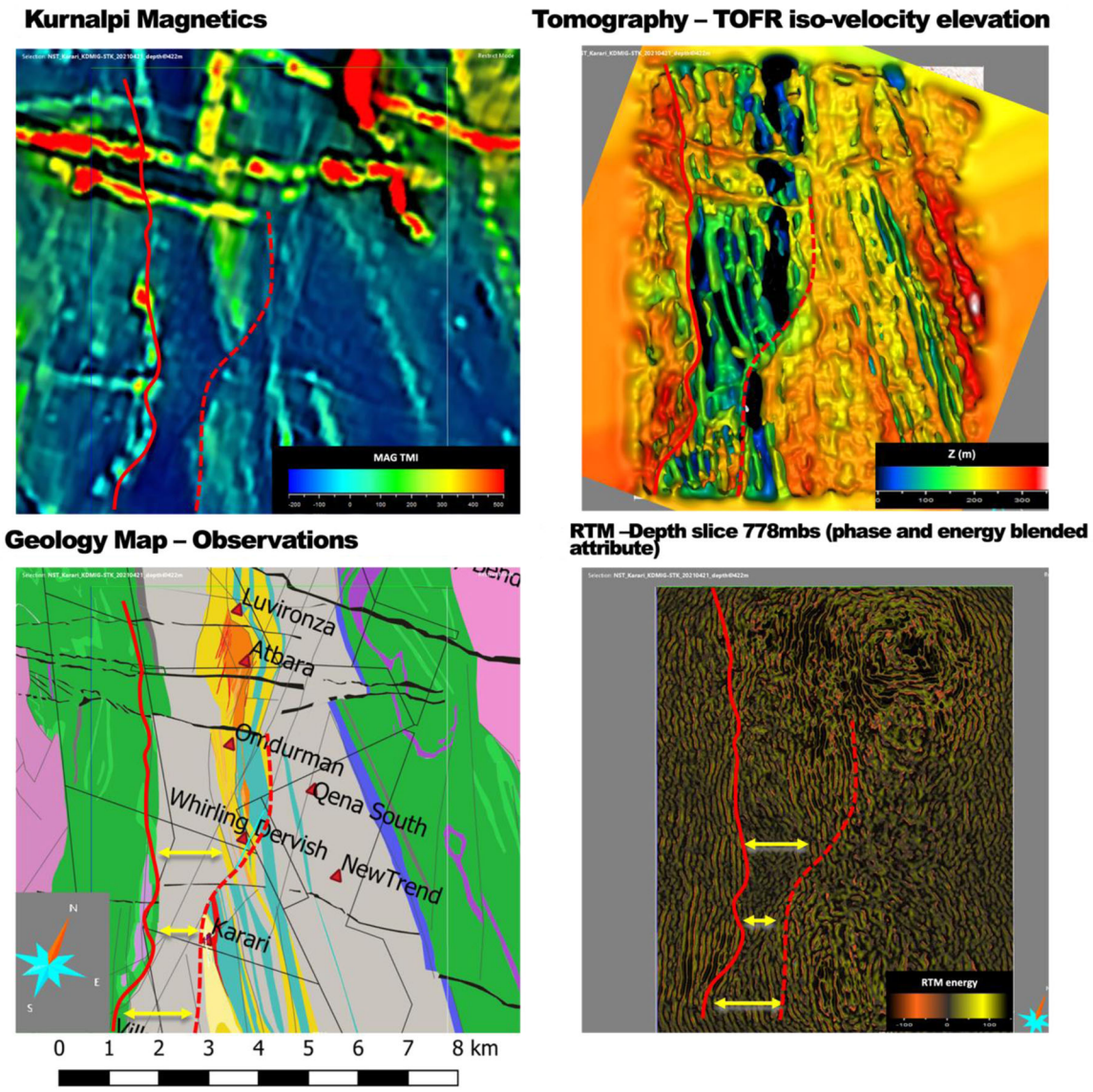

FIGURE 16 Observation of depth slice and comparison with other data sets. Red line demarcates high reflectivity mafic and possible domain bounding Keith Kilkenny thrust. Overall, a good correlation is observed between different data sets with respect to the separation of lithologies and major structures. Rock description in the geological map is given in Figure 1

A specific velocity model building technique, that involves drillhole data integration and tomographic refinement proved effective for hard rock seismic imaging producing accurate images even in the near surface. Excellent correlation between resultant seismic images, refraction tomography, VSP and drillholes can be attributed to the appropriate velocity model used for depth migration. Although the RTM method is computationally more expensive than Kirchhoff's depth migration, it is preferred when detailed subsurface imaging is required.

This study sets a foundation for the future application of depth imaging approaches for the exploration of mineral resources. While we still work on improving the performance of our imaging approach applied to a hard rock environment, it is becoming clear that depth imaging will play a crucial role in the mineral sector due to its accuracy and resolution. Specific challenges associated with each new hard rock environment mean that some site-specific optimization may still be needed for improving the performance of depth imaging. Hence, at this stage, each depth imaging project should be considered as a unique study to extract maximum value from the seismic data set.

The proposed depth imaging methods led to improved ore identification which enabled the interment of an improved geological model that will guide drilling for future mine expansion.

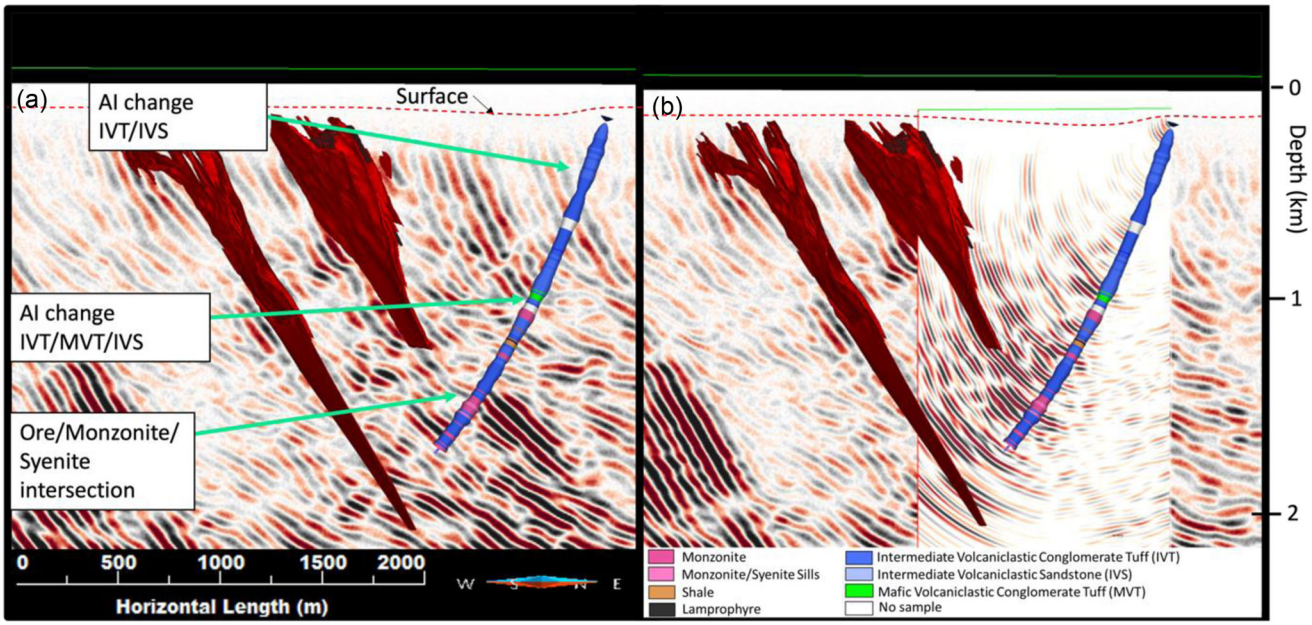

FIGURE 17 Overlay of deviated WDEX047 drillhole with RTM W-E section (a) and embedded with a VSP section (b). The shape of the drillhole is the acoustic impedance (AI) and colour corresponds to lithology. Reflections on the seismic image are expected where we have a change in acoustic impedance. We can observe that reflectors broadly correlate to AI changes and in particular with monzonite intrusions (red surface). In addition, a good correlation exists between RTM and VSP section, where VSP exhibits a higher resolution

ACKNOWLEDGEMENTS

We thank Northern Star Limited for permission to publish the work and for their support throughout the project. We acknowledge the support from Hisies team, especially from Ian James, Alexey Artemov, Reece Cunnold and Sana Zulic during various stages of the project, since the seismic feasibililty study began in 2017.

DATA AVAILABILITY STATEMENT

Research data are not shared.

REFERENCES

Adamczyk, A., Malinowski, M. & Melehmir, A. (2014) High-resolution near-surface velocity model building using full-waveform inversion – a case study from southwest Sweden. *Geophysical Journal of International*, 197, 1693–1704.

Adamczyk, A., Malinowski, M. & Górszczyk, A. (2015) Full-waveform inversion of conventional vibroseis data recorded along a regional profile from southeast Poland. *Geophysical Journal International*, 203, 351–365.

Berson, I.S. (1957) High-frequency seismic: Moscow, *USSR Academy of Science*, 239.

Bohlen, T., Mueller, C. & Milkereit, B. (2003) 5. Elastic Seismic-Wave Scattering from Massive Sulfide Orebodies: On the Role of Composition and Shape. https://doi.org/10.1190/1.9781560802396.ch5

Brodic, B., Malehmir, A., Pacheco, N., Juhlin, C., Carvalho, J., Dynesius, L. et al. (2021) Innovative seismic imaging of volcanogenic massive sulphide deposits, Neves-Corvo, Portugal – Part 1: In-mine array. *Geophysics*, 86, 165–179.

Broüning, L., Buske, S., Malehmir, A., Backström, E., Schön, M. & Marsden, P. (2020) Seismic depth imaging of iron-oxide deposits and their host rocks in the Ludvika mining area of central Sweden. *Geophysical Prospecting*, 68, 24–43.

Buzlukov, V. & Landa, E. (2013) Imaging improvement by prestack signal enhancement. *Geophysical Prospecting*, 61(6), 1150–1158.

Cassidy, K.F., Champion, D.C., Krapez, B., Barley, M.E., Brown, S.J.A., Blewett, R.S., Groenewald, P.B. & Tyler, I.M. (2006) A revised geological framework for the Yilgarn Craton: Western Australia Geological Survey, Record 2006/8.

Claerbout, J.F. (1971) Toward a unified theory of reflection mapping. *Geophysics*, 36(3), 467–481.

Dean, T., Tulett, J. & Barnwell, R. (2018) Nodal land seismic acquisition: the next generation. *First Break*, 36, 47–52.

de Wet, J.A.J. & Hall, D.A. (1994) Interpretation of the Oryx 3-D seismic survey. In: Anhaeusser, C.R. (ed.) *Proceedings XV CMMI Congress: SAIMM Symposium Series*, S14, 3, 259–270.

Ding, Y. & Malehmir, A. (2021) Reverse time migration (RTM) imaging of iron oxide deposits in the Ludvika mining area, Sweden. *Solid Earth*, 12, 1707–1718.

Dondurur, D. (2018) *Acquisition and processing of marine seismic data*. Amsterdam: Elsevier.

Durrheim, R.J. & Maccelari, M.J. (1991) Seismic exploration for preciousmetals in the hard rock environment: 61st Annual International Meeting, SEG, Expanded Abstracts, 159–162.

Eaton, D.W., Milkereit, B. & Adam, E. (1997) 3-D seismic exploration: *Proceedings of Exploration*, 65–78.

Etgen, J., Gray, S.H. & Zhang, Y. (2009) An overview of depth imaging in exploration geophysics. *Geophysics*, 74(6), WCA5–WCA17.

Hloušek, F., Hellwig, O. & Buske, S. (2015) Improved structural characterization of the Earth's crust at the German Continental Deep

Drilling Site using advanced seismic imaging techniques. *Journal of Geophysical Research: Solid Earth*, 120, 6943–6959.

Jones, I.F. (2003) A review of 3D preSDM velocity model building techniques. *First Break*, 21(3), 45–58.

Karaev, N.A. & Rabinovich, G.Y. (2000) *Ore seismic*. Moscow: Geoinformmark, 366 (in Russian).

Malehmir, A., Urosevic, M., Bellefleur, G., Juhlin, C. & Milkereit, B. (2012) Seismic methods in mineral exploration and mine planning. *Geophysics*, 77, WC1–WC2.

Milkereit, B., Adam E., Barnes A., Beaudry, C., Pineault, R. & Cinq-Mars, A. (1992) An application of reflection seismology to mineral exploration in the Matagami area, Abitibi Belt, Quebec. *Current Research, Part C*, 13–18.

Naghizadeh, M., Snyder, D., Cheraghi, S., Foster, S., Cilenšek, S., Floreani, E. & Mackie, J. (2019) Acquisition and processing of wider bandwidth seismic data in crystalline crust. *Progress with the Metal Earth Project: Minerals*, 9, 145. https://doi.org/10.3390/min9030145.

Nelson, D.R. (1997) Compilation of SHRIMP U-Pb zircon geochronology data, 1996. *Geological Survey of Western Australia*, Record 1997/2.

Pertuz, T., Melehmir, A., Bos, J., Brodic, B., Ding, Y., Kunder, R. & Marsden, P. (2022) Broadband seismic source data acquisition and processing to delineate iron oxide deposits in the Blötberget mine, central Sweden. *Geophysical Prospecting*, 70, 79–94.

Pretorius, C.C., Jamison, A.A. & Irons, C. (1989) Seismic exploration in the Witwatersrand Basin, Republic of South Africa. Proceedings Exploration 87, Third Decennial International Conference on Geophysics and Geochemoical Exploration for Minerals and Groundwater. Special Publication, Ontario Geologic Survey, 3, 241–253.

Pretorius, C.C. & Trewick, W.F. (1997) Application of 3D seismics to mine planning at Vaal Reefs Gold Mine, number 10 shaft, Republic of South Africa. Proceedings of Exploration 97: Fourth Decennial International Conf. on Mineral Exploration, Prospect. and Development Assoc. of Canada, 399–408.

Robein, E. (2010) *Seismic imaging: a review of the techniques, their principles, merits and limitations (EET 4)*. Houten: Earthdoc.

Schetselaar, E. Bellefleur, G. & Hunt, P. (2019) Elucidating the effects of hydrothermal alteration on seismic reflectivity in the footwall of the Lalor Volcanogenic Massive Sulfide Deposit, Snow Lake, Manitoba, Canada. *Minerals*, 9, 384. https://doi.org/10.3390/min9060384.

Singh, B., Malinowski, M., Górszczyk, A., Melehmir, A., Buske, S., Sito, Ł. & Marsden, P. (2022) 3D high-resolution seismic imaging of the iron oxide deposits in Ludvika (Sweden) using full-waveform inversion and reverse time migration. *Solid Earth*, 13, 1065–1085.

Singh, B., Malinowski, M., Hloušek, F., Koivisto, E., Heinonen, S., Hellwig, O. et al. (2019) 3D seismic imaging in the Kylylahti mine area, Eastern Finland: comparison of time versus depth approach. *Minerals*, 9(5), 305. https://doi.org/10.3390/min9050305.

Stolz, E., Urosevic, M. & Connors, K. (2004) Reflection seismic surveys at St. Ives gold mine, WA. *Preview*, 111, 79.

Swager, C.P. (1997) Tectono-stratigraphy of late Archaean greenstone terranes in the southern Eastern Goldfields, Western Australia. *Precambrian Research*, 83, 11–42.

Tanis, M.C., Shah, H., Watson, P.A., Harrison, M., Yang, S., Lu, L. & Carvill, C. (2006) Diving-wave refraction tomography and reflection tomography for velocity model building: 76th Annual International Meeting. SEG, Expanded Abstracts, 3340–3344.

Urosevic, M., Stolz, E. & Massey, S. (2005) Seismic exploration of complex mineral deposits – Yilgarn Craton, Western Australia. 67th Conference of European Association of Exploration Geophysics, Madrid, Spain, Z-99.

Urosevic, M., Kepic, A., Stolz, E. & Juhlin, C. (2007) Seismic exploration of mineral deposits in Yilgarn Craton, Western Australia. Proceedings of Exploration 07: Fifth Decennial International Conference on Mineral Exploration, Toronto, Canada.

Urosevic and Evans. (2007a) Feasibility of seismic methods for imaging gold deposits in Western Australia, M363 project. Report No. 267, Minerals and Energy Research Institute of Western Australia, Report No. 267, 1–99.

Urosevic, M., Bhat, G. & Grochau, M.H. (2012) Targeting nickel sulfide deposits from 3D seismic reflection data at Kambalda, Australia. *Geophysics*, 77, 123–132.

Urosevic, M. (2013) What can seismic do for you?, 23rd International Geophysical Conference and Exhibition, Melbourne, Australia.

Urosevic, M., Bona, A., Ziramov, S., Pevzner, R., Kepic, A., Egorov, A. et al. (2017) Seismic for mineral resources – a mainstream method of the future. Proceedings of Exploration 17: Seismic Methods and Exploration Workshop, edited by G. Bellefleur and B. Milkereit.

Witt, W.K., Mason, D.R. & Hammond, D.P. (2009) Archean Karari gold deposit, Eastern Goldfields Province, Western Australia: a monzonite-associated disseminated gold deposit. *Australia Journal of Earth Sciences*, 56(8), 1061–1086.

Woodward, M.J., Nichols, D., Zdraveva, O., Whitfield, P. & Johns, T. (2008) A decade of tomography. *Geophysics*, 73(5), VE5–VE11.

Yilmaz, Ö. (2001) *Seismic data analysis: processing, inversion, and interpretation of seismic data*. Houston, TX: Society of Exploration Geophysicists.

Zhang, J. & Toksöz, N. (1998) Nonlinear refraction traveltime tomography. *Geophysics*, 1726–1737.

Ziramov, S., Dzunic, A. & Urosevic, M. (2015) Kevitsa Ni-Cu-PGE deposit, North Finland? A seismic case study. *ASEG Extended Abstracts*, 2015(1), 1–4.

Ziramov, S., Kinkela, J. & Urosevic, M. (2016) Neves-Corvo 3D: a high-resolution seismic survey at a Mine Camp Scale: Near Surface Geoscience 2016, 22nd European Meeting of Environmental and Engineering Geophysics, Barcelona, Spain, 4–8 September 2016, cp-495-00188.

How to cite this article: Ziramov, S., Young, C., Kinkela, J., Turner, G. & Urosevic, M. (2023) Pre-stack depth imaging techniques for the delineation of the Carosue Dam gold deposit, Western Australia. *Geophysical Prospecting*, 1–19. https://doi.org/10.1111/1365-2478.13314

2.3. Application of 3D optical fibre reflection seismic in challenging surface conditions

Application of 3D optical fibre reflection seismic in challenging surface conditions

Sasha Ziramov[1*], Andrej Bona[1], Konstantin Tertyshnikov[1], Roman Pevzner[1] and Milovan Urosevic[1]
show how the mineral sector could deliver an order of magnitude saving, while substantially increasing the data density and hence allowing optimum performance of modern seismic imaging algorithms.

Abstract

Distributed Acoustic Sensing (DAS), which uses strain-induced optical distortion effects to use optical fibres as multi-channel seismic arrays, enable efficient and inexpensive high-resolution seismic surveying in the challenging surface conditions, such as salt lakes. In this study, we present a first published 3D seismic survey completed with a fibre optic network.

Since DAS cables freely deployed on surface can be sensitive to ambient noise such as strong wind, which is common in many field conditions, we developed an efficient methodology for cable burring by fast ploughing it in both soft and hard ground conditions. Even a standard telecommunication fibre optic cable deployed beneath the surface by this ploughing method delivers reflection seismic recording performance comparable to conventional geophone systems, offering substantial cost savings in practice.

Combined with light and mobile seismic sources such as Betsy gun, DAS technology deployed in 3D surface reflection configuration across a hyper-saline salt-lake environment delivered a performance akin to modern nodal seismic systems. We show that the introduction of DAS technology into seismic surveying practice in the mineral sector could deliver an order of magnitude saving, while substantially increasing the data density and hence allowing optimum performance of modern seismic imaging algorithms.

Introduction

The rate of new mineral discoveries in Australia has been declining for several decades. Hence resolving and mapping complex underground structures is of significant value in exploring for structurally hosted gold mineralisation that could reverse such a negative trend. While airborne geophysics can provide initial indications of potential mineralised zones, seismic reflection provides the only method by which complex structures can be mapped in detail (Urosevic *et al.,* 2007; 2016). Seismic imaging is essentially unchallenged over a very large depth range in its capacity to provide clear images of subsurface structures (Pretorius *et al.,* 2003; Urosevic *et al.,* 2007; Melehmir *et al.*, 2012). Reflection seismic is particularly effective in resolving complex structures (Stolz *et al*., 2004; Milkereit *et al.,* 2000; Pretorius *et al*., 2011, Urosevic *et al.,* 2017), and is often used in exploration for structurally controlled and structurally hosted gold mineralisation.

However, a range of factors including inconsistent application of seismic reflection methodologies, a lack of integration of seismic data with other geophysical, geological and mining information, a lack of experienced seismic analysts working in the mining sector and, of course, high cost and difficulty in implementation of seismic reflection methods, have long prevented seismic surveying from becoming a mainstream exploration method. Urosevic and Evans (2007) have addressed many of these issues and demonstrated that reflection seismic analysis delivers substantial value in understanding complex geological structures that can host gold. Since that time many 3D seismic surveys have been acquired over gold prospects across the world to resolve such structurally hosted mineralisation (Urosevic *et al,* 2017), including several 3D seismic surveys of exceptional quality acquired across the hyper-saline lake Lefroy in Western Australia. Despite their significant exploration value (Urosevic *et al.,* 2012), common equipment loss and corrosion in the harsh salt lake operating environment has meant such surveys entail high risk of writing off the sensitive electronic hardware required, which may amount to multi-million dollar losses for service providers. This has resulted in many highly prospective areas under salt lakes in WA remaining underexplored, creating a potential value case for more appropriate exploration concepts and technologies suited to work in these challenging environments (Urosevic et al., 2019b). The most likely solution to this challenge is DAS as the sensitivity to a highly invasive hyper-saline environment is only on the data receiving end – interrogator. Securing the interrogator from the harmful environment is trivial, while on the sensor side, DAS technology is corrosion-proof, easy to deploy, and several orders of magnitude cheaper than equivalent conventional seismic acquisition systems. Considering that salt lakes of Australia are often hosting mineral deposits, DAS technology is of a particular importance for advancing mineral exploration in such environments.

[1] Curtin University
[*] Corresponding author, E-mail:
S.Ziramov@curtin.edu.au

Distributed acoustic sensing

DAS systems utilise interferometry of backscattered laser light through a Distributed Optical Fibre Sensors approach to identify fibre strain changes caused by impinging seismic or acoustic wave by comparing sequential back-scattered laser pulses (e.g., Hartog, 2018). Because of the high rate of information transfer involved, fibre strain is measured through optical interferometry (Hartog, 2018; Issa *et al.,* 2020).

Since DAS relies on interferometry of a backscattered laser pulse; the longer the pulse, the higher the signal-to-noise ratio (SNR) of the measured signal. However, a pulse of laser light will also average out any fibre deformations whose wavelength is shorter than the pulse length. This undesired effect can be avoided by reducing the pulse length at the expense of the SNR, hence introducing a trade-off between pulse length and SNR that needs to be optimised for a particular survey, depending on the seismic resolution required for the specific underground targets.

For interrogator systems that natively (optically) measure the spatial changes of the backscattered pulses, the distance between compared points is called Gauge Length (GL). Because these systems are measuring elongation of the fibre between locations separated by this gauge length, gauge length influences the recorded signal analogous to discrete differentiation, and the native measurement corresponds to the discrete strain (or strain rate). Hence Gauge Length has a smoothing effect on strain measurement like that of pulse length – it multiplies the spatial spectrum of the strain by a sinc function and introduces 'notches' in the spectrum (e.g., Correa *et al.* 2017).

The nature of DAS measurements influences the directional sensitivity of the measurement when a seismic P-wave impinges on the fibre at an angle. For systems that natively measure strain or strain change rate (e.g. Fotech or Silixa systems), signal strength decreases as the cosine squared of the incidence angle, whereas for deformation-based systems (e.g. Terra15 systems) the signal behaves like a geophone oriented along the fibre, with signal strength decreasing as the cosine of the incidence angle (Sidenko *et al.,* 2020). In either case, the signal (backscattered light) is measured simultaneously along the entire length of the fibre-optic (FO) cable. The sensing locations along the cable are closely spaced at 0.5 to 1m intervals depending on the interrogator type and settings used, providing extraordinary data density in comparison to standard geophone seismic technology. This high data density offers many advantages:

- A possibility to form digital arrays prior to processing.
- Apply multi-channel filters more effectively and achieve improved imaging due to better (correct) spatial sampling.
- Compensate DAS intrinsically low signal-to-noise ratio trough utilisation of high data density processing particularly in stacking and imaging.

Signal to noise ratio of an optical cable sensing seismic waves is controlled by many factors, including fibre thickness, purity, properties of the protective layers, geometry (straight, helical, hybrid), and length. Length of the cable influences the SNR by at least two factors. First, the longer the cable the smaller Pulse Repetition Frequency (PRF). PRF describes how many laser pulses are sent along the fibre per second. Since each pulse represents one measurement, PRF is an indicator of a 'stacking' power of the measurement. Second, the longer the cable the higher is the attenuation of the backscattered signal. Significant ongoing research efforts are devoted to development and testing of these cables to maximise the signal-to-noise ratio, improve consistency, improve directivity (omni-directivity) increase cable strength and flexibility, etc. Researchers at Curtin University have conducted various studies involving permanent DAS installation in a 900m-deep well at Curtin ground (Van Zaanen et al., 2017). Following early work of Daley et al (2013) at a CO_2 sequestration site in Otway, Victoria, Australia, Curtin researchers have conducted various studies at that site testing different cable types, configuration, sensitivity, directivity, attenuation properties in both borehole and surface modes (Yavuz et al, 2016; Correa et al., 2017a and 2017b) as a function of different source types (Freifeld et al., 2016, Urosevic et al., 2019a). Sensor geometry represents the key distinction

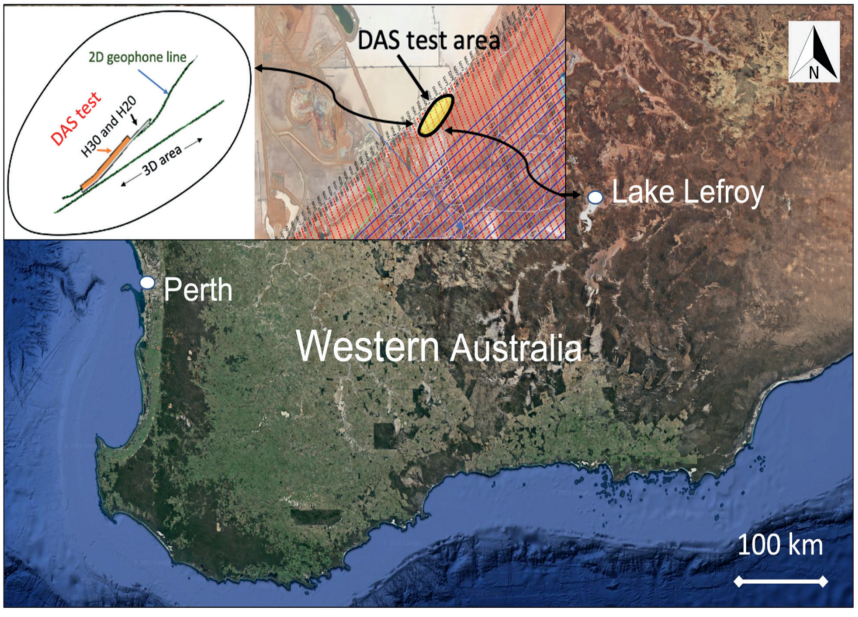

Figure 1 Satellite image of the southern half of Western Australia capturing the position of Lake Lefroy and the experimental setup: Conventional 3D seismic grid (middle insert) and DAS test area (left insert). Some 450 m length of helical 300and 600 m of helical 200 were laid alongside 2D geophone line and close to the edge of a conventional 3D survey. Hypersaline virgin lake area has beige tonnes due to salt crust. Google earth (April 10, 2022). Western Australia, 33° 23' 21"S, 118° 59' 12"W, Eye alt 814 km. http://www.earth.google.com.

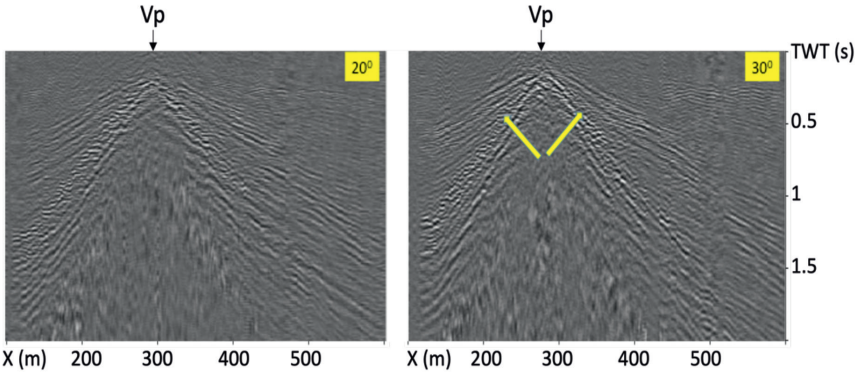

Figure 2 Raw shot records for vibroseis position (Vp) 18 (out of total 44 shots). Yellow arrows denote reflected waves, which are more prominent in the H30 cable data.

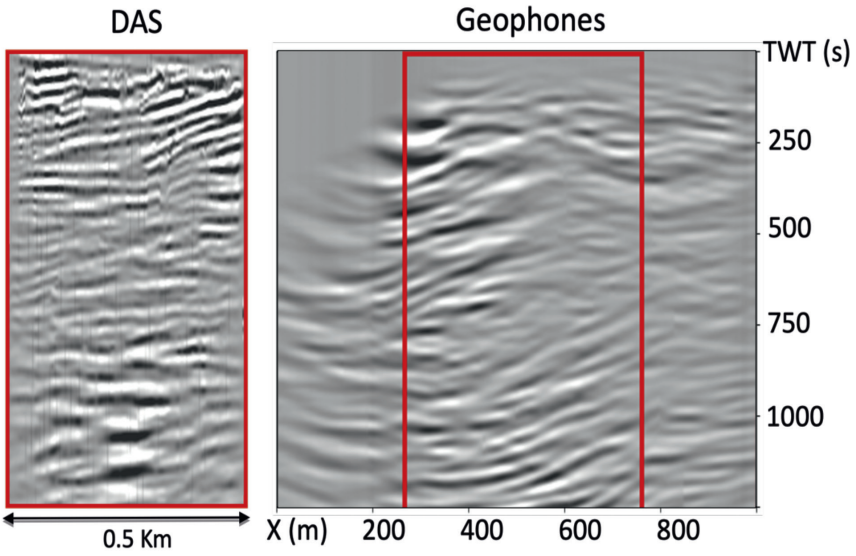

Figure 3 Comparison of short (450m) reflection profiles obtained in the initial vibroseis source Lake Lefroy survey using 300 DAS (left) and geophone receivers (right). Both stacks were depth-migrated after stacking. DAS image is of a superior quality at shallow depths.

between borehole and reflection seismic tests. VSP surveys utilise sensors positioned along a vertical axis, while reflection studies utilise sensors positioned along the ground surface. This geometric difference results in wave modes delivering different information in the two survey types. However, when comparing conventional sensors like geophone to DAS the difference exists between the two, even for the same geometry. The main reason lies in the directional sensitivity. Geophone has an omnidirectional response while fibre sensitivity is highest in the direction of fibre and drops of as cos^2 of the angle (or *cos* of the angle for rate of deformation). This can be improved by winding the cable around some central support. A 60^0 pitch angle (cable helicity) will produce close to omnidirectional fibre optic sensitivity. Unfortunately, the higher the pitch the higher is the bend radius or the fibre wound in the same cable diameter, which often results in greater attenuation for the same distance. Moreover, specialised highly helical cables are an order of magnitude more expensive than straight or low pitch angle cables that are used in the telecommunication industry.

In the following sections we describe a series of surface seismic DAS acquisitions on salt lakes and the associated learnings that culminated in the first successful 3D DAS survey.

Lake Lefroy study

Initial field testing of DAS technology for surface reflection seismic analysis in a hyper-saline environment was undertaken in 2018 during a conventional 3D seismic reflection survey conducted by HiSeis P/L at Lake Lefroy, WA (Fig.1). Some 44 shots were recorded into s 450 m length of helical 30^0 (H30) and 600 m of helical 20^0 FO cables that were laid directly onto the hypersaline lake surface, alongside a 2D geophone traverse located close to the edge of 3D seismic area (Figure 1). The geometry of the survey lines allowed for a direct comparison of the two DAS cable types, as well as qualitative comparison of the performance of new and conventional sensors. Raw shot records from the two optical fibres are shown In Figure 2. DAS data quality is similar for the two helical cables, with better resolution of the reflected waves in the H30 cable data. Overall signal-to-noise ratio (SNR) for the DAS data is low due to variable coupling, wind noise and in general lover directional sensitivity of DAS in comparison to conventional vertical geophones. Recording parameters were: Laser pulse – 50ns, Gauge length – 10m, PRF – 29kHz and output at every 1m. SIlixa iDAS-v2 was used for continuous recording.

Geophone and H30 DAS data were fully processed to a stack and then migrated. DAS produced a good reflection profile over the upper 1000m of the column (Figure 3). This can be attributed to the high data density provided by DAS, with cable sensing output sampled every 0.86m (=cos(30º)*1m), compared to the 15m spacing of geophones along the conventional line. This higher data density enables proper wave field sampling in the spatial domain, delivering alias-free recording. Furthermore, steep structures and discontinuities produce grazing reflections,

which favour DAS directivity and do not suit geophone recorders, which respond best to energy emerging at small angles to the surface (Urosevic et al., 2019a). While very encouraging results were obtained, the challenges identified in the application of DAS in this initial evaluation included:

- Cable deployment is a significant mechanical challenge, particularly for the H30 helical cable, which is heavy, bulky and has low resistance to stretch. For this study we utilised skid steerer to carry the cable wound onto a large drum. The cable was manually unwound, which was a daunting task.
- Deployment of the skid steerer was only possible at the edge of the salt lake where the ground supported its weight. Elsewhere such operation would not be possible.
- The vibroseis seismic source was used along the hard ground parallel to the sensor line. Such source would not be possible to deploy anywhere along salt lakes of WA.
- Cable-ground coupling with the salt lake surface is variable as a function of surface roughness and temperature (due to cable thermal stretching).

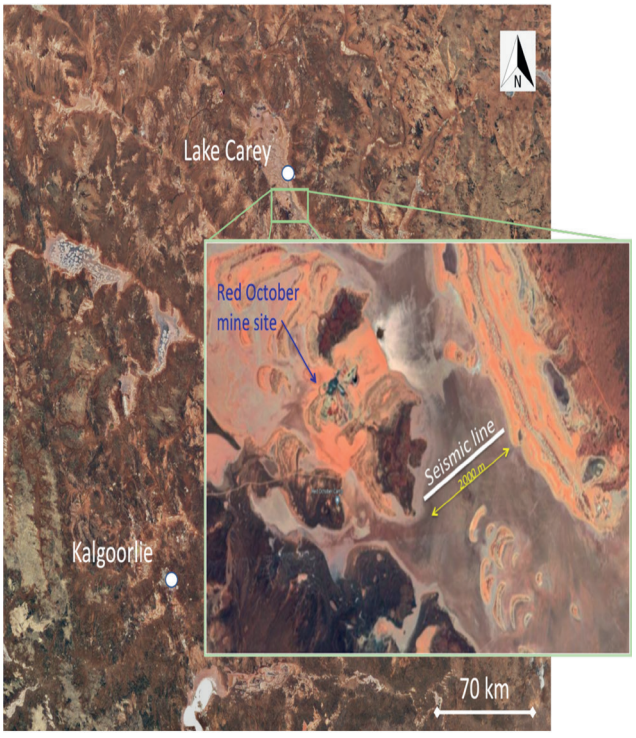

Figure 4 Satellite image of the Fortitude North test site. The studied area is located near to the southeast of the tailings facility from the existing Red October mine site. The experimental seismic line is 2 km long. Google earth (April 10, 2022). Lake Carey, WA, 30° 00′ 35″S, 122° 35′ 57″W, Eye alt 624 km. http://www.earth.google.com.

Lake Carey study

To improve upon the initial tests conducted at Lake Lefroy, the application of DAS across the salt lakes of WA took us to Lake Carey. The DAS experiment was situated across the lake encompassing soft to very soft saturated and hyper saline clay surface that was also flooded in parts (Figure 4). In a shortage of appropriate vehicles that could cope with such surface conditions, we selected much lighter FO cable and portable seismic source: a Betsy gun using a 12-gauge blank cartridge discharged at a depth of 10-15 cm. Geometry of the survey included 2D straight line length of 2000 m with parallel layout of FO cable and NuSeis nodal system that utilises a 10 Hz sensor at 15 cm depth. Hence the conventional sensor was fully protected from the ambient noise, while FO cable was exposed to it. Apart from the noise factor, the coupling of the FO cable with the ground varied along the line and during the day due to temperature variations (Figure 5). Geophones were placed at an interval of 10 m. DAS recording involved a Fotech interrogator with Laser pulse – 30ns, Gauge length – 12m, PRF – 30kHz and output at every 0.68 m.

Weather conditions during the first day of recording were calm, resulting in acceptable record quality for the DAS system (Figure 6a). Excessive wind on day two, however, generated significant DAS noise, resulting in sub-optimal performance (Figure 6b). The best quality DAS shot record is displayed alongside the NuSeis geophone record for the same source (Figure 7). The main wave modes such as reflected and refracted (head) P-waves are clearly identifiable in the geophone data. The DAS data lacks refracted wave modes due its preferred sensitivity along the fibre and very poor sensitivity orthogonal to it (due to a low-fibre pitch angle of 11º), which corresponds to the emergence angle of head waves. However, surface waves are aliased in the geophone data due to the coarse 10m spatial sampling rate, and are much better resolved in the DAS data.

Figure 5 Fortitude North Lake Carey survey conditions: A) 2 km of FO cable stretch across the lake, B) Deployment of NuSeis geophone system alongside the FO cable and C) FO cable was only partially in contact with the ground surface resulting in poor cable-ground coupling. The quality of coupling varied during the day as a function of the ambient temperature, which affected the stiffness of the cable.

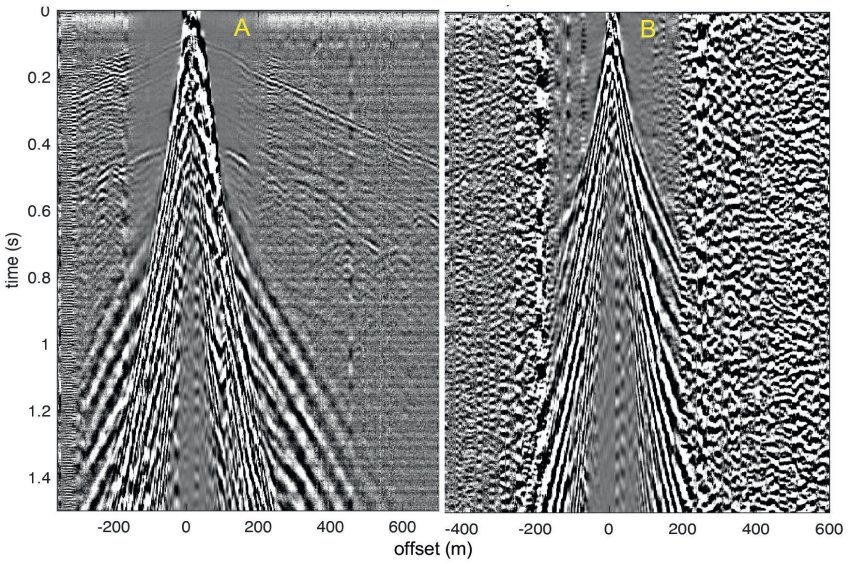

Figure 6 Raw DAS shot record under (A) calm conditions on day 1, and (B) windy conditions on day 2 of the experiment. Note the lack of visible reflections resolved in panel B.

	Geophone Data	DAS Data
1	SEGD reformat to local SeisSpace (SS) format	HDF5 reformatting to SGY then to local SS format
2	Geometry database and header load	Geometry database and header load
3	First arrival onset picking and refraction static computation	Solution from geophone data
4	Spike deconvolution	Spike deconvolution
5	Amplitude compensation	Amplitude compensation
6	Multi-channel filtering (surface wave attenuation in F-K domain)	Multi-channel filtering (Time Frequency De-noise) and Tau-P filetering
7	Constant Velocity Analysis (CVA)	From geophone data for consistency of results
8	Brute stack	Brute stack
9	Residual reflection statics	Residual reflection statics
10	2nd pass CVA	From geophone data for consistency of results
11	Dip move-out corrections (DMO)	Common Reflection Surface (CRS) corrections
12	Final stack + F-X deconvolution	Final stack + F-X deconvolution
13	Time and depth imaging (Migration)	Time and fepth imaging (Migration)

Table 1 Data processing workflows employed on North Fortitude 2D survey data (after Urosevic and Evans, 2007).

Raw signal data acquired from both geophones and DAS was processed using a 'hard-rock' processing flow modified from Urosevic and Evans (2007) (Table 1). Refraction statics were computed from the first arrivals in the geophone data, as this wave mode was not recorded by DAS. Computed delay times were then applied to both datasets for further processing. DAS output spacing of 0.67m (=0.68m*cos(11º)) produced 2857 data points over the ~2 km length of cable deployed, in comparison to the 200 geophone data points over the same distance. The higher DAS data density supported application of time-frequency domain (TFD) ambient noise suppression and coherent noise removal using limited apertured Tau-P transform. This conditioning approach has substantially increased SNR of DAS records.

With respect to imaging, migration after stack resulted in the best outcome. This method takes the full advantage of high fold coverage during common depth point (CDP) stacking, which further improves SNR. We applied a partial pre-stack migration in form of common reflection point stacking (CRS) and a post-stack migration algorithm. The CRS method, which involves post-stack dip modelling, provided a more sophisticated partial pre-stack migration than standard dip move-out (DMO) correction.

Direct comparison of the final processed geophone and DAS signals is provided in Figures 8a and 8b, respectively. Deterioration in DAS image quality from left to right reflects the impact of wind noise during the latter period of data collection. Comparison of the geophone data with the initial km of DAS data collected in calm conditions (Figure 8c) shows the two sensor types produce similar results under calm conditions.

Overall results from the survey are evaluated by comparison to a nearby seismic line produced by Urosevic and Evans (2007) using an array of four 60,000 lb Vibroseis trucks (Figure 9). Comparable resolution of the two lines down to at least 2 km depth establishes the capacity of the Betsy gun source to deliver coherent seismic energy to at least this depth for a cost of less than $1 per shot. This establishes viable potential for low-cost, high-quality reflection seismic acquisition in the near-surface environment combining the cheapest sensor – DAS – with the cheapest source – the Betsy gun.

Overall, the results achieved with surface layout of DAS were satisfactory. However, it became clear that FO cable needs to be trenched and protected from often persistently strong wind. Thus, the optimum methodology for the harsh environment of hypersaline lakes could involve:

- Light, portable seismic source
- Light, buried FO cable
- Sparse geophone grid providing near surface time delay information for processing

Geophone support may be avoided if, for example a highly helical FO cable with a pitch of 60^0, that would provide for close to omni-directional sensitivity, is deployed. However, soft lake surface makes deployment of helical cables difficult, if not impossible. The associated high cost makes currently highly helical cables impractical for a commercial exploration of mineral resources.

To effectively deploy DAS acquisition methodology over a length of exploration interest we need to utilise an inexpensive FO cable that can be efficiently machine trenched. Inexpensive FO cables are less ragged and in general contain only straight fibre. To analyse the possibility of replacing loose-tube telecommunication cable (slightly pitched) with a straight fibre we conducted another test that utilised a 'bare' fibre: 250mm diameter single mode: 8mm core, 125mm cladding and 250mm coat. A direct comparison between the two cables is shown in Figure 10, which shows that the bare fibre produced a higher SNR due to the lack of the protective layers that attenuate the seismic energy. This final test showed that a light weight, and at least one order of magnitude cheaper seismic exploration with DAS, is feasible in the harsh conditions of the hypersaline lake of WA (Urosevic et al., 2019b).

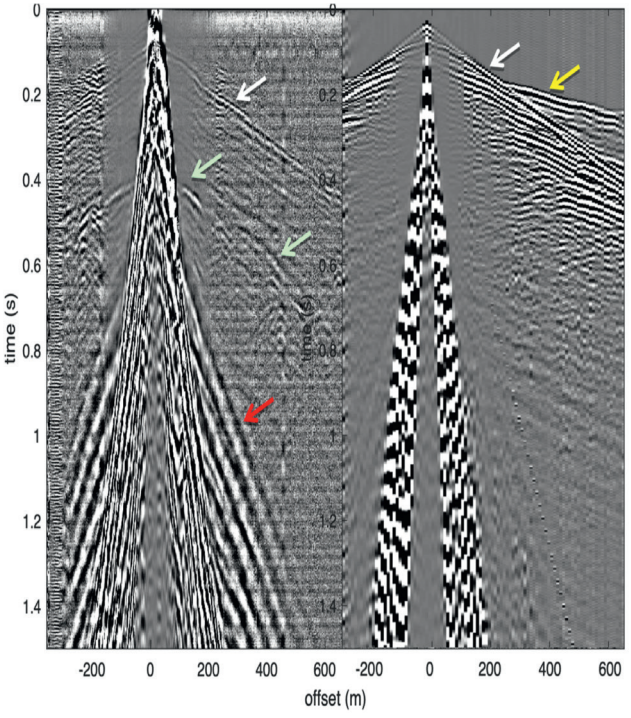

Figure 7 DAS data (left panel) and NuSeis shot record (right panel). Note that the NuSeis geophone array was active over only 1km while DAS was active over a 2km transect. NuSeis was deployed in two sections to match the overall DAS coverage. NuSeis exhibits a much higher SNR. Arrows depict the detection of specific wave arrivals as follows: white – direct wave; yellow – head wave; green – converted shear wave, and; red – surface waves.

3D DAS reflection seismic over lake Carey

The combination of Betsy gun source and ultra-lightweight bare optical cables delivered high-quality reflection seismic results in a salt lake setting. The next and an ultimate evaluation stage involved implementation of 3D reflection seismic survey across the hyper-saline surface of Lake Carey. The area selected was on the lake proper, close to the existing mine site, covering approximately 1.5 km^2. The geometry of the DAS survey and the acquisition strategy is illustrated in Figure 11. Two interrogators by Terra15 were utilised to interrogate 7 km of FO cable each.

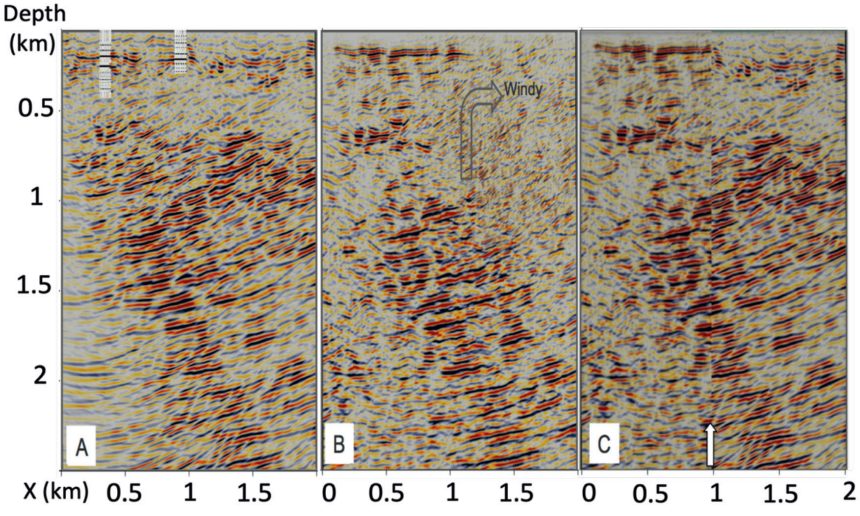

Figure 8 Final images. (A) Geophone data, (B) DAS data, and (C) 1 km of geophone data (left) and 1 km of DAS data (right). Quality of the geophone data (NuSeis) is superior under high-wind conditions, but not so during calm conditions.

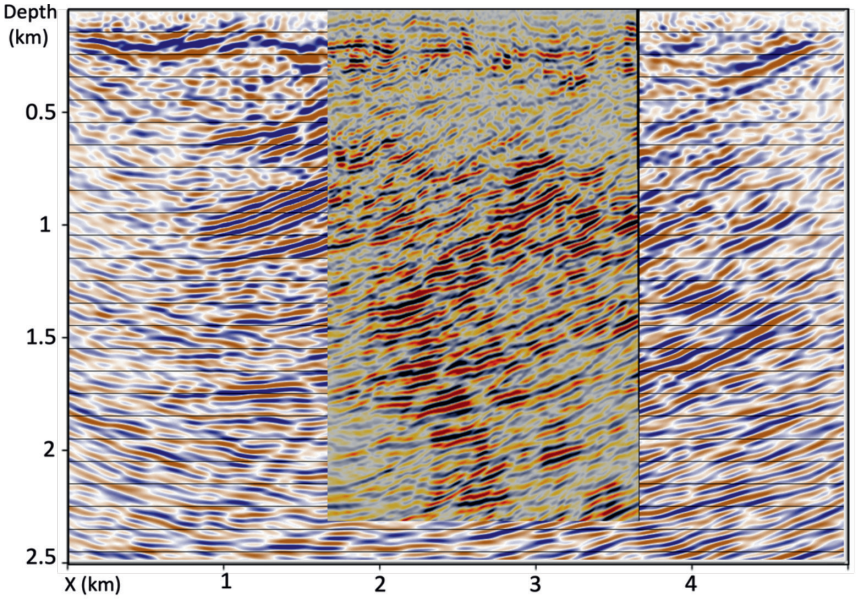

Figure 9 Betsy gun image overlain onto a Vibroseis image. Good correlation can be observed as both lines are recorded in the dip direction of the main geological structures. Lines are approximately 10 km apart but the same large shear structures can be seen in both images.

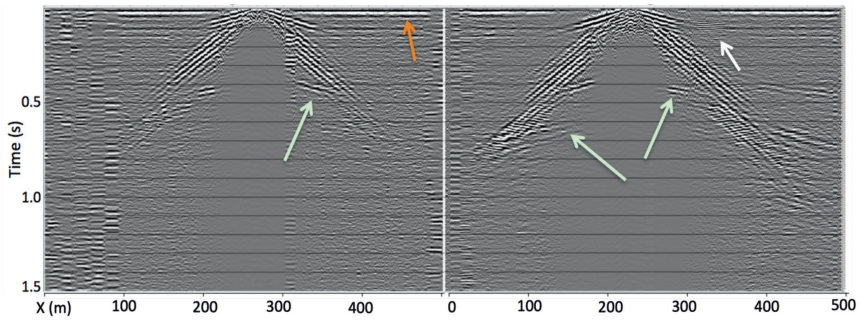

Figure 10 Raw field data comparing blue helical cable (left panel) and bare cable (right panel). Shots are displayed as a mirror image pairing for easier comparison. The ultra-light bare cable delivered superior performance to the blue helical cable, including capturing the P-wave reflection (white arrow) arrival which is not seen in the helical cable results. Green arrow denotes S-wave reflection arrival.

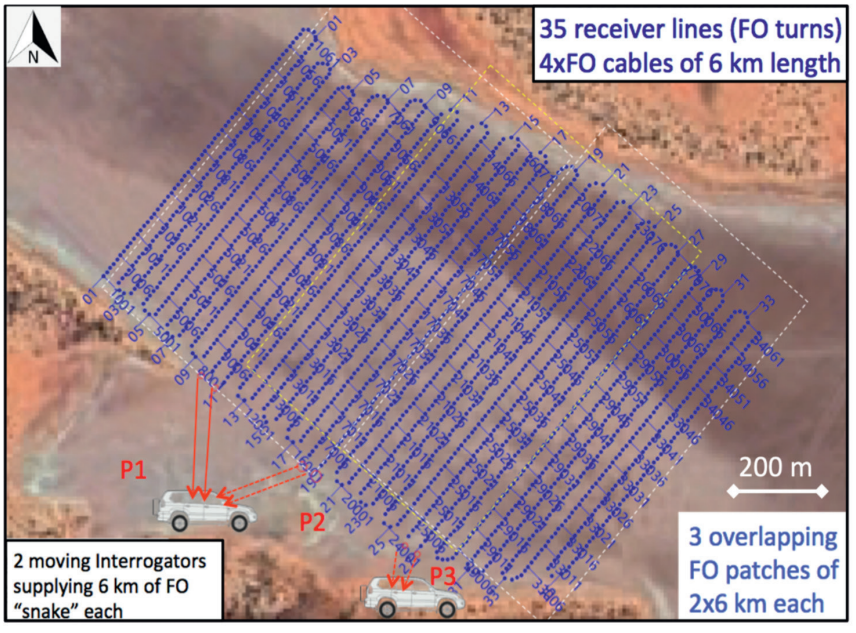

Figure 11 Optical cables were distributed in four patches of 6 km length each in a 'snake-like' pattern. Two patches at a time are connected to the two active interrogators. As shooting progresses from NW-SE the two, interrogators are shifted one patch down at the time. Hence there are three acquisition sets, covering patches 1-2, 2-3 and 3-4, respectively. Google earth (April 10, 2022). Lake Carey, WA, 29° 13' 10"S, 122° 26' 46"W, Eye alt 3.5 km. http://www.earth.google.com.

These interrogators record deformation rate rather than the strain or strain rate as do the other interrogators used in this study. The interrogator was set with Laser pulse – 200ns and output at every 0.82 m. PRF was set automatically to maximum based on the fibre length of up to 7 km.

Two Betsy guns were also utilised for shooting along 20x20 m grid pattern (Figure 12). As the shooting progressed, the two interrogators were shifted by one cable of 7000 m length. In total three DAS patters were utilised to complete the survey.

One hundred and three channels of Sercel Unites (with geophone extensions) were positioned in 90x100 m grid pattern (Figure 12). Utilisation of such sparse geophone grid will enable both refraction and reflection data analysis, provide support to DAS data processing and eventually allow for a direct comparison between the two data sets.

For this experiment, we used somewhat more rugged FO cable compared to the bare fibre used in the preceding experiment. In particular, we used tight buffer fibre with 8 µm core, 125 µm cladding and additional PVC reinforcement, taking the total diameter to 900 µm. While this is still very thin and inexpensive cable it provided sufficient tensile strength to allow for fully automatic trenching by plough mounted on a rubber-tracked Can-Am 4WD off-road vehicle (Figure 13). This plough was designed and manufactured at Curtin University. The trenching operation went flawlessly at a very high speed. A total of ~26,000 m of FO cable was trenched within 10 hours, by a single operator.

Results

The flow of Table 1 is used for processing of both geophone and DAS data. The bin size was 10x10 m for DAS and 20x20 m for geophone data. DAS data, recorded as deformation rate, was differentiated to provide output like geophones. Suboptimal parameters were unfortunately used in the survey. The pulse length of 20 m was too long and resulted in ghosting filtered with a in spatial domain. To avoid this issue, a shorter pulse length could have been used with a trade-off of smaller SNR. To compensate for this effect, we applied a deconvolution in spatial domain as a deghosting filter. However, it resulted in considerable artefacts.

An example of geophone stack and migrated data is provided in Figure 14, while equivalent DAS data is shown in Figure 15. Comparing the stacked sections, it is clear that even sparse geophones produced superior result over DAS, due to considerable artefacts remaining in DAS data after deghosting. However, after migration we have the better outcome and DAS data appears to

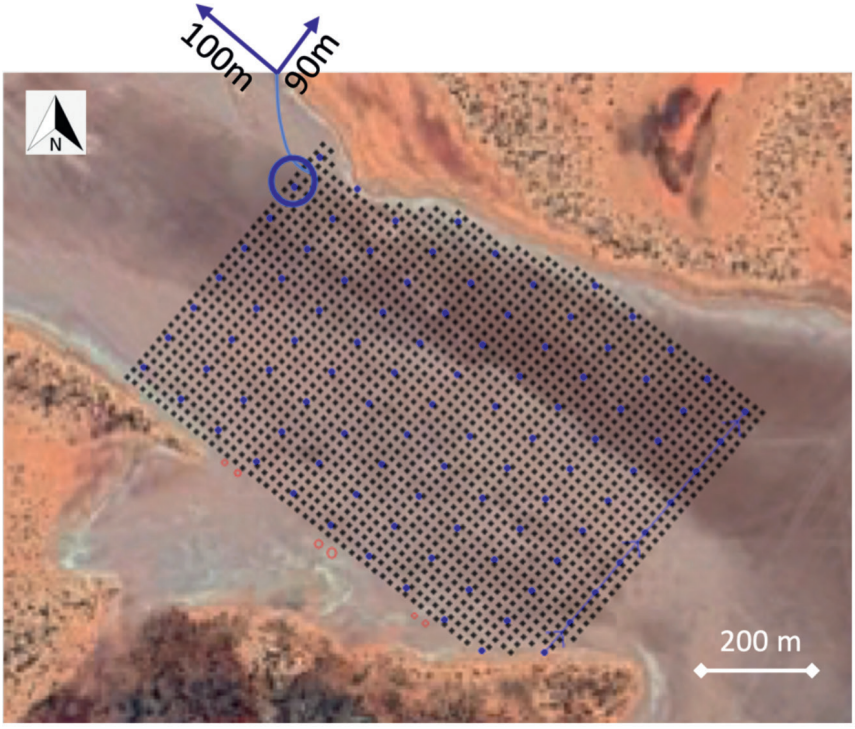

Figure 12 Source array and geophone receiver distribution. Betsy gun shots were delivered in a rectangular pattern on a 20x20m spacing. Geophones are arrayed in 90x100m grid using 100 Unite 3-component units and 200 extension cables to minimise use of electronic equipment. Lake Carey, WA, 29° 13′ 10″S, 122° 26′ 46″W, Eye alt 5 km. http://www.earth.google.com.

Figure 13 Curtin University designed and constructed cable plough attached to Can-Am 4WD vehicle. Provides very rapid deployment of FO cable approximately 0.1m beneath the lake surface. Some 24 km of cable was deployed in 10 h as a single man operation. This is equivalent of 32,000 sensors 0.8 m apart.

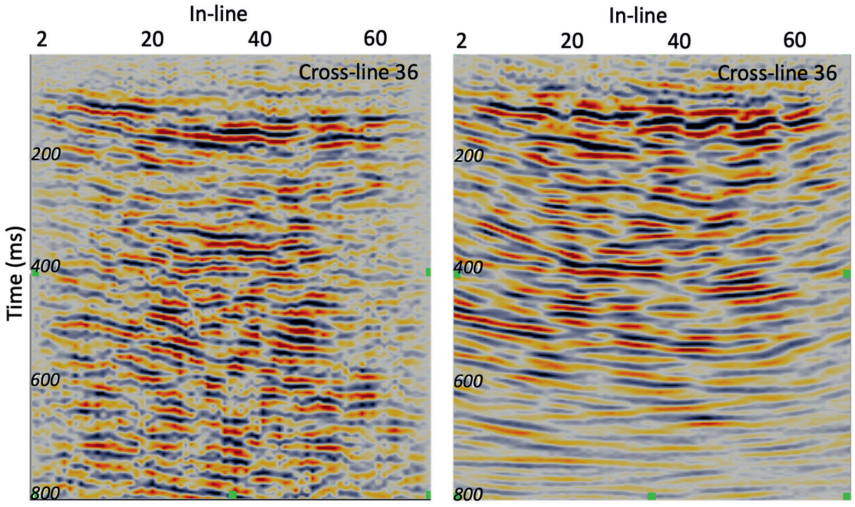

Figure 14 Cross-line 36 from geophone cube before migration (left), and after migration (right).

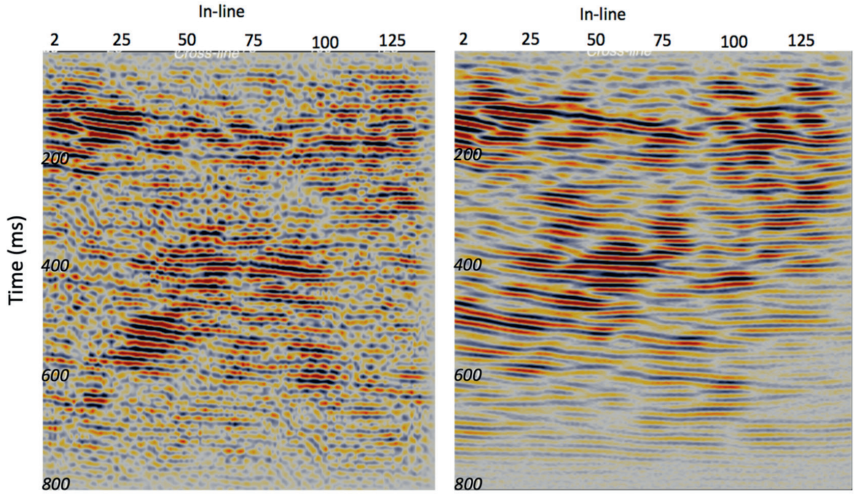

Figure 15 Cross-line 36 from DAS cube before migration (left), and after migration (right). Note significant SNR improvement after migration. This is attributed to high spatial data density.

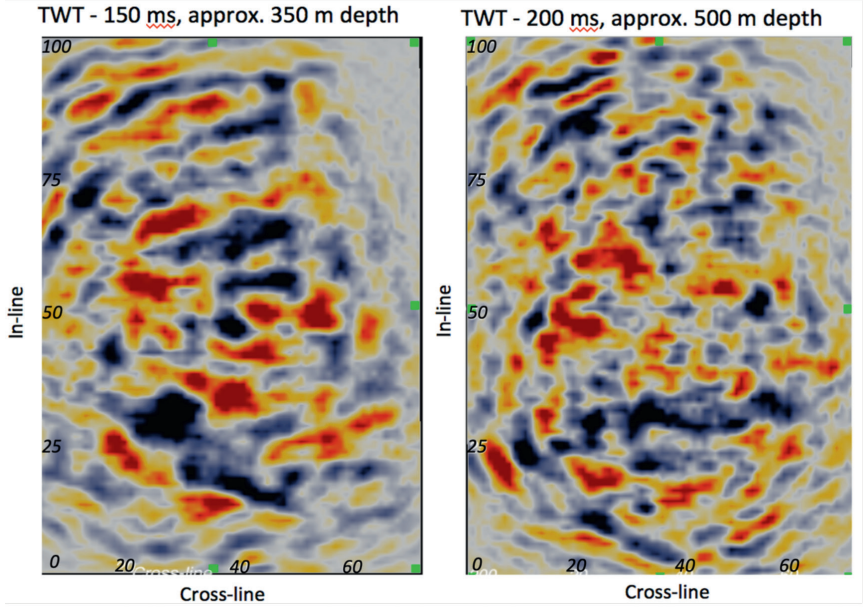

Figure 16 Geophone cube time slices at 150 and 200ms two-way-travel time (TWT) corresponding to approximate depths of 350 and 500 m.

have more continuity and better SNR. This is attributed to higher density of DAS data.

Selected time slices are shown in Figures 16 and 17 for geophone and DAS data cubes after post stack migration, respectively. Again, it appears that DAS data produced a more coherent result. A chair type of data display is shown in Figure 18. The results are of a lower quality than expected but still of a sufficient SNR to be interpretable.

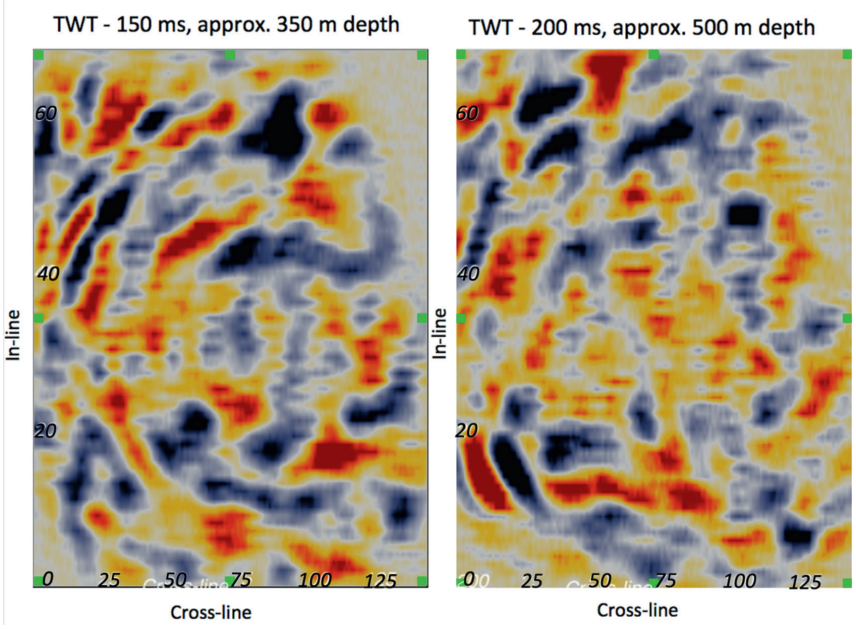

Figure 17 DAS cube time slices at 150 and 200 ms two-way-travel time (TWT) corresponding to approximate depths of 350 and 500 m, respectively.

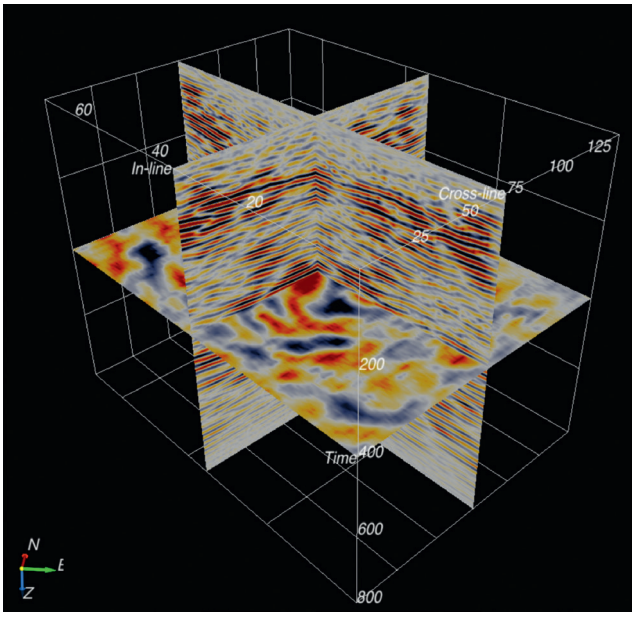

Figure 18 Chair display of migrated DAS data cube.

Conclusion

The first application of DAS sensing technology to 2D and 3D seismic reflection imaging of complex underground structures in a mineral exploration context are presented. An evaluation of DAS technology against current seismic exploration practices is discussed briefly, omitting the long-term ominous efforts conducted in the background that led to the seismic experiments and the results present in this study. The field studies were of key importance in evaluating DAS technology and enabled us to develop an efficient methodology based on the new generation of sensors in combination with a specific type of acquisition geometry, combined with portable, efficient sources of seismic energy.

Some of the key achievements of this study are:

- Completion of the world's first successful 3D reflection seismic survey for mineral exploration using DAS technology
- Design and construction of a plough for rapid trenching deployment of FO cable
- Performance evaluation of different types of optical interrogators and FO cables for DAS imaging under mineral exploration conditions

This study sets a foundation for the future application of cost-efficient DAS seismic technology for exploration of mineral resources. Many lessons were learnt in the utilisation of DAS technology for the objectives of seismic reflection prospecting of mineral resources. While the learning continues it is becoming clear that DAS technology will play a crucial role in the mineral sector due to its efficacy, low cost and exceptional spatial data density that allows for new thinking in data processing and interpretation.

Acknowledgements

We would like to thank Dave Felding and Camilo Guarin of Matsa Resource Company for providing key financial support, and equipment necessary field support and equipment. We thank HiSeis for providing financial and field acquisition support.

We would also like to thank Dominic Howman, Murray Hehir, Alexei Yurikov and Pouya Ahmadi who made these complex data acquisition programs possible. We thank Mehdi Asgharzadehmeh for analysing borehole seismic experiments.

We would like to acknowledge the principal support of the Mineral Research Institute of Western Australia (MRIWA) under the program M514, co-sponsored by Matsa Resources and Hiseis. For more information on the program, refer to MRIWA M514 project report: Novel seismic methodologies for exploration of mineral resources in a hypersaline environment, 2018-2020.

https://www.mriwa.wa.gov.au/research-projects/project-portfolio/novel-seismic-methodologies-for-exploration-of-mineral-resources-in-a-hypersaline-environment/

We thank Haliburton for providing seismic data processing package (SeisSpace).

Some support has also been provided by MinEx Corporative Research Centre, sponsored by the Australian Government.

References

Correa, J., Egorov, A., Tertyshnikov, K., Bona, A., Pevzner, R., Dean, T., Freifeld, B. and Marshall, S. [2017a]. Analysis of signal to noise and directivity characteristics of DAS VSP at near and far offsets — A CO2CRC Otway Project data example. *The Leading Edge* **36**(12), 994-1001.https://www.earthdoc.org/search?value1=J.+Correa&option1=author&noRedirect=true

Correa, J, Van Zaanen, L., Tertyshnikov, K., Dean, T., Pevzner, R. and Bona, A. [2017b]. DAS Versus Geophones: a Quantitative Comparison of a VSP Survey at a Dedicated Field Laboratory, Fourth EAGE Borehole Geophysics Workshop.

Daley, M. Freifeld, T., Ajo-Fanklin, M.J. and Dou, S. [2013]. Field testing of fiber-optic distributed acoustic sensing (DAS) for subsurface seismic monitoring, *The Leading Edge*, 699-706.

Freifeld, B.M., Pevzner, R., Dou, S., Carrea, J, Daley, T.M, Robertson, M, Tertishnykov, K, Wood, Ajo-Franklin, T.J., Urosevic, M. and Gurevich, B. [2016]. The CO2CRC Otway Project deployment of a Distributed Acoustic Sensing Network Coupled with Permanent Rotary Sources, 78th EAGE Conference and Exhibition, V1, 1-5.

Hartog, A. [2018]. *An introduction to distributed optical fibre sensors, series in fiber optic sensors*. FL, USA: CRC Press Taylor & Francis Group. ISBN 9781138082694.

Issa, N., Roelens, M.A.F. and Frisken, S.J. [2020]. Distributed optical sensing systems and methods, US Pattent App. 16/633,706.

Malehmir, A., Durrheim, R., Bellefleur, G., Urosevic, M., Juhlin, C., White, D. J., Milkereit, B. and Campbell, G. [2012]. Seismic methods in mineral exploration and mine planning: A general overview of past and present case histories and a look into the future: *Geophysics*, **77**, 173-190.

Milkereit, B., Berrer, E.K., King, A.R., Watts, A.H., Roberts, B., Adam, E., Eaton, D.W., Wu, J. and Salisbury, M.H. [2000]. Development of 3-D seismic exploration technology for deep nickel-copper deposits; a case history from the Sudbury Basin, Canada. *Geophysics*, **65**(6), pp.1890-1899.

Pretorius, C.C., Jamison, A.A. and Irons, C. [1989]. Seismic exploration in the Witwatersrand Basin, Republic of South Africa: Proceedings Exploration 87, Third Decennial International Conference on Geophysics and Geochemoical Exploration for Minerals and Groundwater: Special Publication, *Ontario Geologic Survey*, **3**, 241–253.

Pretorius, C.C., Muller M.R., Larroque, M. and Wilkins C. [2003]. A review of 16 years of hard rock seismics on the Kaapvaal Craton,in Eaton, D. W., B. Milkereit, and M.H. Salisbury, eds., Hard rock seismic exploration: SEG, 247–268.

Pretorius, C.C., Gibson, M. and Snyman, Q. [2011]. Development of high-resolution 3D vertical seismic profiles: *Journal of the South African Institute of Mining and Metallurgy*, **111**, 117-125.

Sidenko, E., Pevzner, R., Bona, A. and Tertyshnikov, K. [2020]. Experimental Comparison of Directivity Patterns of Straight and Helically Wound DAS Cables, in Conference Proceedings, 82nd EAGE Annual Conference & Exhibition, Jul 2020, Volume 2020, p.1-5.

Stolz, E., Urosevic, M. and Connors, K. [2004]. Reflection seismic surveys at St. Ives gold mine, WA: Preview, **111**, 79.

Urosevic, M., Kepic, A., Stolz E. and Juhlin, K. [2007]. Seismic exploration of mineral deposits in Yilgarn Craton, Western Australia: *Proceedings of Exploration 07: Fifth Decennial International Conference on Mineral Exploration*, 525-534.

Urosevic, M. and Evans., B.J. [2007]. Feasibility of seismic methods for imaging gold deposits in Western Australia, MRIWA Project, 363, Report #267.

Urosevic, M., Kepic, A., Sheppard, S. and Johnson, D. [2008]. Nickel exploration with 3D seismic – Lake Lefroy, Kambalda, WA: Post-convention workshop on high resolution seismic methods, 77th Annual SEG conference, Las Vegas, USA, Chairman.

Urosevic, M., Bhat, G. and Grochau M.H. [2012]. Targeting nickel sulfide deposits from 3D seismic reflection data at Kambalda, Australia: *Geophysics*, **77**,123-132.

Urosevic, M., Ziramov, S., Kinkela, J. and Dwyer, J. [2016]. Seismic exploration of mineral resources – an Australian prospective: The first conference on geophysics for mineral exploration and mining, *Proceedings; We Min PO5*.

Urosevic, M., Bona, A., Ziramov, S., Pevzner, R., Kepic, A., Egorov, A., Kinkela, J., Pridmore, D. and Dwyer, J. [2017]. Seismic for mineral resources – a mainstream method of the future: Exploration 07: Seventh Decennial International Conference on Mineral Exploration, Toronto, Canada.

Urosevic, M., Bona, A., Ziramov, S., Martin, R., Dwyer, J. and Foley, A. [2019a]. Reflection seismic with DAS, why and where?: Near Surface Geoscience Conference & Exhibition, The Hague, Netherlands.

Urosevic, M., Bona, A., Ziramov, S., Martin, R., Dwyer, J., Felding, D. and Foley, A. [2019b]. Seismic prospecting of mineral reserves with DAS, 16th SAGA Biennial Conference and Exhibition, Durban, South Africa.

Van Zaanen, L., Bona, A., Carrea, J., Pevzner, R. and Tertyshnikov, K. [2017]. A comparison of borehole seismic receivers, SEG International Exposition and 867th Annual Meeting, in press.

Yavuz, S., Freifield, B., Pevzner, R., Tertyshnikov, K., Dzunic, A., Shulakova, V., Robertson, M., Daley, T. M., Kepic, A. and Urosevic, M. [2016]. Subsurface Imaging Using Buried DAS and Geophone Arrays – Preliminary Results from CO2CRC Otway Project: 78th EAGE Conference & Exhibition, SBT4-04.

3. Appendices

3.1. Carbon storage characterisation using pre-stack depth migration in Harvey, Western Australia.

14th International Conference on Greenhouse Gas Control Technologies, GHGT-14

21st -25th October 2018, Melbourne, Australia

Carbon storage characterisation using pre-stack depth migration in Harvey, Western Australia

Ziramov, S.*, Urosevic, M., Pevzner, R., Glubokovskikh, S., Gurevich, B.

Curtin University, 26 Dick Perry Avenue, Kensington 6151, Western Australia

Abstract

In 2013 a first-order assessment of the CO_2 containment, for the South West Hub (SW Hub), suggested possible migration pathways across faults with potential for improving reservoir connectivity but also bypassing the primary and secondary seals (Langhi et al., 2013). The assessment was based on a geological model built upon sparse 2D seismic data with locally high uncertainties specific*ally regarding the structural architecture. The following year regional 3D seismic data was acquired near Harvey, Western Australia. The survey proved to be of great importance for regional characterisation of the reservoir, identification of the large structures and key geological interfaces. Small to medium size, shallow structures were imaged using high-resolution (nested) 3D surveys. These nested surveys were acquired in 2015 at the Harvey 4 well and in 2017 at the Harvey 3 well locations. The results demonstrated that high-density surveys were important even at the characterisation stage and were crucial for development of a detailed static model. A pre-stack time migrated (PSTM) high-resolution cube and the attribute derived from it, such as coherency and impedance, enabled improved structural and stratigraphic analysis around Harvey 3 and 4 wells. To acurately model the distribution of paleosols, lenses of high clay content, which are assumed to serve as baffles for CO_2 upward migration, a pre-stack depth migration (PSDM) and stochastic inverstion were attempted on the Harvey seismic data.
Keywords: Geological storage; geosequestration; pre-stack depth migration; tomography; inversion.

1. Introduction

The SW Hub Carbon Capture and Storage (CCS) project is a leading initiative to reduce carbon dioxide emissions in Western Australia. This comprehensive project has been executed in multiple stages and aimed to fully characterise a potential CO_2 storage reservoir, the Lesueur Sandstone formation, and to test sealing properties of the overlying formation. The Lesueur Sandstone lies in the southern Perth Basin and is the type of saline aquifer identified by scientists around the world as a potential CO_2 storage reservoir (Gurevich et al., 2018).

The site characteristion was initiated by the Harvey 1 stratigraphic well that was drilled in 2012 and a 3D seismic survey was acquired in 2013-2014 over a 115 km2 area in the vicinity of potential future injection sites. Since then new sources of the geophysical data became available:

- Harvey 2, 3 and 4 wells were drilled and a suite of well-logs have been acquired along with a zero-offset Vertical Seismic Profile (VSP);

* Corresponding author. Tel.: +61 8 9266 2296; fax: +61 8 9266 3407.
E-mail address: Sasha.Ziramov@curtin.edu.au

- High-resolution nested 3D seismic surveys around the Harvey 4 well (Ziramov et al., 2017) and, most recently, around the Harvey 3 well that also incorporated 3D VSP and multi-offset VSP surveys (Yavuz et al., 2018).

By integrating all available geophysical data, we were able to fill current information gaps relevant for the CO_2 sequestration modeling. The interpretation started with advanced analysis and processing of VSP data. The results of VSP analysis were then used to help derive an optimum velocity field for depth imaging of the entire 3D seismic dataset plus a composite 2D line that passed in proximity to three Harvey wells. All of these datasets together, with well logs, were then used for reflection tomography and stochastic seismic inversion.

2. Seismic data analyzed

2.1. VSP data

VSP data contain downhole recordings of seismic waves excited by a surface source. At the SW Hub area, VSPs were shot with the source close to the boreholes, known as Zero-Offset VSP (ZVSP). This type of survey was our in situ laboratory since it provided us with transmission wave field. This allowed us to produce accurate P and S-wave velocities in the seismic frequency range as surface seismic data. P-wave velocity field was then used for the seismic to well-tie. The interval velocities derived from VSP data were used to stabilize migration velocities and calibrate sonic logs. Analysis of the amplitudes and signal bandwidth of the transmitted P and S-wave fields provided important information relating to the attenuation of seismic energy through various rock formations. Finally, transmitted shear waves were used to estimate in situ stress orientations. For the purpose of imaging we were mainly concerned with deriving a high accuracy P-wave velocity function.

The ZVSP data were of satisfactory quality for a conventional analysis and interpretation, except for the Harvey 4 which had a significant interval contaminated by noise. We were able to recover reliable time-depth relations for the Yalgorup and Wonnerup Members of the Lesueur Formation, which significantly helped with the well-tie (Fig. 1). This also verified that our surface wave data were dominated by primaries with minimal noise contamination.

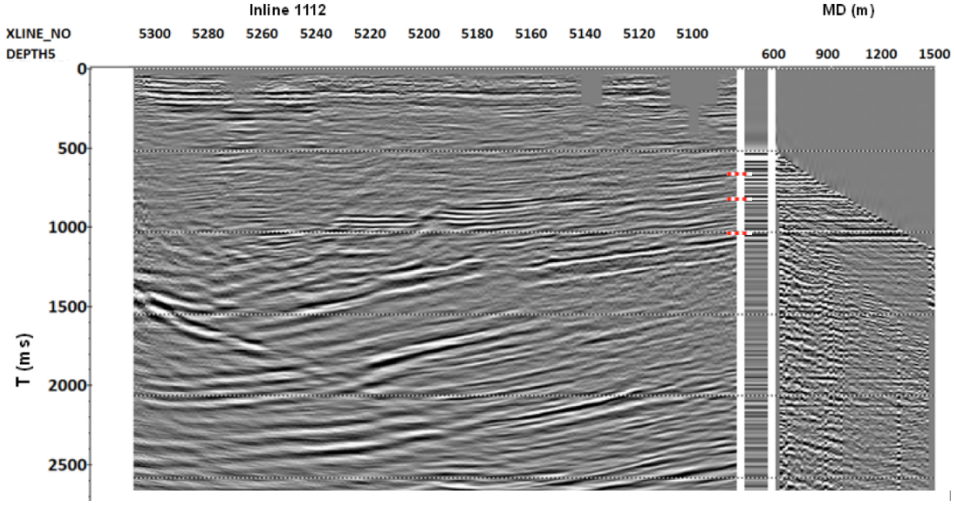

Fig. 1. The Harvey 3 well ZVSP, the result of the seismic to well-tie (principle reflectors are shown marked with red dashed lines).

2.2. Regional and nested surface seismic

The initial assessment of the CO_2 containment was based on a geological model built upon a sparse 2D seismic data analysis. The next stage of the site characterisation involved integration of the regional 3D seismic dataset acquired in 2014 with the available Harvey-2 and Harvey-4 well data. Regional 3D seismic shed new light onto the structural architecture of the SW Hub site and provided an initial assessment of the potential for lateral and vertical

movement of CO_2 through the Wonnerup and Yalgorup Members (Pevzner et al., 2015). It has given us a means to investigate the relationship between the modelled faults and the present-day stress field.

The reginal 3D seismic data set was subsequently re-processed with true relative amplitude preservation, 5D interpolation, model-based noise attenuation, PSTM and PSDM. These new datasets allowed for in depth reservoir characterisation studies including stochastic rock physics inversion. Reprocessed 3D seismic images were far superior to those existing previously with significantly improved reflection continuity and fault expression that allowed for the delineation of fault planes with much higher precision. Additional processing involved tomographic velocity analysis reconstruction to be utilised for both final imaging and inversion.

The regional Harvey 3D seismic survey provided good information of the large-scale subsurface structures and main stratigraphic units. This survey, as it is typical for most of regional land 3D surveys, suffers from low data density, which limits the imaging precision. Hence, the spatial distribution and orientation of shallow fractures and faults remained unresolved. These geological features were targeted by additional high-resolution 3D surveys. The objective of these nested high-resolution 3D surveys was to produce a crisp image of the structures surrounding the Harvey H-4 and H-3 wells with emphasis on the shallow subsurface geology and structures that may impact CO_2 flow.

Careful processing of high-resolution 3D data sets with incorporation of the latest processing techniques produced:

- A high-definition seismic image of the shallow subsurface geology around H-4 and H-3 wells.
- Enabled detailed characterisation of the near-surface structures in the area.
- Validation of the effectiveness of high-resolution data acquisition and processing techniques.

After inserting the nested 3D data cube into the regional 3D data cube (Fig. 2), it can be clearly observed that the fault density and their complexity cannot be fully resolved with the regional seismic data even at greater depths. Low-resolution regional seismic data are also not adequate for a rigorous implementation of seismic stratigraphy and certainly not for the quantitative interpretation.

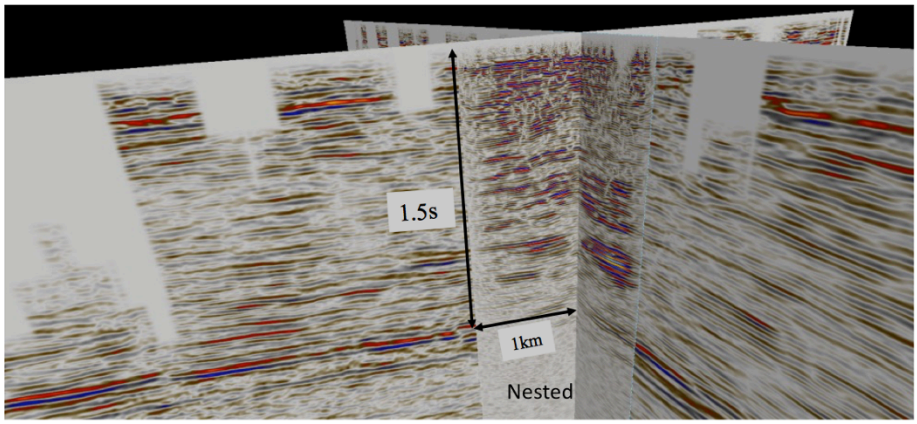

Fig. 2. Regional survey with nested survey inserted. Nested 3D survey demonstrated higher resolution and better overall expression of shallow geology. Vertical scale is in time.

2.3. Composite seismic line

The offset distribution in the large 3D volume was quite irregular and patchy due to acquisition gaps. The nested Harvey 4 survey, while allowing for detailed analysis around the well, lacked the size to enable reservoir characterisation over a sufficient area. For that reason, a composite line was created that cut through the available volumes. It incorporated previously acquired 2D lines with a full complement of offsets and passes close to of Harvey 1, 3 and 4 wells (Fig. 3). This gave us an opportunity to build a relatively detailed P-wave velocity model

using PSDM imaging techniques which provided sufficiently high quality seismic common-offset gathers and made the application of AVO inversion possible.

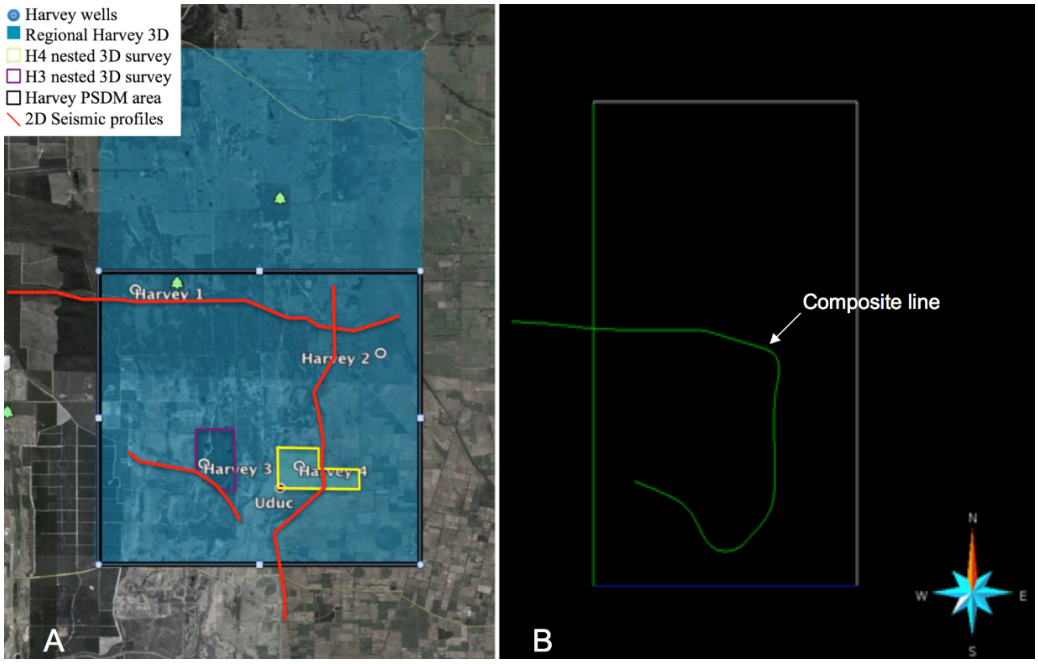

Fig. 3. (A) Seismic vintages in SW Hub; (B) Composite line from 2D/3D seismic data.

The arbitrary line is composed of existing 2D profiles from the H-3 nested survey, while some segments of the composite line were extracted from the regional survey. Segmental extraction was successfully processed using the 2D crooked line binning technique. The resulting composite line did not suffer from significant gaps and footprints, and the data was successfully migrated in both time and depth domains. Composite PSTM seismic section showed a good correlation with regional 3D volume (Fig. 4).

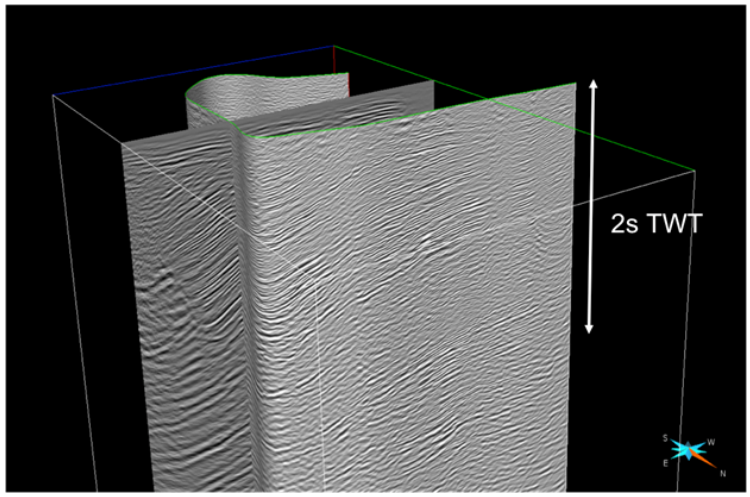

Fig. 4. PSTM section of composite line embedded in regional reprocessed 3D Harvey volume, view from NE.

3. Building accurate P-wave velocity model

The aim of this study was to close current information gaps by integrating all available geophysical data. For that purpose a high quality velocity model needed to be built to infer the distribution of petrophysical properties. This information was subsequently used to constrain static and dynamic models, which formed the core for subsequent feasibility studies of CO_2 sequestration in the SW Hub area.

Two velocity models were built by applying residual-moveout tomography on PSDM gathers. The first velocity model was from the composite line. This resulted in a relatively detailed velocity model built from sufficiently high quality seismic common-offset gathers. The second velocity field came from the regional 3D data that unfortunately lacked the offset distribution. This velocity model was relatively sparse and lacked resolution and detail that composite line provided. The PSDM algorithm used to create both velocity models is illustrated in the flowchart in Fig. 5.

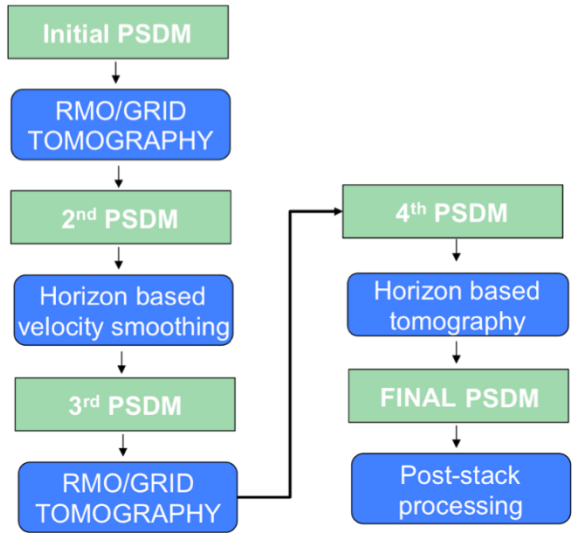

Fig. 5. PSDM Flowchart.

The model based velocity smoothing (layer stripping) method, included parameterisation of velocity within each layer either as constant interval velocity or by setting a linear velocity trend. The velocity field was updated using PSDM gathers for selected target horizons over the project area. Residual depth delays at horizon boundaries were extracted from the imaged gathers. Tomographic analysis method was then used for the final velocity update. The traveltime tomography projected the offset-dependent residual delays along raypaths, joining the subsurface location and the source and receiver locations (Stork, 1992). Iterations of these analyses continued until the pre-stack depth gathers were flat for the horizon events. The VSP and sonic logs from the wells were used to constrain the final velocity field (Fig. 6) used in the PSDM process.

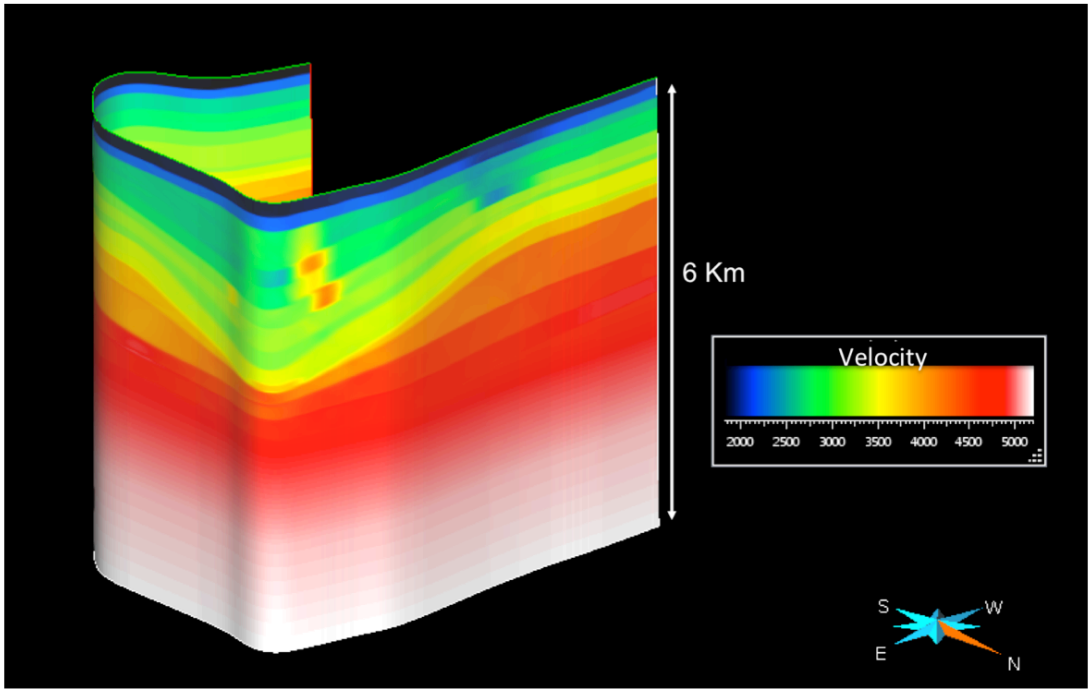

Fig. 6. High-resolution P-wave velocity field in depth of composite line.

Stochastic inversion was then applied to both the composite and 3D data sets. Ideally, AVO inversion should be performed on the 3D seismic volumes. However, this approach was inapplicable on available 3D data due to the patchy geometry, the offset distribution in the large survey and the size of the nested survey. The best that could be done on these 3D volumes was a stochastic post-stack acoustic inversion. A stochastic AVO inversion had been done on the composite 2D seismic line.

The final stage in this study included the integration of all the relevant information from seismic vintages into 3D reservoir models. The aim was to interpret the data in terms of subsurface distribution of petrophysical properties, relevant for the CO_2 sequestration modelling, such as:

- Probabilistic lithology prediction of the sand and shale,
- Sand porosity predictions calculated from velocity (Fig. 7), and,
- Sand porosity prediction calculated from P-Impedance.

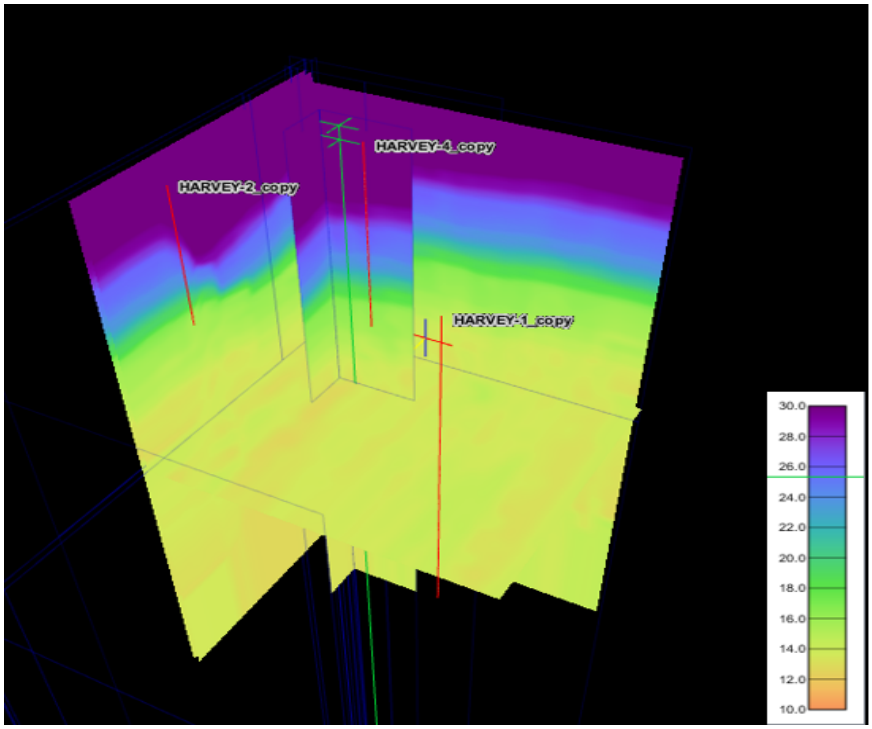

Fig. 7. Vertical and horizontal slices through the porosity cube computed from the reflection tomography velocities on regional and nested H-4 3D volumes. Note the smooth structure of the porosity, which resulted from the low resolution of the velocity analysis.

4. Conclusion

In this paper we present the workflow and the results of geophysical data analysis in the SW Hub area aimed at estimating distribution of rock properties within the Lesueur Formation. The analysis started with processing of VSP data. The velocity information of the VSP analysis was then used in the reprocessing and imaging of the regional 3D seismic dataset and a composite 2D line that passes in proximity to the three Harvey wells. Both of these datasets were then used for stochastic seismic inversion.

The main findings of the overall study are as follows:

Creation of a composite line greatly helped to constrain the velocity model. The high quality common-offset gathers allowed the application of the stochastic AVO inversion.

The most comprehensive analysis was performed on the regional 3D (2014) seismic volume, involving the post-stack stochastic rock physics inversion. Regional seismic volume was carefully reprocessed and produced images far superior to those produced previously with better reflection continuity and fault delineation. Reprocessing involved tomographic velocity reconstruction followed by pre-stack time and depth imaging.

The deterministic inversion of the regional 3D data showed very large uncertainty and hence required a priori constraints. To this end, a quantitative interpretation workflow was developed, which implements the Bayesian approach to stochastic seismic inversion.

Nested 3D seismic data produced high resolution images that allowed for precise structural analysis particularly in the shallow zone. Incorporating these data into the dynamic modelling will provide an insight into migration of CO_2 in the shallow subsurface, which is of greatest interest to the local community. This will also enable the design of more targeted surface and near-surface monitoring schemes to detect potential leakage.

5. Acknowledgements

The authors wish to acknowledge financial assistance provided through Australian National Low Emissions Coal Research and Development (ANLEC R&D). ANLEC R&D is supported by Australian Coal Association Low Emissions Technology Limited and the Australian Government through the Clean Energy Initiative.

The South West Hub project is managed by the Carbon Strategy Group of the Western Australia Department of Mines and Petroleum. It is supported through the Australian Commonwealth Government Flagship Program through the Department of Industry, Innovation and Science (DOIIS); the West Australian State Government through the Department of Mines and Petroleum; and the local community in the south west of Western Australia.

We are grateful to Halliburton Company for their generous donation of Landmark processing software and to CGG for their donation of AVO and seismic inversion software.

6. References

[1] Bretan, P., Yielding, G., Jones, H. (2003) Using calibrated shale gouge ratio to estimate hydrocarbon column heights, AAPG bulletin, 87, 397–413.

[2] Gurevich, B., Glubokovskikh, S., Pervukhina, M., Esteban, L., Müller, T., Pevzner, R., Schaubs, P., Shevchenko, S., Tertyshnikov, K., Yavuz, S., Zhang, Y., and Ziramov, S., 2018. The Lesueur, SW HUB: Improving seismic response and attributes. Fast-track quantitative interpretation for South West Hub. Milestone 7 Report, ANLEC R&D Project – 7-0115-0241.

[3] Langhi, L., Ciftci, B., Strand, J. (2013) Fault seal first-order analysis – SW Hub, CSIRO report EP13879, pp. 50.

[4] Langhi, L. , Zhang, Y. , Nicholson, C., , Bernardel, G., Rollet, N., Schaubs, P., Kempton, R., and Kennard, J. (2012) Geomechanical modelling of trap integrity in the northern offshore Perth basin, CSIRO Open file report: EP 12425.

[5] Morris, A., Ferrill, D.A., Henderson, D.B. (1996) Slip tendency analysis and fault reactivation, Geology 24 (3), 275–278.

[6] Mildren, S.D., Hillis, R.R., Dewhurst, D.N., Lyon, P.J., Meyer, J.J., Boult, P.J. (2005) Fast: a new technique for geomechanical assessment of the risk of reactivation-related breach of fault seals, Boult, P. & Kaldi, J. (eds) Evaluating fault and cap rock seals. AAPG hedberg series, 2, 73–85.

[7] Pevzner, R., Lumley, D., Urosevic, M., Gurevich, B., Bóna, A., Alajmi, M.A., Shragge, J., Pervukhina, M., Mueller, T., Shulakova, V. (2013) Advanced geophysical data analysis at Harvey-1: storage site characterization and stability assessment, ANLEC R&D project number 7-1111-0198.

[8] Pevzner, R., Langhi, L., Shragge, J., Ziramov, S., Potter, T., Tetyshnikov, K., Bona, A., and M. Urosevic, 2015. Advanced processing and analysis of South West hub 3D seismic data. ANLEC R&D Report (7-0314-0231).

[9] Stork, C., 1992, Reflection tomography in the postmigrated domain: GEOPHYSICS, 57, 680–692.

[10] Urosevic, M., Ziramov, S., Pevzner, R. (2015) Acquisition of the Nested 3D seismic survey at Harvey, ANLEC R&D Project 7-1213-0224 Final report, Curtin University, 36 pp.

[11] Urosevic, M., Ziramov, S., Pevzner R. and Kepic, A. (2014) Harvey 2D test seismic survey-issues and optimisation: ANLEC R&D Project 7-1213-0223.

[12] Yavuz, S., Ziramov, S., Shulakova, V., Tertyshnikov, K., Langhi, L., Bona, A., R. Pevzner and M. Urosevic (2018). Potential for preferential flow through faults and fractures. ANLEC Milestone 3 report; project 7-1215-0261.

[13] Ziramov, S., Urosevic, M., Glubokovskikh, S., Pevzner, R., Tertyshnikov, K., Kepic, A., Gurevich, B., 2017, CO2 Storage Site Characterisation using Combined Regional and Detailed Seismic Data: Harvey, Western Australia, ENERGY PROCEDIA, Volume 114, 2017, Pages 2896-2905, ISSN 1876-6102.